Recombinantly expressed spermadhesin AWN and fluorescence based characterization of porcine sperm membranes - prerequisites for functional interaction studies

Inaugural-Dissertation
to obtain the academic degree
Doctor rerum naturalium (Dr. rer. nat.)

submitted to the Department of Biology, Chemistry and Pharmacy
of Freie Universität Berlin

by Filip Schröter

from Cottbus, Germany

2017

The dissertation was performed during the years 2013 to 2017

at the Leibniz Institute for Zoo and Wildlife Research

under the supervision of Dr. Beate C. Braun and Dr. Karin Müller.

1st Referee: Prof. Dr. Heribert Hofer

2nd Referee: Prof. Dr. Rupert Mutzel

Disputation date: 12.05.2017

This cumulative dissertation is composed of an introduction and discussion of two publications in peer-reviewed journals:

Article 1: Recombinant expression of porcine spermadhesin AWN and its phospholipid interaction: indication for a novel lipid binding property

Filip Schröter[1], Karin Müller[1], Peter Müller[2], Eberhard Krause[3], Beate C. Braun[1]

Reproduction in Domestic Animals, March 2017, Epub ahead of print

DOI: 10.1111/rda.12953

Article 2: Lipid dynamics in boar sperm studied by advanced fluorescence imaging techniques

Filip Schröter[1], Ulrike Jakop[1], Anke Teichmann[4], Ivan Haralampiev[2], Astrid Tannert[1], Burkhard Wiesner[4], Peter Müller[2], Karin Müller[1]

European Biophysics Journal; March 2016; 45(2); page 149-63.

DOI: 10.1007/s00249-015-1084-z

https://www.ncbi.nlm.nih.gov/pubmed/26481472

Affiliations:

1: Leibniz Institute for Zoo and Wildlife Research, Department Reproduction Biology, Berlin, Germany

2: Humboldt University of Berlin, Department of Biology/Biophysics, Berlin, Germany

3: Leibniz Institute for Molecular Pharmacology, Department Mass Spectrometry, Berlin, Germany

4: Leibniz Institute for Molecular Pharmacology, Department Cellular Imaging, Berlin, Germany

Acknowledgement

I express my sincere gratitude to Prof. Dr. Heribert Hofer and Prof. Dr. Katarina Jewgenow for the opportunity to prepare my doctoral thesis on this fascinating topic at the IZW and their supervision as well as for Prof. Dr. Rupert Mutzel for his immediate willingness to act as a referee.

Special thanks go to Dr. Beate C. Braun for her great supervision, help and support during every single stage of my PhD work. I am deeply grateful for her ongoing inspiration to overcome my sometimes chaotic nature with her clear structures, experimental regime and documentation. It is my firm conviction that by that she immensely improved my performance not only as researcher but also in life outside the lab. The same goes for Dr. Karin Müller und Dr. Peter Müller, who always lent assistance and advice, especially during the biophysical experiments, manuscript creation and publication as well as the writing of the cumulative thesis. Both have my special thanks for awakening my enthusiasm for research work during my bachelor thesis and showing me early on that science can be quite funny. I would further like to thank my coauthors for their valuable contributions to both manuscripts and the colleagues of the Department of Reproduction Biology at the IZW Berlin, the group of molecular biophysics of the Humboldt University Berlin and the light microscopy group and mass spectrometry group of the Leibniz Research Institute for Molecular Pharmacology (FMP) Berlin for their support and assistance. Thanks also go to the doctoral students of the IZW Berlin for their input during our meetings and especially to Susanne Pribbenow for her advice whenever I had questions.

Last but not least I want to thank my family for their great support along the way without whom this work would have been impossible.

Selbstständigkeitserklärung

Hiermit erkläre ich, die Dissertation selbstständig und nur unter Verwendung der angegebenen Hilfen und Hilfsmittel angefertigt zu haben. Ich habe mich anderwärts nicht um einen Doktorgrad beworben und besitze keinen entsprechenden Doktorgrad. Ich erkläre, dass ich die Dissertation oder Teile davon nicht bereits bei einer anderen wissenschaftlichen Einrichtung eingereicht habe und dass sie dort weder angenommen, noch abgelehnt wurde.

_____

Filip Schröter

_____

Ort, Datum

Table of contents

Abbreviations

AFM	atomic force microscopy
AQN-1	carbohydrate-binding protein AQN-1
AQN-3	carbohydrate-binding protein AQN-3
AWN	carbohydrate-binding protein AWN (origin: domestic pig)
Bdh	bodhesin
CD spectroscopy	circular dichroism spectroscopy
CLSM	confocal laser scanning microscopy
CRP	cAMP-activated global transcriptional regulator CRP
CUB-domain	complement C1r/C1s, Uegf, Bmp1 domain
DAG	diacylglycerol
$DiIC_{12}$	1,1'-didodecyl-3,3,3'3'-tetramethylindocarbocyanine
$DiIC_{16}$	1,1'-dihexadecyl-3,3,3'3'-tetramethylindocarbocyanine
ELBA	enzyme linked binding assay
EPR	electron paramagnetic resonance spectroscopy
FCS	fluorescence correlation spectroscopy
FLIM	fluorescence lifetime imaging microscopy
FRAP	fluorescence recovery after photobleaching
FRET	Förster resonance energy transfer
FLIP	fluorescence loss in photobleaching
Fur	ferric uptake regulator
GAGs	glycosaminoglycans
H_{II} phase	hexagonal II phase
HCCA	alpha-Cyano-4-hydroxy-cinnamic-acid
HSP-7	carbohydrate-binding protein AWN (origin: domestic horse)
lysoPA	lyso phosphatidic acid
LUV	large unilamellar vesicle
NBD	7-nitro-2-1,3-benzoxadiazol-4-yl

NMR	nuclear magnetic resonance spectroscopy
ODAF	5-(N-octa-decanoyl) aminofluorescein
PA	phosphatidic acid
PBS	phosphate buffered saline
PC	phosphatidylcholine
PE	phosphatidylethanolamine
PI	phosphatidylinositol
POC	phosphorylcholine
POE	phosphorylethanolamine
PS	phosphatidylserine
PSP-I	major seminal plasma glycoprotein PSP-I
PSP-II	major seminal plasma glycoprotein PSP-II
PtdIns(4)P	phosphatidylinositol-4-phosphate
PtdIns(4,5)P_2	phosphatidylinositol-4,5-bisphosphate
PtdIns(3,4,5)P_3	phosphatidylinositol-3,4,5-trisphosphate
PXB	polymyxin B
recAWN	recombinantly expressed AWN
ROI	region of interest
SlyD	FKBP-type peptidyl-prolyl cis-trans isomerase SlyD
SAAI	sperm associated acrosin inhibitor
SPFI	single particle fluorescence imaging
SPI	serine proteinase inhibitor
SPR	surface plasmon resonance
TFA	trifluoroacetic acid

Chapter 1: Introduction

The aim of this dissertation was to establish the methodology to study the interaction of the spermadhesin carbohydrate-binding protein AWN (AWN) – a protein of the porcine seminal fluid named after its first three amino acids – with domestic pig sperm membranes, thereby improving the knowledge about the biological role of this protein in porcine reproduction. I focused on the domestic pig (*Sus scrofa domestica*) as model species because of good accessibility of tissue and ejaculates and the large number of studies on its reproduction. The gained information will provide insight into the general role of spermadhesins which may also be applicable to other porcine species and ungulates. In this respect, several endangered Asian species such as the babirusa (*Babyrousa babyrussa*), the pygmy hog (*Porcula salvania*) or the visayan warty pig (*Sus cebifrons*) are to be mentioned.

Two prerequisites have to be fulfilled to carry out studies on the interaction of AWN with sperm membranes, which I have pursued with the work documented in this thesis. Firstly, AWN has to be generated by recombinant technologies and characterized. Previously, this was only done for the spermadhesins bodhesin-2 obtained from the domestic goat (*Capra aegagrus hircus*, Nascimento et al. 2012, Cajazeiras et al. 2009) and the bovine spermadhesin-1 (also referred to as aSFP, Ekhlasi-Hundrieser et al. 2008a), originally obtained from domestic cattle (*Bos primigenius taurus*). Special interest concerns the identification of a putative phospholipid ligand of AWN in the sperm membrane to apply this knowledge for further studies.

Secondly, methods with a high resolution are needed for the examination of said interactions. For this purpose I focused on the adaption of fluorescence microscopic methods using fluorescence labeled lipid analogs incorporated into the sperm cell to acquire information on membrane compartments in the gamete. This adaption is necessary since male gametes differ greatly from other cells because of their small size, low cytoplasmic content, highly structured membrane and intense membrane curvature in some regions.

Taken together this will lead to a better understanding of the role of seminal proteins of the spermadhesin family in the porcine reproductive system and provide references for similar examinations in other ungulates.

1.1 AWN as a member of the spermadhesin protein family

1.1.1 The seminal fluid

Even after their differentiation in the testis, mammalian spermatozoa need to undergo a series of maturation processes in order to acquire their full fertilization competence. The seminal fluid, when coming into contact with the male gametes during ejaculation, plays a crucial role in mediating these processes whose final stage is referred to as capacitation. It is commonly assumed that

spermatozoa are not transcriptionally active (Mackie et al. 2001) and do not express proteins in their cytosol (Miller and Ostermeier 2006). Yet at least a limited amount of protein synthesis from mRNA seems to be retained, by using mitochondrial ribosomes during capacitation (Gur and Breitbart 2008, Kwon et al. 2014, Gur and Breitbart 2006). Nonetheless, the necessary changes of the sperm cells to endure the changing environmental challenges during their passage through both genital tracts are predominantly processed by reorganization of existing components and interactions with external molecules.

The seminal plasma is a mixture of secretions from epididymis and male accessory glands consisting of a broad variety of proteins, peptides, carbohydrates, lipids and other components. It comes into contact with spermatozoa during ejaculation and mediates fertilization-relevant processes in the sperm cells as well as the female genital tract. The main protein families of mammalian seminal plasma are fibronectin type-II proteins (Fn-2 proteins), cysteine-rich secretory proteins (CRISP) and spermadhesins (see Rodriguez-Martinez et al. 2011, Ekhlasi-Hundrieser et al. 2008b, Töpfer-Petersen et al. 1995, Töpfer-Petersen 1999b, Töpfer-Petersen et al. 1998) who have been linked to functions including but not limited to interactions with the sperm membrane, modulation of sperm properties, mediation of sperm-oviduct binding and gamete recognition (Töpfer-Petersen et al. 1998). The incidence of these protein families differs between species. CRISP proteins appear to be present in all mammalian species, whereas Fn-2 proteins were only identified in primates, carnivores and ungulates so far but not in rodents and spermadhesins are exclusively found in ungulates (Ekhlasi-Hundrieser et al. 2008b).

It is a common expectation that proteins of different families will perform homologous functions throughout but this is still somewhat speculative, because the role of the seminal plasma is not limited to simply aid fertilization as it may assume additional roles. These include a possible function to minimize sperm competition (Ramm et al. 2015, for general information on sperm competition see Parker 1982, Parker and Pizzari 2010 and references therein) and influencing the offspring phenotype, likely through influencing protein expression in the female genital tract (Bromfield et al. 2014).

1.1.2 Spermadhesins

The proteins of the spermadhesin family are mainly present in ungulates with members being found in the males of domestic horses, (*Equus ferus caballus*, Reinert et al. 1996), domestic cattle (Einspanier et al. 1993, Tedeschi et al. 2000), domestic goat (Melo et al. 2008), domestic sheep (*Ovis gmelini aries*, Bergeron et al. 2005, International Sheep Genomics et al. 2010, Soleilhavoup et al. 2014) and domestic pig (Töpfer-Petersen et al. 2008 and references therein). On the other hand only inactive copies of spermadhesin genes were discovered in the genomes of humans (*Homo sapies sapiens*), chimpanzees (*Pan troglodytes*) and domestic dogs (*Canis lupus familiaris*) whereas

the entire corresponding region has been deleted in the genomes of mice (*Mus musculus*) and rats (*Rattus norvegicus*, Töpfer-Petersen et al. 2008, Leeb 2007, Haase et al. 2005). Correspondingly, no expressed proteins were detected in the seminal fluid of these species so far.

Structurally spermadhesins are 12-16 kDa proteins consisting of 105-133 amino acids forming a complement C1r/C1s, Uegf, Bmp1 domain (CUB domain), a structural module consisting of a β-sandwich structure with two highly conserved disulphide bridges (Bork and Beckmann 1993). This module is present in several combinations in functionally diverse proteins, often involved in developmental processes. Spermadhesins express multiple binding affinities e.g. to heparin, carbohydrates, phospholipids and the inhibitors for the serine proteinases acrosin and trypsin (Sanz et al. 1992a, Dostalova et al. 1995a, see also Töpfer-Petersen et al. 1998, Töpfer-Petersen et al. 2008 and references therein).

For spermadhesins of different species, similar but also diverse functions and properties were revealed and/or discussed so far. Equine carbohydrate-binding protein AWN (HSP-7) is a member of the spermadhesin protein family identified in male domestic horses seminal fluid (Reinert et al. 1996). It has 98 % sequence identity with porcine AWN and possesses a binding affinity to zona pellucida proteins. It is therefore probably involved in sperm-egg-interaction. Labeling of ejaculated domestic horse spermatozoa with antibodies against AWN revealed a distribution over the equatorial segment of the sperm head membrane (Töpfer-Petersen et al. 1995), supposedly caused by HSP-7. This is in contrast to ejaculated domestic pig spermatozoa where AWN is predominantly localized over the acrosomal region.

In seminal plasma of male domestic cattle, two spermadhesins, spermadhesin-1 (also referred to as aSFP, Einspanier et al. 1993) and spermadhesin Z13 (Tedeschi et al. 2000) were identified. In contrast to other spermadhesins, spermadhesin-1 has neither heparin nor zona pellucida binding potential (Calvete et al. 1996b) and does not bind to capacitated spermatozoa (Dostalova et al. 1994a). It has therefore been implied to function as a decapacitation factor for bovine sperm. It also appears to function as a growth factor, affects ovarian granulosa cells and may protect spermatozoa against oxidative stress (see Einspanier et al. 1994 and references therein). The lack of heparin binding affinity is shared by spermadhesin Z13. In male domestic cattle, a high concentration of spermadhesin Z13 is associated with low fertility (Moura et al. 2006). Both proteins have also been isolated from seminal plasma in the wild yak (*Bos mutus*).

In male domestic goats, four spermadhesins named bodhesin-1 to bodhesin-4 (referred to as Bdh-1 to Bdh-4) have been identified (Teixeira et al. 2002, Melo et al. 2008). However, to my knowledge the functional similarity of bodhesins to the other members of the spermadhesin family has not yet been examined.

A spermadhesin designated as RSP-15.5kDa was detected in the male domestic sheep (Bergeron et al. 2005) accounting for 45% of the seminal plasma's protein content by mass. The first 25 N-terminal amino acids identified in this study showed high sequence similiarities to several spermadhesins including porcine AQN-1 and the four bodhesins of domestic goats. Another study identified Bdh-2, spermadhesin-1 and spermadhesin Z13 in male domestic sheep's seminal plasma (Soleilhavoup et al. 2014). To my knowledge no functional roles for the spermadhesins in the sheeps's seminal plasma have been proposed.

The highest number of spemadhesins can be found in the domestic pig. There, five different spermadhesins, carbohydrate-binding protein AQN-1 (AQN-1, Sanz et al. 1992c), carbohydrate-binding protein AQN-3 (AQN-3, Sanz et al. 1991), AWN (Sanz et al. 1992b) and major seminal plasma glycoproteins PSP-I and PSP-II (PSP-I and PSP-II, Rutherfurd et al. 1992) are present in glycosylated and unglycosylated isoforms, comprising about 75 % of the protein content of the seminal fluid (Ekhlasi-Hundrieser et al. 2002). They share 40-60 % amino acid identity (Töpfer-Petersen et al. 1995) and are able to bind heparin. However, since PSP-I and PSP-II only express affinity for heparin as monomers while normally forming heterodimers in the seminal fluid, they cannot become purified by heparin columns (Calvete et al. 1995). AWN, AQN-1 and AQN-3 bind to the sperm surface during ejaculation and can bind to the zona pellucida. These spermadhesins seem to prevent a premature acrosome reaction (Töpfer-Petersen et al. 1998), participate in the formation of a sperm reservoir in the oviduct (Ekhlasi-Hundrieser et al. 2005, Wagner et al. 2002, Töpfer-Petersen 1999a) and during subsequent sperm egg recognition (Töpfer-Petersen et al. 1998, Rodriguez-Martinez et al. 1998). The PSP-I/PSP-II heterodimer might modulate immune responses in the porcine uterine environment (Assreuy et al. 2002)

1.1.3 AWN

AWN, the focus of this work, was named after the first three amino acids of its sequence. It is a secretion product of the epididymis as well as the seminal vesicles (glandula vesiculosae) of male domestic pigs (Rutherfurd et al. 1992). The latter seem to be the exclusive source of the glycosylated form of AWN (Calvete et al. 1994). There is some evidence that these glycosylated molecules have a truncated C-terminus and lack 8 amino acids, even though this does not seem to influence binding characteristics (Calvete et al. 1993). AWN is also expressed in the uterus, uterotubal junction and oviduct of sows (Ekhlasi-Hundrieser et al. 2002) as well as in the oviductal fluid of sheep (Soleilhavoup et al. 2016).

Two isoforms of AWN were detected, with AWN-2 differing from AWN-1 by the acetylation of the N-terminus (Sanz et al. 1992b). It is noteworthy that the equine spermadhesin HSP-7 only differs from porcine AWN in 3 amino acids, thus being identical by 98 % (Reinert et al. 1996) and therefore surpassing sequence similarity amongst porcine spermadhesins AWN, AQN-1, AQN-3,

PSP-I and PSP-II by far. With the last common ancestor of domestic pigs and horses living over 50 million years ago (Carroll 1988), this implies a high structural and functional conservation of AWN and HSP-7 in both species.

The porcine protein is already present in large numbers on epididymal spermatozoa (7×10^6 molecules per cell) before they become covered by a further $12 - 60 \times 10^6$ AWN, AQN-1 and AQN-3 molecules per cell during ejaculation. It was proposed that this large number of bound protein molecules forms a multilayer hull above the acrosomal cap, thus implicating protein-protein as well as protein-membrane interactions (Dostalova et al. 1994b). During in vitro capacitation, most spermadhesins are released from the sperm surface (Töpfer-Petersen et al. 1998). Since this process also occurs in vivo in the oviduct, the function of this coating of sperm is presumed to be transient for the transit of sperm through the female genital tract. A recent study on protein expression which continues in ejaculated spermatozoa reported a significant increase in AWN expression of the sperm cells themselves after capacitation (Kwon et al. 2014). Since capacitation was performed after removal of the seminal plasma this implies an intracellular expression of the protein through mitochondrial ribosomes of sperm cells (see also Gur and Breitbart 2008).

The heparin and phospholipid binding sites overlap in AWN (Calvete et al. 1996a) and are localized opposite to the glycoprotein binding domain (Dostalova et al. 1995b). AWN also contains an arginine positioned at the 50^{th} position of its amino acid sequence acting as glycosylation site that is highly conserved between the members of the spermadhesin family. Its glycosylation diminished the binding affinity to carbohydrates, zona pellucida glycoproteins and trypsin inhibitors but not to heparin (Calvete et al. 1993, Calvete et al. 1994, Töpfer-Petersen et al. 1995). Owing to the localization of the corresponding binding site, it is likely that the phospholipid affinity is not influenced by glycosylation. Regarding interactions between the different ligands, the interaction of AWN with the acrosin inhibitor did not seem to diminish the zona pellucida binding of the protein. However, its interaction with the zona pellucida appears to release the acrosin inhibitor from AWN and implies a competitive binding of both ligands with a preference for the zona pellucida (Sanz et al. 1992a).

Since phospholipids are the main component of biological membranes, it is likely that the membrane association of AWN is mediated by its phospholipid binding site, yet AWN's phospholipid ligand has been controversially discussed so far. No aggregated forms and only 20 % of non-aggregated AWN bound to phosphorylethanolamine (POE) containing matrices (Dostalova et al. 1995b). On the other hand, an affinity between AWN and phosphorylcholine (POC), which was not detected by these authors, was proposed after application of an enzyme-linked binding assay (ELBA, Jonakova et al. 2000). The phospholipid composition of sperm cells can also differ laterally (see Flesch and Gadella 2000 and references therein), thereby providing a target for localized binding. Immunohistological localization of AWN with mouse and chicken derived

antibodies showed such selective binding to the acrosomal region of the domestic pig sperm head (Sanz et al. 1992b, Dostalova et al. 1995a, Rodriguez-Martinez et al. 1998), which, for some antibodies, was even reduced to the apical ridge of this substructure (Calvete et al. 1997).

1.2 Methods for membrane studies

For the examination of membrane interactions of AWN and its functional role, the application of different fluorescence microscopic methods promise great potential. These methods provide a high resolution for studies of fluorescent labels incorporated in membranes. Examples are fluorescence lifetime microscopy (FLIM, Marriott et al. 1991), fluorescence recovery after photobleaching (FRAP, Meyvis et al. 1999, Axelrod et al. 1976 and references therein) and fluorescence correlation spectroscopy (FCS, Elson and Magde 1974, Magde et al. 1974, Elson 2011). Previous studies have used FRAP to investigate sperm membranes (e.g. Wolfe et al. 1998, Mackie et al. 2001, Christova et al. 2004, Jones et al. 2007) but not yet used FLIM and FCS to examine the sperm plasma membrane.

FLIM measures the lifetime of fluorescent molecules, which is influenced by the presence of possible quencher molecules, polarity and other physical properties in its immediate vicinity (**Figure 1**). The lifetime values can be calculated for each detected pixel separately, thereby allowing for the differentiation of lateral subdomains. Even though fluorescence lifetimes lay in the range of nanoseconds, it has to be kept in mind that fluorescence counts have to be accumulated over seconds, thereby limiting the resolution of events with short temporal stability.

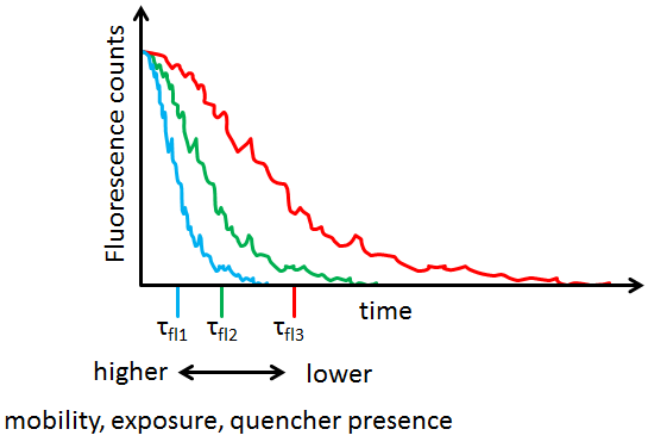

Figure 1: *Principle of FLIM measurements. Excited fluorophores emit photons in a stochastic manner over a characteristic time range. The average timespan between excitation and emission is called fluorescence lifetime (τ_{fl}). This value is influenced by the environment of the fluorescent molecule, especially by the probability to interact with quencher molecules. This interaction leads to an emission free energy loss competing with the fluorescence emission in a time dependent manner thereby decreasing the fluorescence lifetime.*

FCS and FRAP on the other hand both focus on the mobility of molecules. In the FRAP approach, all molecules in a predefined region are irreversibly photobleached by an intense laser beam. Afterwards the redistribution kinetics of the fluorophore is monitored either through the fluorescence intensity recovery inside the bleaching region (**Figure 2**) or the decrease outside. This permits the calculation of diffusion constants, the localization of diffusion barriers and the identification of immobile or less mobile fractions.

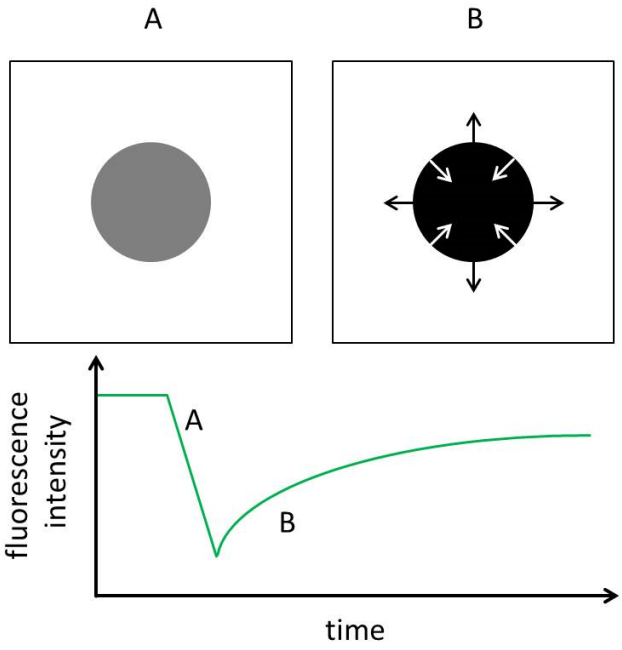

Figure 2: *Principle of FRAP measurements. The fluorescence intensity of a fluorophore is measured in a predefined area. A: The fluorophores within the area are bleached by a laser. B: Intact fluorophores from outside the area and permanently bleached molecules from within exchange by brownian motion. The recovery of fluorescence caused by this exchange can be monitored to calculate physical parameters as for example diffusion coefficients or gain knowledge of diffusion barriers.*

FCS monitors the fluctuation of fluorescence intensity in a very small volume, which is caused by brownian motion of single molecules (**Figure 3**). This permits, for instance, the calculation of diffusion constants and hydrodynamic radii. Interestingly, in other cells and vesicles diffusion coefficients derived by FCS sometimes differ greatly from those measured by FRAP (Adkins et al. 2007, Guo et al. 2008).

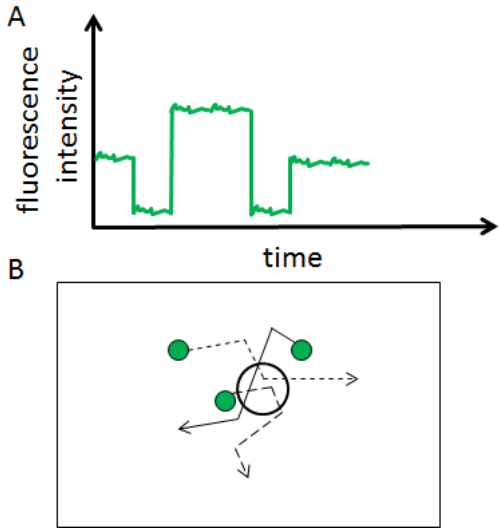

Figure 3: *Principle of FCS measurements.*

If the observed volume is sufficiently small and the concentration of the fluorescent molecule sufficiently low, fluctuations of the fluorescence intensity (A) can be directly correlated to separate molecules (B, green circles) diffusing through the confocal volume (B, black circle).

To correctly correlate fluctuations of fluorescence intensity to the movement of single molecules, FCS measurements require a preferably small detection volume and concentration of fluorophore. In contrast, FLIM and FRAP benefit from a high number of fluorescence counts. All three techniques have varying spatial and temporal resolutions, thereby being of complementary suitability for addressing different biological questions.

A prerequisite for all aforementioned applications is the presence of fluorescent molecules in the membrane which is the subject of the study. The membrane lipids as potential targets can be labeled in several ways, including direct labeling at the head group or one of the acyl chains and indirect labeling using antibodies or toxin domains (for a general overview see Maekawa and Fairn 2014). Several fluorescent lipid analogs and artificial lipid reporters have been incorporated into sperm cells of different species. Some of them are incorporated almost exclusively into one half (also referred to as cytoplasmatic and exoplasmatic leaflet) of the membrane bilayer in proportion to the asymmetric distribution of endogenous lipids (Müller et al. 1994). Size, polarity and positioning on the lipid molecule are important considerations when choosing the fluorescence label. Labeling of the hydrophobic acyl-chains with polar groups might lead to a loop back to the membrane surface (Chattopadhyay and London 1987, Kaiser and London 1998). Head group positioned labels might alter the interaction between the labeled lipid and other membrane components because of their size, charge or polarity. This might also have an impact on the membrane properties like lipid packing, fluidity and formation of bilayers or other lipid arrangements.

Measurements of diffusion coefficients of several probes via FRAP revealed differences between sperm regions and changes upon sperm maturation in the epididymis, after removal of cholesterol or after addition of hydroperoxides (reviewed by Jones et al. 2010, Jones et al. 2007).

Chapter 2: "Recombinant expression of porcine spermadhesin AWN and its phospholipid interaction: indication for a novel lipid binding property"

2.1 Summary

The paper focussed on the recombinant expression of the porcine spermadhesine AWN for further studies on spermadhesine membrane interaction. It contains a purification regime for the recombinant AWN (recAWN) comprising three steps:

1. affinity chromatography using binding of a recombinant His-tag to immobilized Ni-ions
2. affinity chromatography using recAWN's heparin binding affinity
3. size exclusion chromatography.

The protein was further characterized by controlling the presence of the two disulphide bridges highly conserved in spermadhesin structure and experiments to identify the lipid binding partner of recAWN. Interestingly these experiments showed high affinity of the protein to phosphatidic acid (PA) as well as cardiolipin, whereas no significant binding to phosphatidylethanolamine (PE) or phosphatidylcholine (PC) as surmised in the literature could be reproduced. The biological relevance of the cardiolipin binding was discussed and discouraged because of its localization in the mitochondrial membrane and the possibility of a His-tag mediated interaction.

The binding affinity to PA is here proposed for the first time for a spermadhesin, thereby yielding new insights into the possible mechanism of sperm coating and its functional relevance, since PA may represent a key molecule for fusion events in the membrane. We proposed a role for AWN for masking the charge of this phospholipid, thereby preventing the membrane from calcium-induced formation of non-bilayer structures which would lead to membrane destabilization. Immunolocalization of the recAWN showed a distribution across the acrosomal region of ejaculated domestic pig spermatozoa similar to earlier results with porcine AWN.

Author contributions

Filip Schröter: project design, all steps from the insertion of recombinant AWN sequence into the used transfection vector, generation of the *E.coli* expression cell line to the establishment of the purification protocols, characterization of disulphide bridges, identification of the lipid ligand, documentation of experiments, analysis and interpretation of result, writing of the manuscript

Beate C. Braun, Karin Müller, Peter Müller: project design and supervision

Eberhard Krause: protein identification using LC-MS/MS

All authors were involved in discussing data as well as preparing and correcting the manuscript.

Recombinant expression of porcine spermadhesin AWN and its phospholipid interaction: indication for a novel lipid binding property

Filip Schröter[1], Karin Müller[1], Peter Müller[2], Eberhard Krause[3], Beate C. Braun[1]

1: Leibniz Institute for Zoo and Wildlife Research, Department Reproduction Biology, Berlin, Germany

2: Humboldt University of Berlin, Department of Biology/Biophysics, Berlin, Germany

3: Leibniz Institute for Molecular Pharmacology, Department Mass Spectrometry, Berlin, Germany

Running title

Recombinant spermadhesin AWN and lipid binding

Keywords

spermadhesin, recombinant expression, phospholipid binding domain

Abstract

AWN is a porcine (*Sus scrofa domestica*) seminal plasma protein and has been linked to a variety of processes related to fertilization. To acquire the protein in sufficient amount and purity for functional studies, we established its recombinant expression in *E. coli* and a three step purification protocol based on different chromatographies. The test for AWN-phospholipid interaction revealed phosphatidic acid and cardiolipin as potential binding partners. Since phosphatidic acid is surmised to play a role in cation induced membrane destabilization and fusion events, we propose a membrane protective function of the presented binding affinity. Further studies with recombinant AWN will allow new insights in the mechanism of sperm-spermadhesin interaction and might provide new approaches for artificial reproduction techniques.

2.2 Introduction

Ejaculate consists of sperm cells and seminal plasma. The latter is a mixture of secretions from epididymis and male accessory sex glands providing a variety of fertilization-relevant components to sperm cells and to the female genital tract. Representatives of the main protein families found in mammalian seminal plasma, Fn type 2 proteins, CRISP proteins and spermadhesins, have been proposed to interact with the sperm membrane, modulate sperm properties, and mediate processes like sperm-oviduct binding and gamete recognition (Ekhlasi-Hundrieser et al. 2008b). Spermadhesins are a family of seminal plasma proteins mainly found in ungulates with particularly high abundance in pigs, where they represent about 75% of the seminal plasma proteins (Ekhlasi-Hundrieser et al. 2002). Five different members are described for the pig: carbohydrate-binding protein AWN, AQN-1, and AQN-3 as well as major seminal plasma glycoprotein PSP-I, and PSP-II. AWN and AQN were named for their first three amino acids, while PSP is an abbreviation for

porcine seminal protein. Spermadhesins consist of 109-133 amino acids, show 40-60% amino acid identity and possess two conserved disulphide bridges (reviewed by Töpfer-Petersen et al. 1995, Töpfer-Petersen et al. 1998).

AWN is not only secreted in the epididymis and by the seminal vesicles (*glandula vesiculosae*) of boars but even in the uterus, uterotubal junction and oviduct of sows (Ekhlasi-Hundrieser et al. 2002). It was also found in the oviductal fluid of sheep (Soleilhavoup et al. 2016). Notably, the glycosylated form of AWN seems to originate exclusively from the seminal vesicles (Calvete et al. 1994). The first isolation of the protein was performed from boar ejaculates. Freshly collected boar spermatozoa were washed and extracted using a buffer containing acetic acid. After centrifugation the supernatant was separated by size exclusion chromatography. Fractions were tested for their affinity to zona pellucida and positive fractions were pooled and further fractionated by gel chromatography and reverse phase HPLC (Sanz et al. 1992d). AWN possesses a glycoprotein (Sanz et al. 1992d, Dostalova et al. 1995a) as well as a phospholipid binding site and displays an affinity to heparin (Sanz et al. 1993, Calvete et al. 1996a). The heparin and phospholipid binding sites overlap (Calvete et al. 1996a) and are both localized opposite to the glycoprotein binding domain (Dostalova et al. 1995b). Regarding the phospholipid ligand, an affinity between AWN and phosphorylcholine (POC) (Jonakova et al. 2000) as well as affinity of non-aggregated spermadhesins to phosphorylethanolamine (POE) (Dostalova et al. 1995b) were observed.

AWN is present in large amounts already on epididymal spermatozoa (7×10^6 molecules per cell) while the membrane over the acrosome – a substructure in the anterior region of the sperm head – becomes covered by further $12\text{-}60 \times 10^6$ AWN, AQN-1 and AQN-3 molecules per cell upon ejaculation. This amount of bound protein molecules is sufficient to form a multilayer envelope above the acrosomal region and suggests that spermadhesins may interact with components of the sperm membrane as well as with the spermadhesins themselves (Dostalova et al. 1994b). Since the majority of the spermadhesin molecules are released from the sperm surface during *in vitro* capacitation (Töpfer-Petersen et al. 1998), a process which occurs *in vivo* in the oviduct, the spermadhesin coating is assumed to have transient functions in favor of sperm transit through the female genital tract.

Since the isolation of single spermadhesins e.g. from seminal plasma with high purity has been proven difficult, their recombinant expression could alternatively provide sufficient quantities for functional studies. Therefore, in the present study, we have expressed AWN recombinantly in *E. coli*, and successfully purified the protein from the cellular lysate. The isolated protein was characterized by several biochemical methods. First experiments on the interaction of recombinant AWN with lipids point to a specific affinity of the protein to phosphatidic acid (PA). The availability of pure AWN at sufficiently large amounts will allow in the future investigating the modulation of sperm functions by AWN in the female genital tract in detail.

2.3 Materials and Methods

2.3.1 Cloning, transformation, and expression of porcine AWN in E. coli

The methods applied were approved by the Internal Committee for Ethics and Animal Welfare of the Leibniz Institute for Zoo and Wildlife Research in Berlin, Germany (Permit number: 2010-10-03). The tissue from porcine genital tract was obtained from slaughterhouse. Total RNA was isolated from porcine epididymis with Precellys Tissue RNA kit (Peqlab, Erlangen, Germany) and single stranded cDNA was synthesized, both likewise as described before (Braun et al. 2012). AWN cDNA was amplified for the cloning process in a PCR using specific primers. Beside gene specific sequences, the primers comprised restriction enzyme specific binding sites as well as the reverse primer a sequence coding for a factor Xa cleavage site (AWN-fw*:* TCG GGA TCC GGC ATG GAA CAG AAG GTC TC, AWN-rv*:* AGT GCG GCC GCC CTT CCC TCG ATA GGG ATG TTT TTC TCT GTA G). PCR reaction was performed using cDNA and 2 U High FidelityPlus polymerase (Roche, Mannheim, Germany) in a 50 µl reaction volume (1x Expand HiFiPLUS Reaction Buffer with 1.5 mM $MgCl_2$, 200 µM nucleotides, 0.5 µM of each primer; PCR conditions: 2 min denaturation at 94°C, 30 cycles of 45 sec/94°C, 45 sec/51°C, 45 sec/72°C, 7 min final elongation at 72°C). The amplified product was purified, restricted by BamHI and NotI (both Thermo Scientific, St. Leon-Rot, Germany), purified again and then ligated into pET-21b vector (Novagen, Darmstadt, Germany), which carries a sequence coding for a C-terminal His-tag sequence. The ligation approach was transformed into chemically competent *E. coli* JM109 cells according to the manufacture's protocol (Promega, Mannheim, Germany). After identification of positive clones and control sequencing, the vector of one positive clone was extracted, purified and transformed into the expression host strain. Since AWN contains two highly conserved disulphide bridges, the SHuffle® T7 Express strain (New England Biolabs GmbH, Frankfurt am Main, Germany) was selected, this strain is designed to possess a non-reducing cytoplasm.

The cultivation of AWN-producing cells took place in lysogeny broth (LB) medium containing 100 µg/ml ampicillin. The medium was incubated at 30°C at 130 rpm and inoculated with an overnight culture of SHuffle® T7/pET21b-AWN. After reaching an OD_{600nm} of 0.5 the incubator was cooled down to 16°C and after one hour of acclimatization, the spermadhesin expression was induced by adding isopropyl-β-D-thiogalactopyranoside (IPTG, final concentration 0.6 mM) to the growing medium. The cells were incubated four hours while shaking with 130 rpm at 16°C and, subsequently, harvested by centrifuging the culture at 4,000 × g for 5 min. The supernatant was discarded and the cell pellets were stored at -80°C. The effectiveness of recombinant protein expression was controlled via SDS-PAGE, coomassie blue staining and western blot. The isotope-averaged molecular mass of the recombinantly expressed, His-tagged protein precursor was calculated to 17.953 kDa from the given primary sequence, assuming two disulfide bridges.

2.3.2 Purification of recombinant AWN

To purify the recombinantly expressed AWN, 64 ml lysis buffer (50 mM Tris-HCl, pH 7.5, 1 mM EDTA, 2 mg/ml lysozyme, 20% glycerol) was added to a thawed cell pellet corresponding to 1.5 l culture volume. This suspension was treated as described in Hachen et al. 2012.

Purification of AWN from the lysate was performed using a three step approach with a His-affinity column followed by a heparin-affinity column and finally a size exclusion chromatography using an Äkta Pure system (GE Healthcare, Munich, Germany). After each step, elution fractions were analyzed by SDS-PAGE and western blotting and the fractions containing the recombinant protein were pooled for further experiments.

First, the lysate was rebuffered into His-affinity binding buffer (20 mM Imidazole, 0.5 M NaCl, 20 mM Na_2HPO_4/NaH_2PO_4, pH 7.0) and concentrated using Amicon 10K centrifugal filter tubes (Merck Millipore, Darmstadt, Germany). For the His-affinity chromatography, a Tricorn 10/20 High Performance Column packed with Ni-loaded Chelating Sepharose Fast Flow was used (GE Healthcare, Munich, Germany). After applying the concentrated lysate, the column was washed with 10 ml 3% elution buffer (100% = 0.5 M Imidazole, 0.5 M NaCl, 20 mM Na_2HPO_4/NaH_2PO_4, pH 7.0) in binding buffer. Afterwards, the bound proteins were eluted with 9 ml 100% elution buffer before the column was washed with another 10 ml of each, elution and binding buffer.

After buffer exchange of selected elution fractions of up to two His-affinity chromatographies into heparin-affinity-binding-buffer (0.15 M NaCl, 20 mM Na_2HPO_4/NaH_2PO_4, pH 7.3), the protein suspension was applied on a Tricorn 10/20 High Performance Column packed Heparin Sepharose 6 Fast Flow (GE Healthcare, Munich, Germany). The column was washed with 10 ml binding buffer and bound proteins were eluted with 9 ml elution buffer (3 M NaCl, 20 mM Na_2HPO_4/NaH_2PO_4, pH 7.3) before washing the column with another 10 ml of each, elution and binding buffer.

As third purification step and to check for putative multimers, size exclusion chromatographies were performed with neutral sodium phosphate buffer (0.15 M NaCl, 50 mM Na_2HPO_4/NaH_2PO_4, pH 7.0) on a HiLoad™ 26/600 Superdex 200 prep grade (GE Healthcare, Munich, Germany) size exclusion column, having a separation range of 10-600 kDa. A gel filtration standard containing globular proteins in the range between 1.35 and 670 kDa (BioRad, Hercules, USA) was used for calibration.

2.3.3 Analysis of protein fractions and pools by SDS-PAGE and western blotting

The protein fractions/pools were analyzed by SDS-PAGE using 20% polyacrylamide gels (Laemmli 1970). For this, the samples were mixed with 4x concentrated sample buffer (0.2 M Tris-Cl, 4% SDS, 0.5 M DTT, 50% glycerol, 0.04% bromphenolblue, pH 6.8) and heated for 5 min at 95°C before being applied onto the gel. After running, the gels were stained with coomassie blue according to Dyballa and Metzger 2009 or transferred to nitrocellulose membrane (0.2 µm, Protran

BA83, GE Healthcare, Munich, Germany) for western blot analysis. The immunological detection of poly-His-residues was performed as described by Hachen et al. 2012.

In some cases, a sodium desoxycholate/trichloroacetic acid precipitation of the proteins was used prior to SDS-PAGE and western blot. For precipitation, 800 µl of the fraction to be analyzed was mixed with 100 µl 0.15% (w/v) sodium desoxycholate (Roth, Karlsruhe, Germany) in H_2O and 100 µl 72% trichloroacetic acid (Roth, Karlsruhe, Germany) in H_2O, incubated for 20 min at room temperature and centrifuged (20 min, 20,000 × g, 4°C). The pellet was washed with 500 µl acetone and resuspended in 20 µl 2x sample buffer.

2.3.4 Protein identification by LC-MS/MS and protein analysis by ESI-MS

Protein bands were excised from the gel and in-gel tryptic digestion was performed as described before (Lange et al. 2010). Briefly, gel bands were incubated with 50 ng trypsin (Promega, Mannheim, Germany) in 20 µl 50 mM ammonium bicarbonate buffer overnight at 37 °C. The enzymatic reaction was terminated by addition of 20 µl of 0.5% (v/v) trifluoroacetic acid (TFA) in acetonitrile. The liquid was separated, evaporated to dryness under vacuum, and the tryptic peptides were re-dissolved in 6 µl 0.1% (v/v) TFA and 5% (v/v) acetonitrile in water. Peptides were analyzed by a reversed-phase capillary liquid chromatography system (Ultimate 3000 nanoLC system, Thermo Scientific, St. Leon-Rot, Germany) connected to an Orbitrap Elite mass spectrometer (Thermo Scientific, St. Leon-Rot, Germany). LC separations were performed on a capillary column (Acclaim PepMap100, C18, 3 µm, 100 Å, 75 µm i.d. × 25 cm, Thermo Scientific, St. Leon-Rot, Germany) at an eluent flow rate of 300 nl/min using a linear gradient of 3–50% of phase B in 60 min. Mobile phase A contained 0.1% formic acid in water, and mobile phase B contained 0.1% formic acid in acetonitrile. Mass spectra were acquired in a data-dependent mode with one MS survey scan with a resolution of 60,000 (Orbitrap Elite) and MS/MS scans of the 15 most intense precursor ions in the linear trap quadrupole.

The processed MS data were analyzed on a MASCOT server (version 2.2.2, Matrix Science Ltd, London) and searched in-house against a self-made database which contains the SwissProt database (version 2014_12; 547,085 sequences) and the recombinant AWN-sequence (MASMTGGQQMGRDPAWNRRSRSCGGVLRDPPGKIFNSDGPQKDCVWTIKVKPHFHVVL AIPPLNLSCGKEYVELLDGPPGSEIIGKICGGISLVFRSSSNIATIKYLRTSGQRASPFHIYYYA DPEGPLPFPYFERQTIIATEKNIPIEGRAAALEHHHHHH).

The mass tolerance of precursor and sequence ions was set to 10 ppm and 0.35 Da, respectively. A maximum of two missed cleavages was allowed. Methionine oxidation and the acrylamide modification of cysteine were used as variable modifications. Peptides were used for identification if their Mascot score was greater than the homology threshold. Protein identifications were accepted if they based at least on two identified peptides.

ESI-MS analysis was performed on an Orbitrap Fusion mass spectrometer equipped with a Dionex Ultimate 3000 NCS-3500RS capillary liquid chromatography system (Thermo Scientific). The protein (33 pmol/µl) was dissolved in 20mM ammonium acetate with 3% formic acid and LC separation was performed on a capillary column (Vydac C18, 300 Å, 5mm x 300 µm i.d., Dionex) at an eluent flow rate of 300 nl/min using a gradient of 10–40% B in 15 min. Mobile phase A was 0.1% formic acid in water and mobile phase B was 0.1% formic acid in acetonitrile. Mass spectra from m/z 700-1900 were acquired with a nominal resolution of 240,000 and an AGC target value of 2^5. Scans were averaged and deconvoluted using Xtract method of the Protein Deconvolution 3.0 software (Thermo Scientific).

2.3.5 Analysis of thiol groups

AWN was checked for the presence of free thiol groups by using fluorescein-5-maleimide (Thermo Fisher Scientific, St. Leon-Rot, Germany). The substance was incubated with the protein according to the manufacturer's protocol. In brief, recombinant protein purified by the first two purification steps (see above) was transferred into pH-neutral buffer (0.15 M NaCl, 50 mM $NaPO_4$, pH 7.0) and treated with a tenfold molar excess of fluorescein-5-maleimide for 2 hours at room temperature. The solution was then applied on a HiLoad™ 26/500 Superdex 200 prep grade (GE Healthcare, Munich, Germany) size exclusion column installed in a FPLC device (Äkta Pure, GE Healthcare, Munich, Germany) using the same neutral buffer to separate unbound fluorescein-5-maleimide from the proteins. Absorbance of the eluate was detected continuously at 280 nm (total protein concentration) and 485 nm (fluorescein absorbance), the latter corresponding to proteins with bound fluorescein-5-maleimide.

2.3.6 Analysis of interaction with lipids

To characterize the interaction of recombinant AWN with lipids, the monomeric (P3, see **Figure 5**) protein fraction obtained after the three purification steps (see above) were applied on membrane lipid strips (P6002, Echelon, Salt Lake City, USA). All experimental steps were carried out at room temperature. The strips were incubated in blocking buffer (phosphate buffered saline (PBS) with 0.1% (v/v) Tween and 0.1% (w/v) Ovalbumin) for 1 h, washed three times for 5 min in 0.1% Tween-PBS and incubated with 1.5 µg/ml AWN in blocking buffer for 1 h. To detect bound protein, the strip was washed three times with 0.1% Tween-PBS and incubated for 1 h with mouse monoclonal IgG anti-penta-His antibody (Qiagen, Hilden, Germany) diluted 1:2,000 in blocking buffer. This was followed by another three washing steps in 0.1% Tween-PBS and 1 h incubation with goat anti-mouse POD antibody (Sigma-Aldrich GmbH, Taufkirchen, Germany) diluted 1:10,000 in blocking buffer. Immune reaction was detected using ECL Prime western blotting detection reagent (GE Healthcare, Munich, Germany). Spot intensities were quantified by using Quantity One software (Bio-Rad, Munich, Germany) and normalized to the spot intensity of the

blank spot. A respective control in the presence of antibodies but without AWN was performed on a separate strip.

To exclude a putative influence of the His-tag on the results, recombinant His-tagged AWN was labeled according to the manufacturer's protocol with fluorescent DyLight™ 594 NHS Ester (Thermo Fisher Scientific, St. Leon-Rot, Germany) which specifically binds to primary amines. The labeled protein was then incubated with membrane lipid strips as described before and the fluorescence was recorded using a green LED (500-570 nm) for excitation and a BP605 band pass filter for fluorescence detection. Labeling success was controlled via SDS-PAGE and fluorescence imaging.

2.3.7 Immunolocalization of recombinant AWN on washed ejaculated boar spermatozoa

Spermatozoa-rich ejaculate fractions were collected from boars (*Sus scrofa domestica*) in accordance with the rules on the care and use of domestic animals at boar stations in Brandenburg (Germany). The ejaculates were diluted to a final concentration of ~2×10^8 spermatozoa/ml with Beltsville Thawing Solution (BTS, Minitüb®, Tiefenbach, Germany), gradually cooled, stored and transferred to the lab at 17°C.

After 48 h of storage, 3 ml-aliquots of diluted ejaculates from three boars were warmed-up for 10 min at 38°C and washed three times by centrifugation (6 min, 1,200 × g, 23°C) to replace seminal fluid and BTS by PBS. Pellets were pooled and sperm concentration was determined. A 100 µl aliquot of His-AWN (~9 µM) was added to ~9×10^6 sperm in 200 µl resulting in a ratio of ~100 nmol protein per 10^9 sperm. As a control, sperm were mixed with PBS without protein. After an incubation of 1 h at 38°C, unbound protein was removed by three repetitive washing-steps in PBS (1 min, 6,000 × g, 23°C) and air-dried smears of the cells were prepared on microscopy slides.

A volume of 500 µl blocking buffer was spread over the slide which was incubated in a wet chamber for 1 h at 23°C. The solution was removed and 500 µl anti-His-antibody in blocking buffer (1:200) was added for 1 h. After rinsing (3 × 1 ml), the second antibody (1:100, rabbit anti-mouse, FITC, sc-358916, Santa Cruz Biotechnology, Inc.) was added for another hour. Slides were rinsed by PBS (4 × 1 ml) and, finally, 8 µl of 50 % (v/v) glycerol in PBS were added before covering. Respective controls were performed with only one or without an antibody.

Immunostained sperm were observed by wide-field inverted microscope (IX81, Olympus, Tokyo, Japan) with an objective (40×) under differential interference contrast or fluorescence optics for FITC (excitation band pass 485/20 nm, emission band pass 525/30).

2.4 Results

2.4.1 Expression and purification of recombinant AWN

A successful transfection of competent SHuffle® T7 *E. coli* cells with a pET-21b vector containing the AWN-coding sequence was achieved. The resulting cell line (SHuffle® T7/pET21b-AWN) produces recombinant His-tagged AWN (**Figure 4a and b**, compare lanes 1 and 2). To isolate the recombinant spermadhesin, three purification steps were performed.

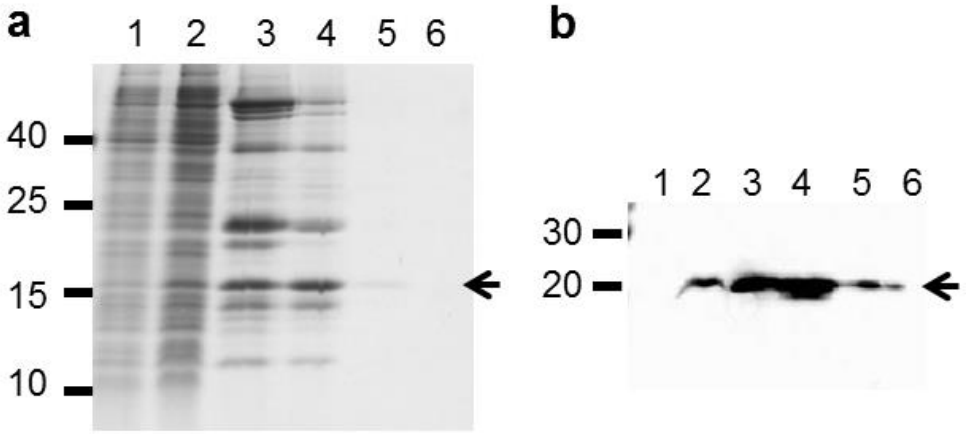

Figure 4: *SDS PAGE verifying the progress of protein expression and purification.*

The arrows indicate the position of recombinant AWN. Proteins of cell lysate before induction (1), cell lysate after induction (2), pooled fractions after His-affinity chromatography (first purification step) (3), pooled fractions after heparin-affinity chromatography (second purification step) (4), monomer fractions (5), and multimer fractions (6) obtained after size-exclusion chromatography on a Superdex200 column (third purification step) were analyzed by sensitive coomassie staining (a) and western blot (b). Molecular masses are denoted in kDa according to the different used molecular mass standards.

The first step was aimed to select for the His-tagged recombinant protein. However, the purification was not satisfactory since a number of proteins of bacterial origin also bound to the affinity column loaded with nickel ions (**Figure 4a**, lane 3). Therefore, AWN-containing elution fractions were pooled and loaded on a heparin-affinity column employing the described affinity of AWN to this substrate (Sanz et al. 1993). This resulted in improved protein purity but some bacterial proteins still remained in the eluate probably because of their heparin-affinity (**Figure 4a**, lane 4). Therefore, AWN-containing elution fractions were pooled again and applied to a size exclusion column. This method also allows to separate AWN monomers from multimers. The chromatogram of a representative run on a Superdex 200 column is shown in **Figure 5a** and revealed three peaks (P1, P2 and P3). Peaks P1 and P3 obviously contained recombinant AWN inferred from SDS-PAGE (**Figure 5b**) and western blot results (not shown). According to the molecular mass calibration with the protein standard, peaks P2 and P3 correspond to molecular masses of about 34 and 23 kDa, respectively. Peak P1, which eluted above the 600 kDa separation range of the Superdex 200

column, is probably caused by protein aggregates. It has to be noted that the use of a calibration standard containing globular proteins only allows an approximation of non-globular protein's masses because of the different migration behavior.

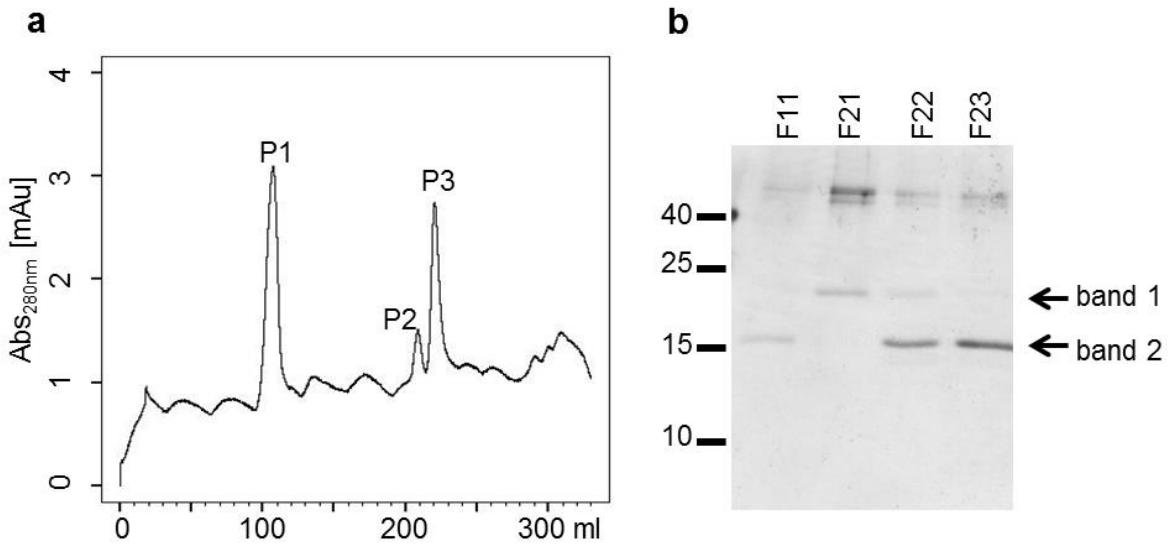

Figure 5: *Purification of recombinant AWN by size exclusion chromatography.*

The pooled eluates after second purification step (heparin-affinity chromatography) were run on a Superdex 200 column and checked for the presence of proteins by detecting the absorbance at 280 nm in arbitrary milli absorption units (mAu). Three peaks (P) were evident eluting at ~100 ml (P1, corresponding mass >600 kDa), ~ 200 ml (P2, corresponding mass ~34 kDa), and ~220 ml (P3, corresponding mass ~23 kDa) (a). The respective fractions (F) were further analyzed by SDS-PAGE and coomassie staining (b) revealing two protein bands (1 and 2) in the range of interest. F11 corresponds to elution volume 100-110 ml and F21-F23 to the three fractions eluting from 200-230 ml respectively. Note that F11, F21 and F23 contain P1, P2 and P3 respectively while F22 is intermediate between P2 and P3. Molecular masses are denoted in kDa according to the used molecular mass standard.

To analyze the protein composition of the two protein bands found between 15 and 25 kDa in the SDS-PAGE gel of some analyzed fractions (**Figure 5b**) three representative bands were excised and analyzed by mass spectrometry after trypsin digestion. All bands contained AWN, however, also some *E. coli* proteins were detected (**Table 1**).

According to the MASCOT score, AWN is more abundant in band 2 which is only prominent in fractions comprising the peaks P1 and P3 but not P2. This indicates that peak P3 primarily contains AWN monomers whereas P1 mainly consists of AWN aggregates. The proteins of the pronounced band in the fraction corresponding to peak P2 (**Figure 5b**, F21 band 1) were identified as the *E. coli* proteins cAMP-activated global transcriptional regulator CRP (CRP, molecular mass 23.6 kDa) and FKBP-type peptidyl-prolyl cis-trans isomerase SlyD (SlyD, molecular mass 20.9 kDa).

Table 1: *Mass spectrometric analysis of the protein bands shown in* ***Figure 5b****.*

The bands were excised and analyzed by mass spectrometry after trypsin digestion. Processed MS data were analyzed on a MASCOT server (version 2.2.2, Matrix Science Ltd, London) and searched in-house against a self-made database which contains the SwissProt database (version 2014_12; 547,085 sequences) and the recombinant AWN-sequence. Only AWN and proteins of E.coli origin are listed.

querries matched: number of found peptides of the corresponding protein

sequence coverage: detected amino acids/total sequence length

band	protein	MASCOT score	querries matched	sequence coverage
F11, band 2	AWN	606	33	124/162
	Alkyl hydroperoxide reductase subunit C	253	13	106/187
F21, band 1	cAMP-activated global transcriptional regulator CRP	1979	123	165/210
	FKBP-type peptidyl-prolyl cis-trans isomerase SlyD	409	12	91/190
	AWN	87	4	65/162
F23, band 2	AWN	976	60	130/162
	Ferric uptake regulation protein	179	4	60/148

ESI-MS was performed to further characterize the protein solution (**Figure 6**). A protein with an averaged mass of 17.820 kDa was detected. The difference to the calculated recombinant protein mass of 17.953 kDa can be explained by the activity of methionine aminopeptidase from *E.coli*, cleaving the N-terminal methionine from the protein (Xiao et al. 2010) and resulting in a calculated averaged mass of 17.821 kDa. This is in agreement with the LC-MS/MS results, were the protein fragments also lacked the first methionine.

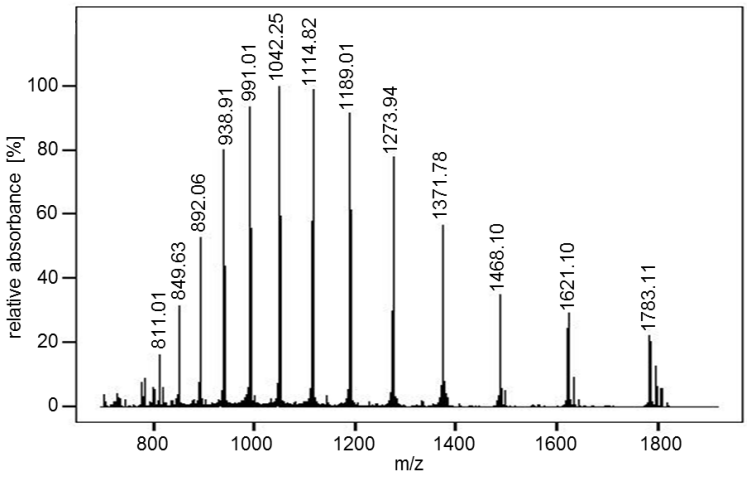

Figure 6: *ESI-MS spectrum of three step purified recombinant AWN.*

The peaks are labeled with their mass/charge ratios and correspond to an ion series with charges between 10 (m/z = 1783.11) and 22 (m/z = 811.01).

2.4.2 Determination of free thiol groups in recombinant AWN

According to the proposed tertiary structure, AWN should have two disulphide bridges but no free thiol groups (Sanz et al. 1992d). Here, AWN containing protein pools purified with the first two (His- and heparin-affinity) purification step were incubated with fluorescein-5-maleimide to detect free thiol groups. The protein-bound label was separated from unbound maleimide by size exclusion chromatography on a Superdex 200 column (**Figure 7a**). The absorbance of the eluate was recorded at 280 nm (for protein) and at 485 nm (for fluorescein). Based on the extinction coefficients for AWN (ε_{280} of about 20,000 $M^{-1}cm^{-1}$) and for fluorescein-5-maleimide (ε_{485} of about 80,000 $M^{-1}cm^{-1}$), the amount of protein-bound maleimide was determined and gives an estimate of free cysteine residues in one AWN molecule.

Figure 7: *Test for free thiol groups.*

AWN was purified by His- and heparin-affinity chromatography before it was incubated with fluorescein-5-maleimide and separated on a Superdex 200 size exclusion column (a). Peaks correspond to proteins above 600 kDa (P1), ~32 kDa (P2), ~25 kDa (P3), free fluorescein-5-maleimide (P4), free fluorescein (P5). The solid curve denotes the absorbance at 280 nm corresponding to the protein concentration while the dashed curve represents the fluorescein-5-maleimide fluorescence at 485 nm. Inlets show the enlarged region encompassing P2 and P3. The corresponding western blot (b) is shown below the chromatogram. F21-F25 correspond to the five fractions between elution volume 200 and 250). Molecular masses are denoted in kDa according to the used molecular mass standard.

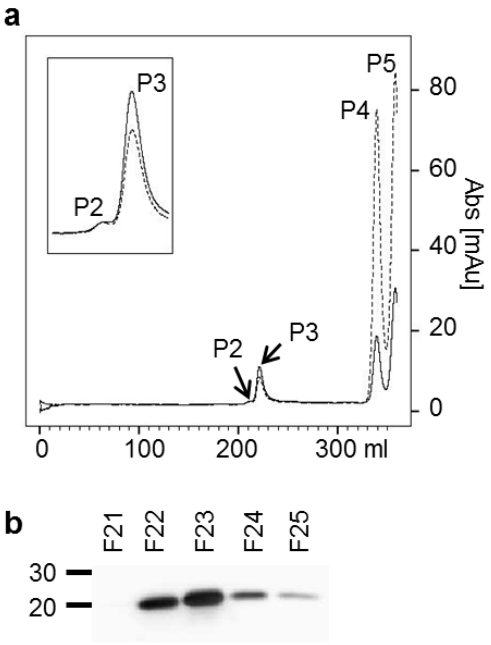

Peaks corresponding to P2 and P3 (see **Figure 5**) appeared in the size exclusion chromatography of the protein incubated with fluorescein-5-maleimide and were named respectively. The fluorescein absorbance in the range of P3 containing the monomeric AWN was lower than the absorbance at 280 nm (molar ratio fluorescein : AWN about 0.18) indicating that the majority of the AWN molecules in this fraction does not contain free thiol groups, but possesses formed disulphide bridges (**Figure 7a**). The region of peak P2 showed a relatively higher level of fluorescein absorption compared to the protein absorption, indicating a stronger presence of free thiol groups which probably originate from *E. coli* proteins in this peak (see above). Peak P1 containing multimeric AWN was absent in the size exclusion chromatogram of the protein incubated with maleimide. The presence of AWN in the respective fractions was verified by western blot analysis (**Figure 7b**).

The peaks P4 and P5 shown in **Figure 7a** correspond to molecular masses of unbound fluorescein-5-maleimide and fluorescein, respectively. The absorbance detected at 280 nm for both signals is probably caused by the broad absorption spectrum of fluorescein interfering with this wavelength range.

2.4.3 Interaction of recombinant AWN with lipids

To search whether recombinant AWN interacts with lipids, monomeric AWN obtained after three purification steps (see above) was incubated with membrane lipid strips. **Figure 8** shows that the protein selectively interacts with phosphatidic acid (PA) and at a lower level with cardiolipin. No staining caused by the used antibodies was observed in the absence of AWN (**Figure 8b**). After labeling the recombinant AWN with fluorescent DyLight 594 NHS Ester, the protein still showed an interaction with cardiolipin, but no affinity to PA could be observed (**Figure 9**)

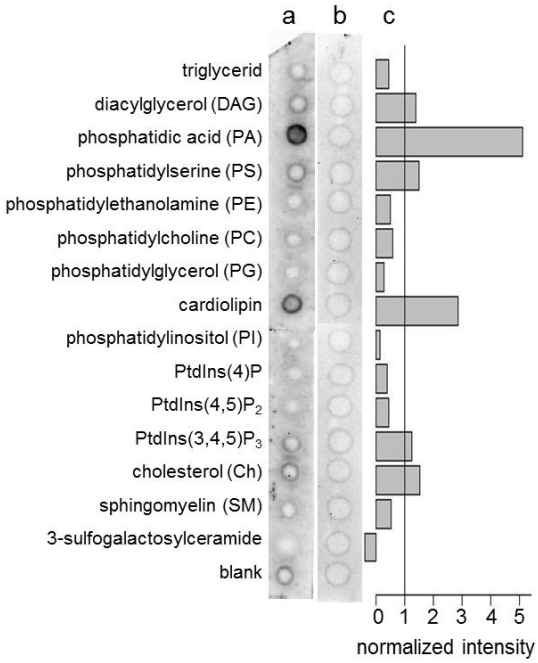

Figure 8: *Interaction of recombinant AWN with lipids.*

Lipid strips were incubated with monomeric AWN (a) obtained after three-step purification. As control, strips were incubated in buffer without AWN (b). Recombinant AWN was detected via immunoaffinity for its His-tag. The intensities of the spots in (a) were quantified by Quantity One and normalized to the intensity of the blank (c).

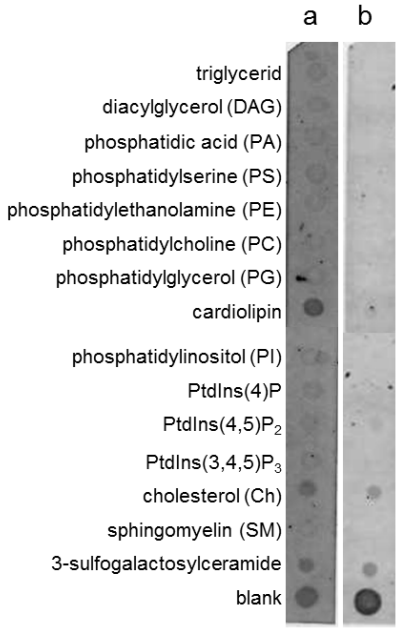

Figure 9: *Interaction of fluorescence labeled recombinant AWN with lipids.*

Lipid strips were incubated with monomeric AWN (a) obtained after three-step purification and labeled with DyLight™ 594 NHS Ester. As control, the fluorescence of untreated strips was imaged (b). Note that fluorescence signals at blank, cholesterol and 3-sulfogalactosylceramide were also present in the protein free control (b).

2.4.4 Immunolocalization of recombinant AWN on ejaculated boar spermatozoa

Immunolocalization of His-tagged AWN incubated with thoroughly washed ejaculated boar spermatozoa revealed a punctual distribution over the acrosomal head region of single spermatozoa (**Figure 10**, white arrows). Labeling was only detected in spermatozoa with membrane remnants visible under differential interference contrast optics, however, not all of those cells were labeled. AWN immunostaining could not be detected on spermatozoa with completely removed acrosome (characterized by an eggcup shape of the head).

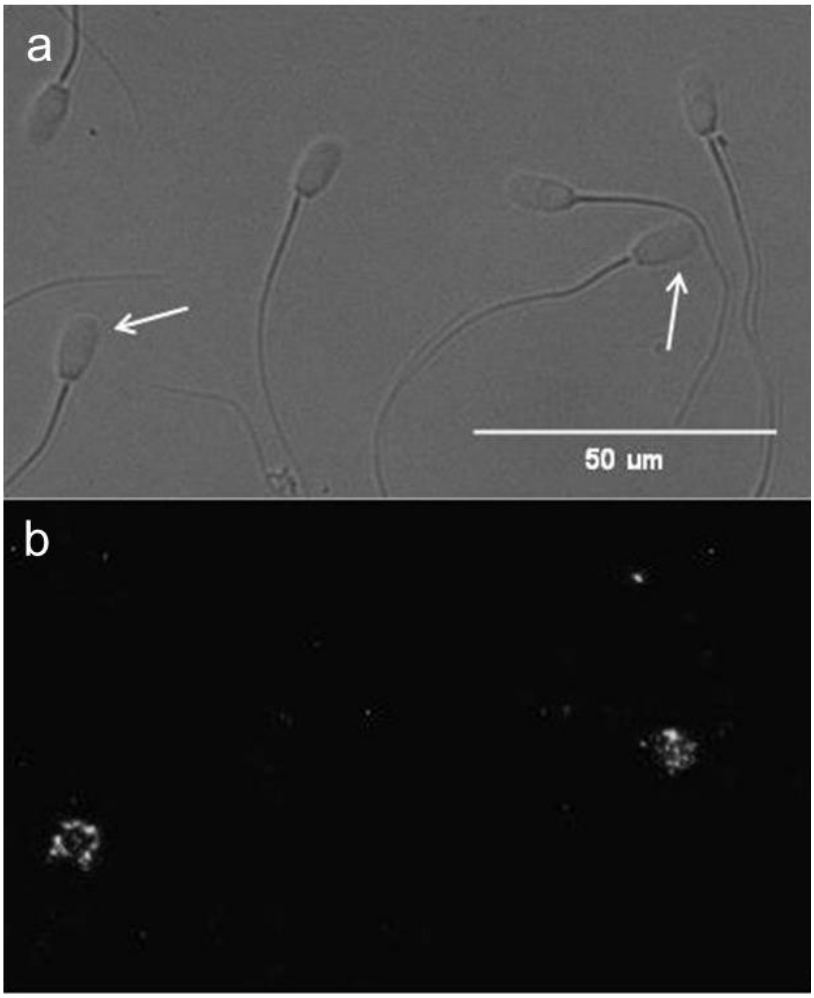

Figure 10: *Immunolocalization of recombinant AWN on washed ejaculated boar spermatozoa*

Ejaculated boar spermatozoa were washed and incubated with his-tagged recombinant AWN before immunostaining by anti-His-antibody and a FITC-labeled second antibody. A differential interference contrast image (a) as well as the corresponding green fluorescence (FITC) (b) are presented. Fluorescence was found to be distributed over the acrosomal head region of single sperm with adhering membrane remnants (white arrows).

2.5 Discussion

Here, we generated a transfected *E. coli* strain and produced for the first time recombinantly expressed porcine spermadhesin AWN. This expands the range of recombinant spermadhesins already including Bodhesin-2 from goat (Cajazeiras et al. 2009) porcine AQN-1 and bovine spermadhesin-1 (referred to as aSFP, Ekhlasi-Hundrieser et al. 2008a). A three step protocol was successfully developed to purify this His-tagged AWN in sufficient purity for functional studies.

2.5.1 Recombinant protein expression and purification

To select AWN from the mixture of proteins harvested from cultured transfected bacteria three purification steps were successfully applied. The first step employs the binding of the accessible His-tag to the matrix loaded with nickel ions. The second purification step is based on the affinity of the heparin binding site of AWN to the used heparin-matrix (Sanz et al. 1993, Calvete et al. 1996a). The analysis of His- and heparin-purified protein fractions revealed that not only recombinant AWN, but also *E.coli* proteins were present in the eluate after these purification steps (see **Table 1** and **Figure 5b**, F21 band 1). The mascot score of these bacterial proteins after LC-MS/MS (**Table 1**) imply that these proteins are minor contaminations of the purified protein solution. SlyD, CRP and Ferric uptake regulator (Fur, **Table 1**, F23, band 2) are all known to be co-purified during immobilized metal affinity chromatography (IMAC) (Bolanos-Garcia and Davies 2006) that we used for the first purification step. Notably, these proteins are still present after the second purification step on a Heparin-column as observed from the analysis of the proteins in these fractions. This could be caused by their sequences/structures that not only contain His-rich motifs but also similarities to heparin-binding domain consensus sequences (Bolanos-Garcia and Davies 2006, Cardin and Weintraub 1989, Fromm et al. 1997). Another reason might be an association between the recombinant AWN and the aforementioned proteins of the prokaryotic host.

The size exclusion chromatography of prepurified AWN allowed a partial separation of these contaminating *E.coli* proteins as well as partitioning of a monomeric (P3) and a multimeric (P1) AWN form for further studies. The absence of a multimeric peak after fluorescein-5-maleimid reaction of AWN indicates that cystein residues not involved in disulphide bridges might have a role in the formation of this multimer. An equilibrium between aggregated and monomeric AWN extracted from the seminal plasma was already reported (Dostalova et al. 1995b).

Whether glycosylation of AWN is essential for its multimer formation *in vivo* cannot be answered as the used recombinant expression system (prokaryotic cells) is unable to add this posttranslational modification. Even though glycosylation influences the binding affinity of AWN to zona pellucida proteins and a trypsin inhibitor (Calvete et al. 1994) as well as to other carbohydrates, it does not influence heparin- or phospholipid-binding (Töpfer-Petersen et al. 2008) and occurs at positions offside the potential phospholipid binding domain (Calvete et al. 1994, Ekhlasi-Hundrieser et al.

2008a). We therefore conclude that our lipid binding study was not influenced by the lack of this posttranslational modification. While the glycosylated isoforms of AWN have been shown to originate from the seminal vesicles (Calvete et al. 1994) *in vivo*, the majority of AWN is non-glycosylated, particularly AWN of epididymal origin (Calvete et al. 1994). Therefore, our non-glycosylated recombinant protein should be useful to enlighten many potential functions.

We used fluorescein-5-maleimide to target and detect free thiol residues in the recombinant AWN after the second purification step. The majority of the cysteine residues of monomeric AWN did not react. Therefore, the utilized special *E.coli* strain, providing non-reductive conditions in the cytoplasm, seems to be indeed appropriate to express the recombinant protein with intact disulphide bridges.

2.5.2 Phospholipid binding of AWN

One main open question so far addresses the interaction of AWN with the sperm membrane, most likely being mediated by its phospholipid binding site. Therefore the first functional study we did with our recombinantly expressed protein was the search for a lipid binding partner using lipid strips.

We clearly detected a strong affinity of the monomeric recombinant AWN for PA and on a lower level for cardiolipin. Since cardiolipin seems to be exclusively synthesized in mitochondria of mammals (Schlame et al. 2000) and seems to be almost exclusively present in the inner and outer membrane of this organelle in eukaryotic cells (Schlame 2008) we suggest PA as the potential AWN ligand in the cell membrane of sperm. Our recombinant AWN did neither bind to phosphatidylcholine (PC) nor phosphatidylethanolamine (PE). This is in contrast to results of other groups (Enßlin et al. 1995, Jonakova et al. 2000, Dostalova et al. 1995b), but since the lipid strip assay presents the whole lipids instead of the head group and the other groups did not test PA, our findings do not really contradict but expand those of others observed with AWN.

The sequence of recAWN differs from naturally occurring AWN by N- and C-terminal extensions, which are spatially close in the proposed 3D-structure of the protein. However, these extensions lack stretches rich in arginine or lysine which are proposed as consensus characteristic for PA binding motives. We therefore conclude that they are not likely to form an epitope interacting with this lipid.

Our recombinant protein furthermore differs from native AWN by possessing a His-tag. After being labeled with DyLight™ 594 NHS Ester, His-AWN lost its affinity to PA while retaining cardiolipin binding. This indicates that the His-tag is not responsible for the observed PA binding. Rather, the PA binding site of the protein is obviously blocked by labeling with the fluorophore. NHS ester covalently binds primary amines, especially at the N-terminus, as well as lysine residues. Furthermore it was shown, that NHS esters can also react with unprotonated arginine (McGee et al.

2012), as well as serine, threonine and tyrosine in the vicinity of histidine (Mädler et al. 2009, Miller et al. 1997). From these studies, it can be concluded that the His-Tag should not react with the fluorophore. However, we cannot exclude that the observed cardiolipin binding of His-AWN is an artifact caused by the His-tag.

It was reported that aggregated AWN and AQN-3 isolated from porcine seminal plasma did neither bind to POC agarose nor to POE agarose columns while only a fraction of non-aggregated spermadhesins were eluted from the POE matrix (Dostalova et al. 1995b). To identify the localization of the phospholipid binding site, overlapping synthetic AWN fragments were applied on POE affinity columns where peptides consisting of the amino acids 1-12 and 104-108 showed a delayed elution (Enßlin et al. 1995). On the other hand, an interaction of AWN with a biotinylated polyacrylamide derivative of POC in an enzyme linked binding assay (ELBA) was reported (Jonakova et al. 2000). Regarding these controversial results it might be possible that a fraction of the presented phospholipid head groups were degraded thus only presenting their phosphate groups and mimicking PA. Focusing on the mechanism for AWN-PA binding it is noteworthy that the aforementioned AWN fragment 1-12 contains a loop with three arginines at position 4, 5 and 7 providing positive charges as well as hydrogen bonding donor groups able to interact with the phosphate group of PA. A further implication for the position of the binding site is the possibility to elute AWN bound to a heparin matrix by the use of POC (Jonakova et al. 1998), since the sequence 3-8 (NRRSRS) also resembles the heparin binding consensus sequence (Cardin and Weintraub 1989, Fromm et al. 1997). Note that this unbound form of the POC head group presents its phosphate at a terminal position quite similar to PA. Notably cardiolipin consists of two phosphatidic acids connected by a glycerol backbone and forms a bicyclic structure presenting the phosphate groups in a way resembling that of PA. Both lipids have been shown to be present in total lipid content of ejaculated boar spermatozoa without significantly changing their concentration after capacitation *in vitro* or *in utero* (Evans et al. 1980).

The fact that the recombinant protein does not express a comparable affinity to other negatively charged phospholipids like phosphatidylserine (PS) or phosphatidylinositol (PI) and its phosphorylated variants (phosphatidylylinositol-4-phosphate (PtdIns(4)P), phosphatidylinositol-4,5-bisphosphate (PtdIns(4,5)P_2) and phosphatidylinositol-3,4,5-trisphosphate (PtdIns(3,4,5)P_3)) implies that this interaction is indeed specific and not exclusively based on the head group charge. A reason for this selectivity towards PA might be the terminal position of its phosphate group and its pronounced ability to form intermolecular hydrogen bonds (Boggs 1987).

It has been shown that addition of PA to mouse sperm cells led to rapid actin polymerization causing hyper-activated motility, a movement pattern observed at the site and time of fertilization (Itach et al. 2012). Furthermore it is an important precursor in *de novo* phospholipid synthesis, which is still active in sperm cells (Vazquez and Roldan 1997). PA also seems to play an important

role in membrane fusion events. Vesicle membranes containing anionic lipids fused upon contact to divalent cations (Papahadjopoulos et al. 1978) which was also shown *in vitro* for vesicles consisting of PC and PA (Simmonds and Halsey 1985, Koter et al. 1978). The initiation of fusion is hypothetically triggered by calcium induced phase transitions of acidic lipids creating disorganized lipid arrays (Papahadjopoulos et al. 1978). PA as well as cardiolipin are known to form the hexagonal II phase in dependence of pH and the presence of divalent cations (Verkleij 1984). This kind of lipid organization has been linked to membrane fusion and acrosome reaction of sperm cells (Martinez and Morros 1996). Notably the immunolocalization of recombinant AWN in the anterior region of the head (**Figure 10**) showed similarity to the localization of natural AWN on sperm cells (Töpfer-Petersen et al. 1995). The rare labeling pattern indicates that the respective membrane binding partners were either inaccessible, lost by the immunostaining procedure and/or natural AWN molecules were not sufficiently removed from ejaculated spermatozoa by washing.

According to its affinity for PA, AWN could mask the anionic charge of these lipid molecules to prevent calcium induced phase transitions and creation of disorganized lipid arrays which would result in premature membrane destabilization. Since AWN is able to bind zona pellucida glycoproteins by a binding site not overlapping with the proposed phospholipid binding site (Calvete et al. 1994, Ekhlasi-Hundrieser et al. 2008a) the contact with the zona pellucida could trigger the release of AWN from the sperm. This would then lead to the uncovering of the anionic phospholipids and initiate their phase transition which precedes the acrosome reaction. Notably a study of Rodriguez et al. (Rodriguez-Martinez et al. 1998) reported the presence of AWN on plasmalemma remnants of spermatozoa bound to the zona pellucida of naturally mated sows *in vivo*. Further studies on spermatozoa and artificial membranes would be useful as well to elucidate the functional sequence of AWN-membrane interaction.

2.6 Conclusions

For the first time, the porcine spermadhesin AWN was recombinantly expressed in *E. coli*. A three step protocol was developed to purify His-tagged AWN for functional studies. A high and selective affinity of the monomeric protein for PA on lipid strips was observed and the recombinant AWN interacted with sperm cells. The recombinant expression offers a broad range of potential applications of AWN not only in functional studies but also in assisted reproduction. This is particularly important in the field of species conservation breeding where predominantly epididymal sperm deficient in seminal plasma are available from dead or euthanatized males for gamete banking and artificial insemination.

Acknowledgements

We thank Michael Schümann and Heike Stephanowitz (Leibniz Institute for Molecular Pharmacology, Berlin, Germany) for carrying out the ESI-MS analysis. We would furthermore like

to thank Nina Dommaschke and Sandra Augustin (Leibniz Institute for Zoo and Wildlife Research, Department Reproduction Biology, Berlin, Germany) for their assistance in the recombinant expression and purification of AWN.

Conflict of interest statement

We hereby declare that we have no conflict of interest regarding this publication.

Chapter 3: Lipid dynamics in boar sperm studied by advanced fluorescence imaging techniques

3.1 Summary

The studied combination of different microscopic methods provided a comprehensive picture of lipid dynamics in the cell membrane of vital sperm even if conclusions from each individual method are limited within each temporal and spatial window.

It was the first time that fluorescence lifetimes of lipid analogs were measured in spermatozoa and determined in a range characteristic for the liquid-disordered phase in artificial lipid membranes. Severe differences in the diffusion coefficients measured by FCS and FRAP were encountered and discussed. It had to be concluded that FRAP leads to a severe underestimation of lipid mobility caused by aberrations resulting from the small size of the used bleach spot.

The results underlined the potential to extract information about different membrane environments by the usage of the aforementioned labeled lipids.

Author contributions

Filip Schröter: project design, preparation of sperm samples, FRAP and FLIM measurements, documentation of experiments, analysis and interpretation of result, writing of the manuscript

Karin Müller, Peter Müller: project design and supervision

Anke Teichmann: FCS measurements and data analysis.

Burkhard Wiesner: FRAP data interpretation and calculation of diffusion coefficients

Ivan Haralampiev: supplementary experiments regarding the phase incorporation of NBD-SM

All authors were involved in discussing data as well as preparing and correcting the manuscript.

Lipid dynamics in boar sperm studied by advanced fluorescence imaging techniques

Filip Schröter[1*], Ulrike Jakop[1], Anke Teichmann[2], Ivan Haralampiev[3], Astrid Tannert[1], Burkhard Wiesner[2], Peter Müller[3], Karin Müller[1*]

[1]*Leibniz Institute for Zoo and Wildlife Research, Dept. Reproduction Biology, Berlin, Germany*

[2]*Leibniz Institute for Molecular Pharmacology, Berlin, Germany*

[3]*Humboldt-University Berlin, Department of Biology, Berlin, Germany*

Abstract

The (re)organisation of membrane components is of special importance to prepare mammalian sperm to fertilization. Establishing suitable methods to examine physico-chemical membrane parameters is of high interest. We characterized the behavior of fluorescent (NBD) analogs of sphingomyelin (SM), phosphatidylserine (PS) and cholesterol (Ch) in the acrosomal and postacrosomal macrodomain of boar sperm. Due to their specific transverse membrane distribution, a leaflet specific investigation of membrane properties is possible. The behavior of lipid analogs in boar sperm was investigated by fluorescence lifetime imaging microscopy (FLIM), fluorescence recovery after photobleaching (FRAP), and fluorescence correlation spectroscopy (FCS). The results were compared with regard to the different temporal and spatial resolution of the methods. For the first time, fluorescence lifetimes of lipid analogs were determined in sperm cell membrane and found to be in a range characteristic for the liquid disordered phase in artificial lipid membranes. FLIM analyses further indicate a more fluid microenvironment of NBD-Ch and NBD-PS in the postacrosomal compared to the acrosomal region. The concept of a more fluid cytoplasmic leaflet is supported by lower fluorescence lifetime and higher average D values (FCS) for NBD-PS in both head compartments. Whereas FLIM analyses did not indicate coexisting distinct liquid ordered and disordered domains in any of the head regions, comparisons between FRAP and FCS measurements suggest the incorporation of NBD-SM as well as NBD-PS in postacrosomal subpopulations with different diffusion velocity. The analog-specific results indicate that the lipid analogs used are suitable to report on the various physicochemical properties of different micro-environments.

Keywords: boar sperm, acrosome, postacrosome, fluorescence lifetime imaging microscopy, fluorescence recovery after photobleaching, fluorescence correlation spectroscopy

3.2 Introduction

Mammalian sperm undergo a multitude of complex processes during their maturation which finally prepare them to fertilize the oocyte. After formation in the testis and passing through the epididymis, sperm still have an inchoate competence for fertilization. Upon ejaculation they are decorated with proteins priming them for transit through the female genital tract where they have to

adapt to changing environmental conditions. At these final steps of maturation, while becoming prepared for the fertilization event, sperm are not able to express proteins on their own (Mackie et al. 2001). Therefore, all necessary adaptations must occur via incorporation of external components or reorganisation of existing cellular molecules and structures. As the (re)organisation of membrane components of the sperm membrane is of special importance to understand the processes which are prerequisite to fertilization, the establishment of suitable methods to examine physico-chemical membrane parameters is of high interest.

Although mammalian sperm of different species perform similar functions, the membrane lipid composition is highly heterogenic (Lessig et al. 2004a, Fuchs et al. 2009). Therefore, it is a challenge for any measurement to apply probes that mimic ubiquitous membrane components and have a minimal influence on the membrane itself. Studies on sperm have mainly used fluorescently labeled lipids and lipid analogs. Fluorescent phosphatidylcholine (NBD-PC), phosphatidylethanolamine (NBD-PE) and cholesterol (NBD-Ch) as well as artificial lipid reporters like 5-(N-octa-decanoyl) aminofluorescein (ODAF), 1,1'-didodecyl-3,3,3'3'-tetramethylindocarbocyanine ($DiIC_{12}$) and 1,1'-dihexadecyl-3,3,3'3'-tetramethylindocarbocyanine ($DiIC_{16}$) have been applied to analyze diffusion coefficients in sperm of several species by fluorescence recovery after photobleaching (FRAP). Dependent on the species, diffusion of these probes may differ between sperm regions and change upon sperm maturation in the epididymis, after removal of cholesterol or after addition of hydroperoxides (for review see Jones et al. 2007, Jones et al. 2010).

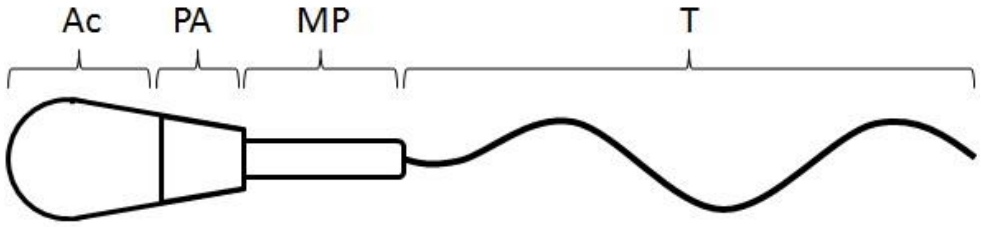

Figure 11: *Schematic image of the lateral organization of mammalian sperm.*

Ac: acrosomal region, PA: postacrosomal region, MP: midpiece, T: tail.

Mammalian sperm are strongly laterally organized cells (**Figure 11**). Especially the properties of the acrosomal and postacrosomal region during cell maturation have been characterized. In ejaculated boar sperm it has been shown by fluorescence recovery after photobleaching (FRAP), fluorescence loss in photobleaching (FLIP), atomic force microscopy (AFM) and single particle fluorescence imaging (SPFI) that a "molecular filter" separates the postacrosomal from the acrosomal macrodomain of the sperm head (Jones et al. 2010, James et al. 2004): Whereas $DiIC_{12}$ was freely diffusible between the anterior and posterior head membrane, $DiIC_{16}$ formed aggregates of 0.3-1.0 µm in diameter which only rarely crossed the equatorial segment. The lateral

heterogeneity of plasma membrane components by formation of microdomains and its relevance for physiological processes has been investigated intensively in mammalian cells, and is currently also under investigation for mammalian sperm (Kawano et al. 2011). Diffusion characteristics and their local variation in response to external stimuli, may play a crucial role in the formation of this lateral membrane structures and can be studied amongst others by FRAP.

Whereas SPFI is mainly restricted to proteins and lipid aggregates, there are further fluorescence methods besides FRAP which allow gathering information on parameters of membrane inherent lipid markers as for example fluorescence correlation spectroscopy (FCS) and fluorescence lifetime imaging microscopy (FLIM). Each of these methods has a different temporal and spatial resolution so that the information gained can be interpreted as snapshot of the conditions over a defined time period and area (see below).

Experiments with FRAP are carried out by irreversibly bleaching the fluorophores in a defined bleaching spot and detecting the recovery rate of fluorescence. Thereby a diffusion coefficient of the fluorophore can be calculated. The size of bleaching spots has a dimension of micrometers in diameter and bleaching times of 5-50 milliseconds are used. Measurements with this technique are usually performed within seconds with the data points most relevant for fitting the recovery curve being collected within the first two seconds.

FCS measures fluorescence fluctuation in a very small volume thus detecting the changes in fluorescence intensity caused by Brownian motion of the fluorophores. These data allow amongst others the calculation of diffusion coefficients of the fluorescent molecules. The detected diffusion times in the confocal volume (ω_1(488 nm) = 230 nm) are in the dimensions of milliseconds.

The measurement of fluorescence lifetime mainly provides information on the immediate vicinity of the examined fluorophore and depends particularly on mobility and polarity of its surroundings. If the fluorophore possesses a dipole moment in the ground state that changes upon excitation, as NBD does, a red shift of the emission spectrum in polar solvents can be detected. This is caused by the reorientation of the surrounding polar solvent molecules to realign the dipole moments. While this reorientation/relaxation process does not significantly affect the fluorescence lifetime in fluid environments, it does when the viscosity of the surroundings is high. Since the speed of the relaxation crucially depends on the movement of the involved molecules, an increased environmental fluidity decreases the fluorescence lifetime by shortening the relaxation process. Along the vertical axe and horizontal plane of a membrane, different micro-environments varying in mobility and polarity exist (de Almeida et al. 2009, Amaro et al. 2014).

Since the abundance and distance of possible interaction partners like said polar solvent molecules or quencher molecules also affects the fluorescent lifetime, FLIM enables the investigation of

domain formation by tracing interactions between reporter molecules and their surroundings whereas FRAP and FCS mainly address the diffusion properties of reporter molecules.

Fluorescence lifetime measurements reflect the environmental conditions of labels in a very short time frame (nanoseconds). However, it is important to note that the fluorescence lifetimes of all fluorophores in a given membrane area are recorded over a longer period (microseconds per pixel). Only if substantial structural inhomogeneities lead to explicit lifetime differences for embedded label molecules and are stable over a time period of about three times their fluorescence lifetime, they might be detected down to a size of about 10 nm^2 (Stöckl et al. 2008).

Here, we have characterized the behavior of fluorescent (NBD) analogs of SM, PS, and Ch in the acrosomal and postacrosomal macrodomain of boar sperm. Although these analogs have a short fatty acyl chain and an artificial NBD moiety, they have been successfully employed to investigate the role of lipids for various biological processes, such as transbilayer movement of lipids, lipid-protein interactions, lipid-bile salt interactions and intracellular transport processes of lipids (Wüstner et al. 1998, Pomorski et al. 1994, Wüstner et al. 2001, Eckford and Sharom 2005, Kol et al. 2003, Im et al. 2004, Tannert et al. 2007a). It has been shown that these analogs - albeit with certain limitations (Haldar and Chattopadhyay 2013, Wüstner 2007) - reflect properties of the respective endogenous lipids. E.g. they have been used for characterizing the transbilayer distribution and mobility in plasma membranes of numerous cells. Those measurements have shown that NBD-SM is exclusively localized in the outer membrane leaflet. In contrast NBD-PS is rapidly transported to the inner membrane leaflet accumulating in this layer (Zachowski 1993). This behavior of NBD-SM and NBD-PS has also been shown in the plasma membrane of sperm cells including those of the boar (Müller et al. 1994, Gadella et al. 1999, Kurz et al. 2005, Nolan et al. 1995). Notably, these transbilayer characteristics of phospholipid species has been found by other approaches also using differently labeled analogs (Daleke 2003, Pomorski et al. 2001, Zachowski 1993). For NBD-Ch, a very rapid, protein-independent transbilayer movement and a symmetrical transverse distribution can be assumed (Müller et al. 2011). Moreover, NBD-labeled lipid analogs have also been successfully applied especially for FLIM (Ostasov et al. 2013, Stöckl et al. 2008, Klein et al. 2012) and FRAP analysis (Pucadyil et al. 2007, Christova et al. 2004).

Membrane fluidity and domain formation in the acrosomal and postacrosomal part of the mammalian sperm cell membrane are key elements for membrane stabilization before and creation of fusion competence after capacitation. Therefore, the behavior of the NBD-labeled lipid analogs in boar sperm was investigated by performing FLIM, FRAP, and FCS measurements. An advantage of using these reporter molecules is that due to their specific transverse distribution in the membrane, a leaflet specific investigation of membrane properties is possible. The results obtained by the various methods were critically compared with regard to their different temporal and spatial resolution reflecting different organizational membrane structures or properties in vital cells. The

outcome of the presented approaches in ejaculated sperm is prerequisite to their further application examining the diverse sperm membrane interactions with molecules in seminal fluid, female genital tract as well as changes during capacitation and further stages of the fertilization process.

3.3 Material and Methods

3.3.1 Material

All chemicals and solvents were obtained in the highest commercially available purity. NBD-labeled lipids were purchased from Avanti Polar Lipids (Birmingham, AL, USA): N-[6-[(7-nitro-2-1,3-benzoxadiazol-4-yl)amino]caproyl]-sphingosylphosphocholine (NBD-SM), 1-Acyl-2-[6-[(7-nitro-2-1,3-benzoxadiazol-4-yl)amino]caproyl]-*sn*-glycero-3-phosphatidylserine (NBD-PS), 25-[N-[(7-nitro-2-1,3-benzoxadiazol-4-yl)methyl]amino]-27-norcholesterol (NBD-Ch). Beltsville *thawing* solution with (BTS+) and without antibiotics (*BTS*) was obtained from Minitüb GmbH (Tiefenbach, Germany). Propidium iodide (PI) was purchased from Invitrogen Life Technologies GmbH (Darmstadt, Germany). Agarose with a gelling temperature of 36 ± 1.5°C for immobilization of the sperm was obtained from Carl Roth GmbH + Co. KG (Karlsruhe, Germany).

3.3.2 Labeling of sperm

Sperm-rich ejaculate fractions were collected from fertile boars (*Sus scrofa domestica*, race Piétrain or Duroc) in accordance with the rules on the care and use of domestic animals at commercial boar stations in Brandenburg (Germany). The ejaculates were diluted to a final concentration of 2.2×10^8 sperm / ml with BTS+ composed of 10 mM KCl, 20.4 mM trisodium citrate, 15 mM $NaHCO_3$, 3.36 mM EDTA, 205 mM glucose, and antibiotics, pre-warmed to 38°C. The prepared sperm were then gradually cooled, transported and stored at 17°C until use within 24 h after collection. 12.5 ml of diluted boar ejaculate were transferred into falcon tubes and incubated for 10 minutes at 38°C followed by 6 minutes centrifugation at 750 x g at room temperature with reduced acceleration and deceleration (accel/decel 4/4, Biofuge Stratos, Heraeus). The pellet was carefully resuspended in 1 ml BTS, transferred into a 1.5 ml Eppendorf tube and centrifuged at 500 x g at room temperature (Biofuge fresco, Heraeus). The pellet was resuspended in 100 µl BTS containing approximately 2.4×10^8 sperm. All subsequent measurements were performed within 3 hours to preserve a high viability of the sperm.

NBD-labeled lipids were stored as chloroform solutions at -20°C. For usage, the chloroform was evaporated in a nitrogen flow and the NBD-labeled lipids were dissolved in BTS as stock solutions by mixing with a vortex. In case of NBD-PS and NBD-SM the stock solutions had a concentration of 400 µM. Labeling of cells with NBD-Ch was performed by using methyl-β-cyclodextrin. The NBD-Ch stock solution consisted of 36 µM NBD-Ch, 1 mM methyl-β-cyclodextrin and 500 µM cholesterol in order not to modify the cholesterol content of the cells during labeling. Cells were labeled by mixing 50 µl sperm suspension with 10 µl (NBD-SM, NBD-PS) or 50 µl (NBD-Ch) of

the stock solutions followed by an incubation in the dark at room temperature for 5 minutes (NBD-SM) or 15 minutes (NBD-PS, NBD-Ch). Subsequently, 1 ml of BTS was added and cells were washed by centrifugation (6 minutes, 500 x g, room temperature). The resulting pellet was resuspended in 50 µl BTS.

Ten µl of the labeled sperm were mixed with 500 µl BTS solution and, for FLIM measurements, 2.5 µl PI. PI served as a marker for non-vital cells. Agarose solution (0.5% in BTS) was melted by cooking, cooled down to 38°C and mixed with the prewarmed (38°C) NBD- and PI-labeled sperm. 7.5 µl of the mixture were applied on an object slide for the measurements. Cooling the slide to room temperature triggered gelation of the agarose and therefore, an immobilization of embedded sperm which allowed to perform the fluorescence measurements. Even at 38°C the sperm were sufficiently immobilized due to the high viscosity of the fluid agarose. Because of the potential cytotoxicity of PI, sperm were used for a maximum of 30 minutes after PI staining.

The FLIM, FRAP, and FCS measurements were carried out at ambient room temperature (RT, 26.3 ± 1.5°C). FLIM measurements were additionally performed in a tempered acrylic glass box at 38°C to examine the extent of temperature-related changes of fluorescence lifetime upon cooling to RT. Chromatographic analyses of organic sperm extracts revealed that the enzymatic degradation of NBD-PS as well as NBD-SM was negligible in the time frame of the experiments (not shown).

3.3.3 Analysis of transversal membrane distribution of NBD-cholesterol

Sperm were labeled by NBD-Ch as described above (15 minutes incubation with NBD-Ch followed by centrifugation and resolution of the cell pellet). Twenty, 45, and 65 minutes after start of the labeling procedure, an aliquot of the resolved pellet (10 µl) was transferred into 240 µl BTS at 38°C and after addition of 2.5 µl PI incubated for 5 minutes. An aliquot of stained sperm suspension (~0.25 x 10^6 sperm) was diluted in 2 mL BTS at 38°C for measurement in a flow cytometer (CyFlow space and Flowmax software, Partec, Germany) equipped with a 50 mW solid-state laser (Ex 488 nm), a 515-560 nm band-pass for NBD (green), and a 620 nm long-pass filter for PI (red). The system was triggered on the forward light scatter, and 15,000 cells per sample were characterized for their fluorescence at a flow rate of about 250 cells per second. After gating sperm signals by forward and sideward light scatter, mean intensity of NBD fluorescence was determined for vital and non-vital (PI-positive) cells. The measurement was repeated in the presence of 25 mM sodium dithionite added from a cold stock solution (1 M in 100 mM Tris-buffer, pH 10). The initial quenching of accessible NBD-Ch molecules i.e. decrease of fluorescence intensity was recorded after 0.5 minutes co-incubation with dithionite and the progressive quenching of NBD fluorescence with time was followed. A previous experiment revealed that the extent of initial quenching was not increased by using higher dithionite concentrations up to 50 mM (see **Supplementary Figure 1**, insert).

3.3.4 FLIM measurements

To determine the fluorescence lifetimes of NBD-analogs in the sperm membrane, time-correlated single photon counting was performed using an inverse Fluoview 1000 microscope (Olympus, Tokyo, Japan) with an oil objective (60x/1.35) for confocal laser scanning microscopy supplemented with a commercial FLIM upgrade kit from PicoQuant (Berlin, Germany). The excitation laser was a pulsed diode laser with a wavelength of 468 nm (pulse length 60 ps, pulse frequency 10 MHz, 4 µs/pixel). The emission was detected by an avalanche photo diode (APD) after passing a 540/40 band pass filter. Pictures were collected with a frame size of 512 x 512 pixels. 60 frames were collected for every data set. The photon count rate varied between 1 x 10^3 and 1 x 10^5 counted photons/s. Pseudocolored pictures were created with the average lifetime per pixel (2x2 binning). The summed up number of photons per pixel (2x2 binning) revealed the picture of fluorescence intensity.

The recorded pictures were analyzed using the Olympus FluoView FV1000 software to document sperm morphological integrity and vitality by PI staining. Acrosomal and postacrosomal head regions were manually selected as regions of interest (ROIs). For each ROI, an overall fluorescence decay curve was generated by summing up the photons registered for that region. The width of the bins of the decay histogram was chosen to 30.5 ps. To determine the fluorescence lifetimes by a non-linear least squares iterative fitting procedure, FLIM data sets were loaded into the software SymphoTime (Analysis) 4.7.2 according to Stöckl et al. (Stöckl et al. 2008).

The decay curves could be principally fitted by two components giving two lifetimes. The shorter lifetime of approximately 2 ns was not considered (Stöckl et al. 2008, Klein et al. 2012). This component represents a comparatively small amount of fluorophores and we assume that these fluorophores, due to a back-loop of their NBD-labeled fatty acyl chains (Chattopadhyay 1990), have access to extra- or intracellular aqueous surroundings. Therefore, the very short lifetime does probably not reflect the properties of the respective membrane leaflet under investigation. This assumption is supported by the fact, that the fluorescence lifetime of NBD is reduced to 0.9 ns in water, while being in the range of 7-10 ns in aprotic solvents (Lin and Struve 1991). A typical lifetime histogram and fitted data for the two head regions of a NBD-SM labeled sperm cell are shown in **Supplementary Figure 2**.

3.3.5 FRAP-measurements

FRAP was used to evaluate the diffusion coefficient (D) of NBD-SM, NBD-PS, and NBD-Ch in the sperm head membrane by selecting circular ROIs in its acrosomal and postacrosomal region. We note that the fluorescence intensity in the postacrosomal region of the sperm head was remarkably low for NBD-Ch.

The measurements were performed using a LSM710ConforCor3 system (Carl Zeiss Microscopy, Jena, Germany) equipped with an argon laser (488 nm), a main beam splitter MBS 488, an emission META detector (34 PMTs,505 - 650 nm), and an oil immersion objective (100x/1.4). The data were recorded by ZEN2010 software (Carl Zeiss MicroImaging, Jena, Germany) using a time series consisting of 400 images, time interval of 25 ms, bleaching after the 10th image (25 iterations 300 ms, laser power 100 times stronger than the imaging performance).

The attained FRAP data were processed with Prism (Version 5.01, 2007, GraphPad) by fitting to a biexponential decay curve (see formula (1)) to evaluate the half-time of fluorescence recovery ($t_{½}$).

(1) $$I(t) = A_1 + (B_1 - A_1)e^{-t/T_1} + A_2 + (B_2 - A_2)e^{-t/T_2}$$

To obtain D, the formula (2) was used with w representing the radius of the ROI in case of an uniform disc bleaching profile (Axelrod et al. 1976):

(2) $$D = \gamma_D \frac{w^2}{4\tau_{½}}$$

Due to the fact, that the region of interest was stimulated by a series of laser spots, with a diameter of 7 pixels, w was calculated to a value of 0.343 µm. γ_D is a factor corresponding to the beam shape, type of transport and bleaching parameter. For uniform bleaching of a circular disc and a fluorescence recovery dominated by lateral diffusion this parameter can be estimated as 0.88 (Axelrod et al. 1976). Since in our case the ROI was bleached by a series of laser spots instead a uniform disc bleaching profile, the true bleaching profile resembles more an uniform disc with Gaussian edges (Braga et al. 2004) and therefore, the assumption for γ_D might be suboptimal, but deviations in this factor should have only a minor influence on the resulting D.

A typical decay curve and fitted data for the two head regions of a NBD-SM labeled sperm cell are shown in **Supplementary Figure 3**.

3.3.6 FCS- measurements

FCS measurements were performed at room temperature on a LSM710-ConfoCor3 system (Carl Zeiss Microscopy GmbH, Jena Germany). NBD fluorescence signals were recorded after excitation by an argon laser (488 nm) using a water objective (40x/1.2) and a main beam splitter MBS488, through a 505-nm longpass filter. Membranes were located by z-scans. Intensity fluctuations were recorded for 4 s and 25 repetitions and further data analysis was carried out using the ZEN 2010 software (Carl Zeiss Microscopy GmbH, Jena, Germany) which also calibrated the PSF. An auto-correlation curve was derived for each raw data set by applying the following formula:

$$G(\tau) = 1 + \frac{\langle \delta F(t) \delta F(t+\tau) \rangle}{\langle F(t) \rangle^2} \quad (3)$$

where $\langle\rangle$ denotes averaging over time and δ (x) is an abbreviation of x-<x>. The correlation curves were fitted using a two component model of free diffusion in two dimensions with triplet fraction and an offset for membrane-associated proteins (Teichmann et al. 2014) analytically given by

$$G(\tau) = 1 + G_{\infty} + \frac{1}{N}\left(1 + \frac{T \times e^{-\tau/\tau_T}}{1-T}\right) \times \left(\frac{1}{\left(1+\frac{\tau}{\tau_{D1}}\right)} + \frac{1-f}{\left(1+\frac{\tau}{\tau_{D2}}\right)}\right) \quad (4)$$

where G_{∞} is the offset from 1. N and T represent the total number of particles and the triplet fraction respectively. The free diffusion times are represented by τ_{D1} andτ_{D2} (the subscripts indicate the different molecule species). τ_T is the triplet time, f and 1 - f are the fractions of species 1 and 2 and τ is the correlation time. The first component was too fast to reflect membrane diffusion and likely reflects a protonation kinetic of the fluorescent molecules leading to blinking (Haupts et al. 1998). Thus the diffusion time of the second component was considered to be significant (Elson 2001). Finally, all data sets with convergent fit results, out of the 25 recorded, were averaged.

Diffusion coefficients were calculated from the obtained diffusion times by the formula

$$D = \frac{\omega^2}{4 * \tau} \quad (5)$$

where ω represents the radius of the confocal volume and $\boldsymbol{\tau}$ is the characteristic diffusion time.

A typical autocorrelation curve and fitted data for the two head regions of a NBD-SM labeled sperm cell are shown in **Supplementary Figure 4**.

3.3.7 Statistics

Significances were tested using the open software R 2.15. Acrosome and postacrosome were compared using a paired Wilcoxon signed rank test while a Mann-Whitney-U-test was applied to compare different temperatures, vitalities, and analogs in the same sperm region.

3.4 Results

3.4.1 Analysis of transversal membrane distribution of NBD-cholesterol

Although there are many data supporting an even distribution of cholesterol and its analogs between both membrane leaflets in several plasma membranes (Müller et al. 2011), such a distribution has not been shown for sperm cells so far. Therefore, a dithionite based assay was applied to analyze the transversal distribution of fluorescent cholesterol analogs at different times after their incorporation in the boar sperm membrane. Immediately after addition of 25 mM dithionite to labeled sperm, about 50% of the NBD fluorescence in vital and about 97% in non-vital (PI-positive) cells was quenched without influence on the proportion of vital sperm (**Table 2**). This implies that 50% of the NBD-Ch in vital cells are accessible for the extracellular quencher and, obviously, located in the outer membrane half. This transversal distribution of NBD-Ch was observed for the whole time period in which labeled sperm were used for analysis by FLIM, FRAP, and FCS (25-70 minutes after start of labeling, **Table 2**).

Table 2 *Quenching of NBD-labeled lipid analogs for cholesterol (Ch) in the boar sperm membrane by sodium dithionite. Vital and non-vital boar sperm cells were discriminated by propidium iodide and analyzed by flow cytometry for their NBD fluorescence at different times after labeling with NBD-Ch. The amount of label accessible towards dithionite was determined 0.5 minutes after addition of 25 mM dithionite to the sperm cells. Means and standard deviations are given (n=3).*

time after start of NBD-Ch labeling [minutes]	**non- vital** % of sperm	+ dithionite % of sperm	**% quenching**	**vital** % of sperm	+ dithionite % of sperm	**% quenching**
25	65.3 ± 6.5	66.3 ± 4.0	**96.8 ± 0.7**	34.7 ± 5.6	33.7 ± 4.0	**55.0 ± 1.4**
50	43.3 ± 15.2	42.9 ± 18.0	**96.2 ± 1.3**	56.7 ± 15.2	57.1 ± 18.0	**50.0 ± 5.2**
70	54.6 ± 14.0	49.1 ± 12.8	**96.6 ± 0.5**	45.4 ± 14.0	50.9 ± 12.8	**51.7 ± 5.8**

Upon extended incubation in the presence of dithionite (up to 20 minutes), the NBD-Ch fluorescence in vital sperm was progressively quenched to values comparable to those in non-vital cells (**Supplementary Figure 1**) while the amount of vital sperm was reduced by 10% at most. A progressive permeation of dithionite through the membrane of PI-negative cells would inevitably result in a loss of sperm vitality and concomitant incorporation of PI. The latter was observed after addition of 0.5% Triton X-100 (data not shown). Therefore, the reason for the progressive

quenching might rather be a flipping of NBD-Ch between both membrane leaflets, exposing initially inaccessible molecules to the quencher outside the cell.

3.4.2 FLIM measurements

Fluorescence lifetime imaging was applied to visualize the distribution of fluorescence lifetimes for the different NBD-labeled lipid analogs in single vital sperm after co-staining the cells with PI. FLIM was performed at room temperature (RT) and at 38°C.

Fluorescence intensities of the cells recorded during FLIM measurements were used to verify the incorporation of the lipid analogs into sperm. Summarized intensity values for pixels in defined ROIs were normalized to the respective areas. The fluorescence intensity should correlate to the amount of analog incorporated into the membrane assuming that no bleaching occurs at the given label concentrations. All analogs incorporated to a higher extent into the acrosomal compared to the postacrosomal region (**Figure 12**). Sperm labeled with NBD-SM and NBD-Ch were only weakly fluorescent compared to sperm labeled with NBD-PS. NBD-SM incorporation increased in non-vital compared to vital cells which was also found for $DiIC_{12}$ (James et al. 1999). These authors assume that in non-vital cells also underlying organelles become stained because of cell membrane ruptures. This seems, however, not to be the case for NBD-Ch and NBD-PS, whose intensities are similar or even lower in non-vital sperm, respectively. In case of NBD-PS, non-vital cells do not actively translocate the analogs to the cytoplasmic membrane half during the labeling procedure. They are obviously not spontaneously included in the exposed leaflet of underlying membranes. The latter also applies to NBD-Ch and was confirmed by the intensity data revealed by flow cytometry for vital and non-vital sperm in the dithionite assay (not shown).

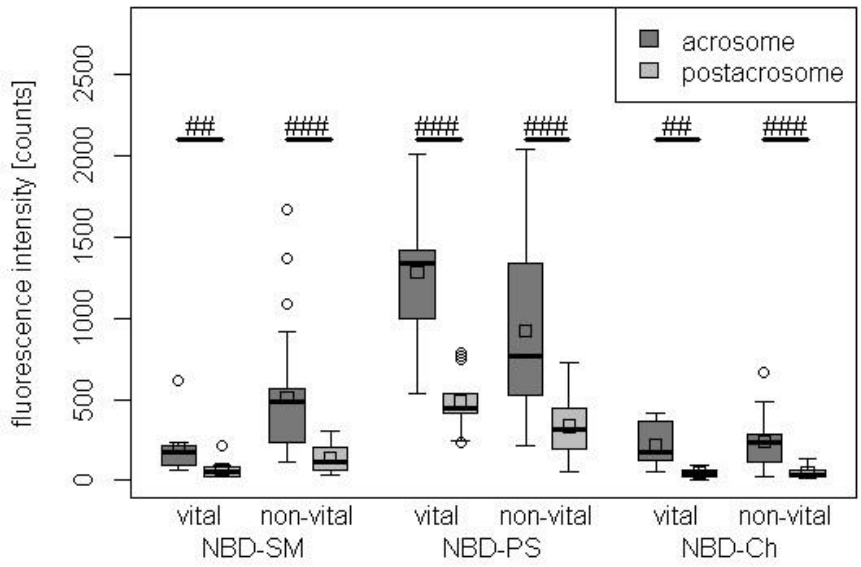

Figure 12: *Fluorescence intensities of NBD-labeled lipid analogs for sphingomyelin (SM), phosphatidylserine (PS), and cholesterol (Ch) incorporated in the acrosomal (dark grey) and postacrosomal (light grey) membrane regions of vital and non-vital boar sperm cells derived from FLIM measurements at 38°C. Data are displayed by means of boxplots (R 2.15). Medians and the 10th, 25th, 75th, 90th percentiles are shown as vertical boxes with error bars, outliers are denoted by open circles and means are shown as small squares. Values were corrected for the different size of both regions (see Materials and Methods). Significant differences between regions (paired Mann-Whitney U-test) are indicated (#P<0.05, ##P<0.01, ###P<0.001). Different fluorescence intensities were observed between vital and non-vital sperm by Mann-Whitney U-test (NBD-SM, acrosomal region: P<0.01, postacrosomal region: P<0.05; NBD-PS, acrosomal region: P<0.05, postacrosomal region: P<0.01). Significant differences between NBD-SM and NBD-PS as well as between NBD-PS and NBD-Ch (Mann-Whitney U-test) in vital cells were found in both regions (P<0.001).*

Representative pseudocolored images as well as fluorescence lifetime data of vital (PI-negative) cells are shown in **Figures 13** and **14**. Differences of fluorescence lifetimes between sperm head and tail regions are obvious in **Figure 13**. However, the number of photon counts per area was insufficient in the sperm tail. Therefore, only data from both head regions were determined and presented in **Figure 14**. For all following considerations it is important to note that the fluorescence intensity in the postacrosomal region of NBD-Ch labeled cells was rather low and that the data obtained for this label and region should be regarded with caution.

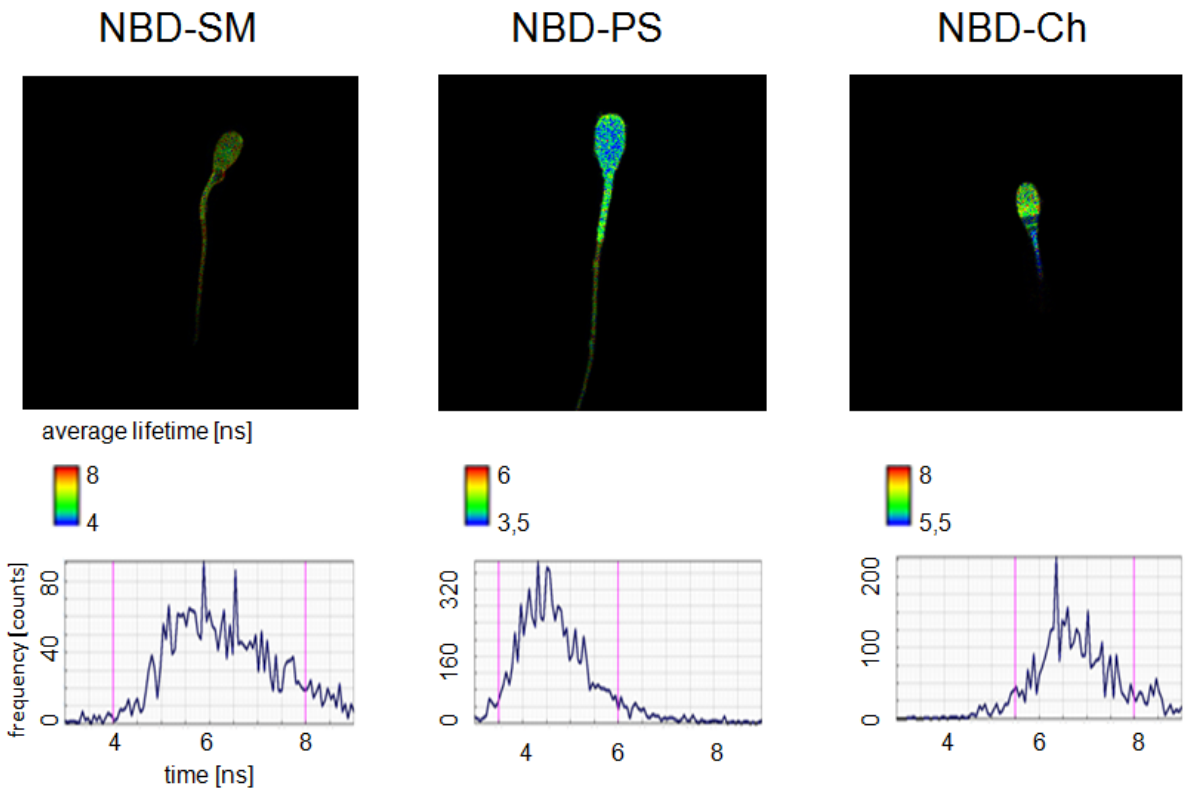

Figure 13: *Fluorescence lifetime images and histograms of NBD-labeled lipid analogs for sphingomyelin (SM), phosphatidylserine (PS), and cholesterol (Ch) incorporated in the membranes of vital domestic boar sperm. FLIM measurements were performed at 38°C. Average lifetime is shown as pseudocolor image (see scale). Pink colored lines in the histograms mark the borders of color coding of the FLIM images.*

All fluorescence lifetimes measured at 38°C were lower compared with the respective data for analog and sperm region at RT which is in agreement with a previously published dependence of NBD fluorescence lifetime on temperature (Fery-Forgues et al. 2003). This temperature effect was - with a difference of about 2 ns - most pronounced for NBD-SM.

When compared to NBD-PS, fluorescence lifetimes at 38°C were significantly higher for NBD-Ch and in the acrosomal region also for NBD-SM. At RT, NBD-PS showed the lowest fluorescence lifetimes, highest values were measured for NBD-SM followed by NBD-Ch. The most pronounced lifetime variability between both temperatures was detected for NBD-SM.

Comparing the results between both sperm head regions, significantly higher fluorescence lifetimes were determined in the acrosomal region with the exception of NBD-SM showing no differences between both sperm head regions. The largest differences of fluorescence lifetimes between acrosomal and postacosomal region were observed for NBD-Ch (**Figure 14**). Note, that data evaluation by exponential fitting procedures (see Material and Methods) revealed, besides a component with a very low lifetime (which was neglected, see Materials and Methods), no indication for the co-existence of clearly distinct label populations with different lifetimes within

one region. However, the lifetime distributions in each head region were relatively broad, particularly for NBD-SM (Δ about 3-4 ns, **Figure 13**).

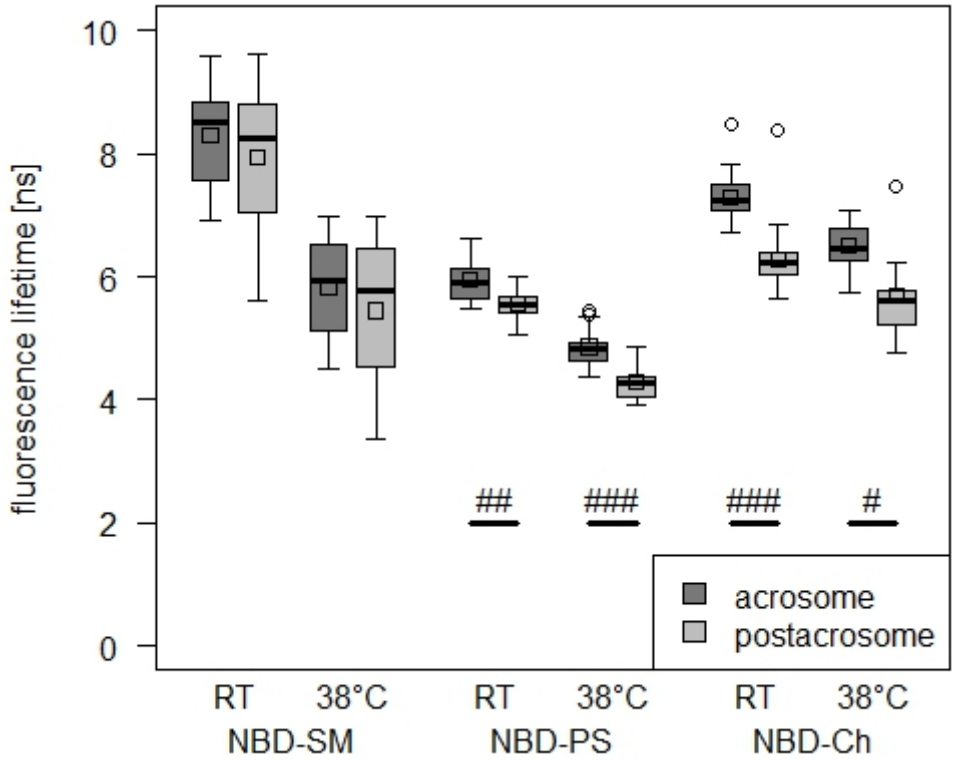

Figure 14: *Fluorescence lifetimes of NBD-labeled lipid analogs for sphingomyelin (SM), phosphatidylserine (PS), and cholesterol (Ch) incorporated in the acrosomal (dark grey) and postacrosomal (light grey) membrane regions of vital domestic boar sperm cells. FLIM measurements were performed at room temperature (RT; NBD-SM: n=8, NBD-PS: n=9, NBD-Ch: n=32) and at 38°C (NBD-SM: n=11, NBD-PS: n=13, NBD-Ch: n=9). Data are displayed by means of boxplots (R 2.15). Medians and the 10th, 25th, 75th, 90th percentiles are shown as vertical boxes with error bars, outliers are denoted by open circles and means are shown as small squares. Significant differences between regions (paired Mann-Whitney U-test) are indicated (#P<0.05, ##P<0.01, ###P<0.001). For each distinct region and analog, fluorescence lifetimes were lower at 38°C compared to RT (Mann-Whitney U-test, P<0.01). Significant differences between analogs (Mann-Whitney U-test) are presented in the table below:*

temperature	***RT***		***38°C***	
region	***acrosomal***	***postacrosomal***	***acrosomal***	***postacrosomal***
NBD-SM versus NBD-PS	***	***	**	***
NBD-SM versus NBD-Ch	**	**	-	-
NBD-PS versus NBD-Ch	***	***	***	***

3.4.3 FRAP measurements

FRAP measurements were performed in the acrosomal and postacrosomal region of sperm and diffusion coefficients (D) for the NBD-labeled lipid analogs were determined from the recovery curves. In the acrosomal region, diffusion coefficients of all three analogs were similar with values of around 1.5 x 10^{-9} cm^2/s (**Figure 15**). Comparing the two sperm head regions, D values of NBD-SM as well as NBD-PS were significantly lower (by about 50%) in the postacrosomal compared to the acrosomal region. No difference between these regions was found for NBD-Ch. Therefore, diffusion of NBD-Ch in the postacrosomal region was faster compared to NBD-SM and NBD-PS.

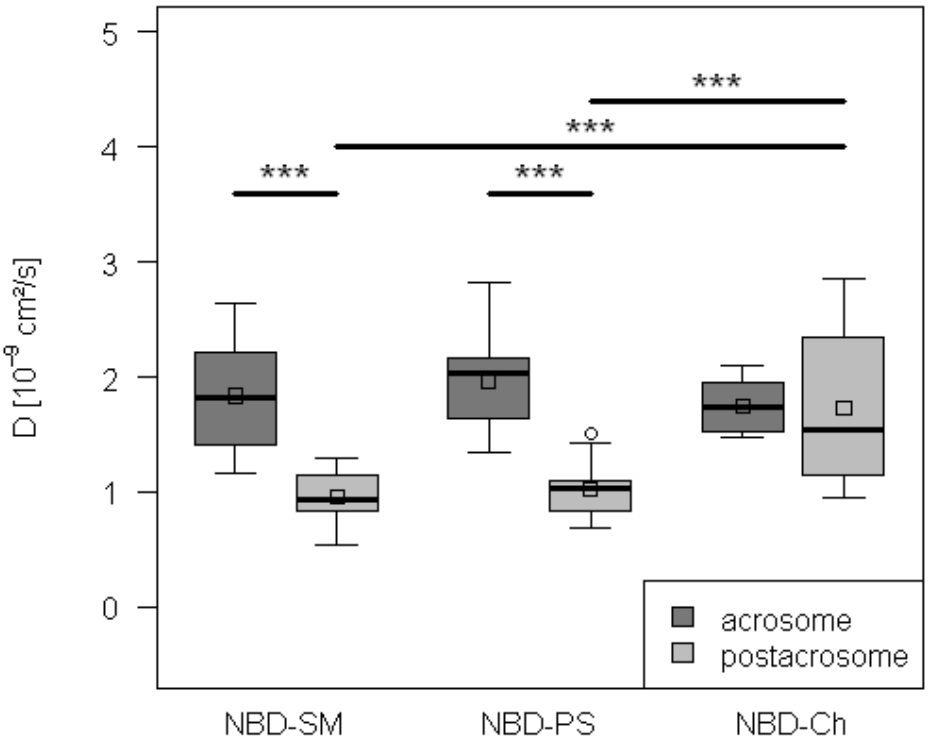

Figure 15: *Diffusion coefficients (D) of NBD-labeled lipid analogs for sphingomyelin (SM), phosphatidylserine (PS), and cholesterol (Ch) localized in the acrosomal (dark grey) and postacrosomal (light grey) membrane regions of domestic boar sperm heads calculated from FRAP measurements (NBD-SM: n=37/34, NBD-PS: n=15/11, NBD-Ch: n=7/8). Data are displayed by means of boxplots (R 2.15). Medians and the 10th, 25th, 75th, 90th percentiles are shown as vertical boxes with error bars, outliers are denoted by open circles and means are shown as small squares. Significant differences either between regions or analogs (Mann-Whitney U-test) are indicated (*P<0.05, **P<0.01, ***P<0.001).*

3.4.4 FCS measurements

Diffusion coefficients of NBD-labeled lipids were also determined from FCS measurements revealing a different picture (**Figure 16**). Generally, much higher (by a mean factor of 45) D values were found in FCS compared to FRAP measurements. No differences were observed between acrosomal and postacrosomal region for all three lipid analogs, contradictory to the results obtained

by FRAP using NBD-SM or NBD-PS. The postacrosomal D values of NBD-Ch were significantly lower than those of NBD-PS. A conspicuously large inter-cellular variability of D was found for NBD-PS in both regions.

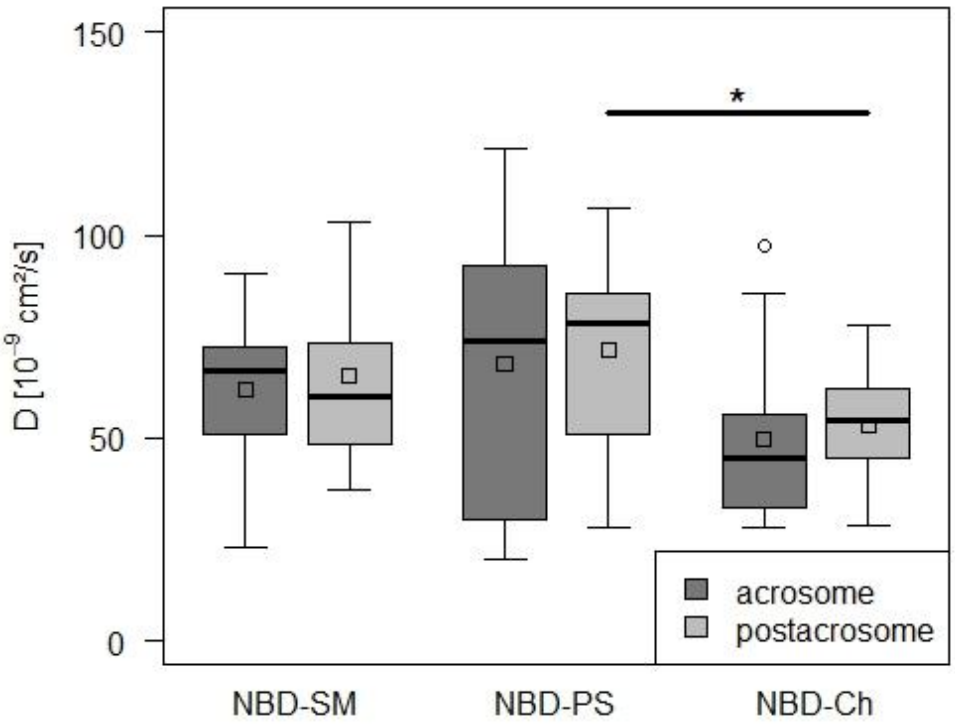

Figure 16: *Diffusion coefficients (D) of NBD-labeled lipid analogs for sphingomyelin (SM), phosphatidylserine (PS), and cholesterol (Ch) localized in the acrosomal (dark grey) and postacrosomal (light grey) membrane regions of domestic boar sperm heads calculated from FCS measurements (NBD-SM: n=12/14, NBD-PS: n=17/17, NBD-Ch: n=13/13). Data are displayed by means of boxplots (R 2.15). Medians and the 10th, 25th, 75th, 90th percentiles are shown as vertical boxes with error bars, outliers are denoted by open circles and means are shown as small squares. Significant differences either between regions or analogs (Mann-Whitney U-test) are indicated (*P<0.05, **P<0.01, ***P<0.001).*

3.5 Discussion

In the present study, the behavior of different fluorescent lipid analogs in the acrosomal and in the postacrosomal region of ejaculated boar sperm was characterized by various approaches of fluorescence microscopy. During transit of sperm through the female genital tract, the acrosomal region interacts with the epithelial cells from the oviduct e.g. forming a sperm reservoir and supporting sperm capacitation as a prerequisite to fertilization. Moreover, the acrosomal region provides the structures and components which mediate the first contact to the z*ona pellucida* which is the main stimulus for the acrosome reaction enabling the sperm penetration through the oocyte surrounding layer. While the anterior part of the sperm head is destroyed during acrosome reaction, the postacrosomal region is important for maintaining cell stability via connections to underlying

cytoskeletal components (Jamil 1984), but is also the region of initial contact and subsequent fusion with the oocyte membrane (Ikawa et al. 2010).

3.5.1 FLIM measurements

With the raising knowledge on comparably stable substructures within membranes, so-called rafts, constituted by certain lipids (essentially Ch and SM) and proteins with a high affinity for interaction in liquid ordered domains (Simons and Gerl 2010), the analysis of these temporally and spatially organized units came increasingly into the focus of cellular investigations. With regard to the physico-chemical properties within the domains, it is assumed that lipid subpopulations captured in those structures exhibit a restricted diffusion compared to freely fast diffusing lipids outside the structures. They could also be limited in their interaction with surrounding molecules which would affect the fluorescence lifetime of incorporated fluorescent markers.

The NBD fluorophore is a very subtle sensor of environmental changes since various spectral properties including its fluorescence lifetime are strongly dependent on solvent polarity and the presence of hydrogen donors (Fery-Forgues et al. 2003). While the fluorescence lifetime of NBD is in the range of 7-10 ns in non-polar aprotic solvents, its fluorescence lifetime is reduced to 1 ns in the polar, strongly protic solvent water. The reason for this behavior was attributed to a strongly increased rate of non-radiative deactivation in more polar and protic solvents (Fery-Forgues et al. 2003, Lin and Struve 1991). NBD-labeled lipid analogs have been successfully applied to analyze the membrane properties both in model membranes (Stöckl et al. 2008) and living cells (Klein et al. 2012, Ostasov et al. 2013, Mukherjee et al. 2006). Even though NBD-labeled lipids, like any anlog, may reflect physical properties of endogenous lipids in some cases only to a certain extent (Chattopadhyay 1990), they have been proven to faithfully reflect the transversal distribution of endogenous lipids in sperm (Gadella et al. 1999, Kurz et al. 2005, Müller et al. 1994, Nolan et al. 1995) and were succesfully applied to analyse membrane environments using their longer fluorescence lifetime (Stöckl et al. 2008, Klein et al. 2012). Since it has been shown in model membranes that the fluorescence lifetime of markers like NBD-labeled lipids is not the same in different lipid domains (Stöckl et al. 2008), FLIM analyses of NBD-analogs were performed in the discrete (acrosomal and postacrosomal) sperm head regions.

FLIM allows a fast high-resolution measurement of the complete areas of both head regions in vital sperm. Decay curves of fluorescence intensity could be properly fitted with two lifetime components for each analog in both membrane compartments. We solely used the higher lifetime which characterizes the motional freedom of the NBD-label of the respective lipid analog and surrounding solvent molecules (see Material and Methods). Since we observed no further pronounced analog population having a different lifetime, we assume that the analogs in the acrosomal as well as in the postacrosomal region are not organized in substructures clearly

distinguishable by their influence on fluorescence lifetimes. FLIM analyses of NBD-PC and NBD-PS in cell membranes of HepG2- and HeLa-cells could also not resolve distinct domain specific lifetimes (Stöckl et al. 2008). An overlapping broad lifetime histogram centered on lifetimes corresponding to values detected for liquid ordered domains in artificial membranes was revealed (11.5 ns for NBD-PC, 10.9 ns for NBD-PS at 25°C). If domains exist in these cell types, the cell membrane seems to consist of several lipid domains differing in properties like composition, size and stability (Stöckl et al. 2008). Moreover, it is assumed that native cell membranes create a rather continuous liquid ordered phase with embedded small disordered domains (Mukherjee and Maxfield 2004, Almeida et al. 2005). Also in boar sperm, broad lifetime histograms were revealed per region, however, even at room temperature (26°C) values never exceed 10 ns. In giant unilamellar vesicles (GUVs) of lipid mixtures known to form ordered and disordered domains as well, lifetimes of 12 and 7 ns were resolved for NBD-PC at 25°C, respectively (Stöckl et al. 2008). We conclude that lifetimes of all NBD-analogs in the boar sperm head rather correspond to those in disordered domains and are much lower when compared to HepG2- and HeLa-cells. This has important implications for the functionality of mammalian sperm which need to sustain their fusogeneity for the exocytotic acrosome reaction (acrosomal region) and fusion with the oocyte (postacrosomal region). This suggests a strong need for stabilization of sperm membranes before fertilization by proteins or binding to oviduct.

As outlined in the introduction, the NBD-analogs used here allow to selectively sense the leaflets of the sperm membrane. The localization of more than 95% NBD-PS on the inner membrane leaflet as well as of more than 95% NBD-SM on the outer membrane leaflet is well documented in the literature (Müller et al. 1994, Gadella et al. 1999, Kurz et al. 2005, Nolan et al. 1995) and can be presumed in both large head regions. For NBD-Ch, we could confirm here for sperm that it is indeed symmetrically distributed across both membrane leaflets and shows a rapid flip-flop across the bilayer (Müller et al. 2011). However, we cannot exclude that the transversal distribution and mobility of NBD-Ch differs between the macrodomains of the head. Furthermore the fluorescence of the NBD group is amongst others sensitive to the polarity and hydrogen-bonding donor strength of its surroundings, therefore being able to sense even small differences between different membrane substructures.

Comparing the lifetimes of the three different analogs, NBD-PS showed the shortest lifetimes at body as well as at room temperature. This is in agreement with the assumption of a more fluid cytoplasmic membrane leaflet in eukaryotic cells (Seigneuret et al. 1984, Julien et al. 1993). Because NBD-PS as well as endogenous PS is rapidly transported to the cytoplasmic leaflet in vital boar sperm it is nearly exclusively located on that membrane half under our experimental conditions (Kurz et al. 2005, Müller et al. 1994). Similar to the lifetime measurements, NBD-PS also tends to have a larger diffusion mobility reflected by highest average diffusion coefficients deduced from

FCS in both head compartments. When the temperature was reduced from 38°C to room temperature, the lifetime of all analogs increased. However, this increase varied for the analogs suggesting a different behavior/reorganization of each analog within the membrane. The largest increase was observed for NBD-SM in the outer leaflet and comes nearest to values in liquid ordered domains in GUVs (see above). It remains open whether the smaller response to temperature change of NBD-Ch is explained by its particular arrangement in the membrane or by a reduced temperature sensitivity of the particular type of NBD bonding compared to chain-labeled analogs (Fery-Forgues et al. 2003). Notably, the variation of lifetimes between single sperm was remarkably high for NBD-SM compared to NBD-Ch or NBD-PS. The induced changes upon cooling could be relevant for stabilizing reorganization processes during sperm storage at slightly lower temperature in the epididymis. This would additionally have implications for low-temperature sperm storage before artificial insemination which could in future be investigated by NBD-analogs in similar approaches.

The existence of liquid ordered membrane (raft) domains has been postulated for boar sperm after analyzing functional protein complexes like for instance GM1 related domains (typical raft marker) in detergent resistant membrane fractions by several authors (Peterson et al. 1987, Bou Khalil et al. 2006, Tanphaichitr et al. 2007, Boerke et al. 2008, Jones et al. 2010, van Gestel et al. 2005). However, for no type of NBD-analog, FLIM analyzes revealed clearly distinguishable coexisting lipid populations, comparable to liquid ordered and disordered domains, within one head region. At least for NBD-Ch it is not sure that the analog locates to liquid ordered and disordered domains as well, since it has been shown for artificial membranes that NBD-PC and NBD-Ch, like most fluorescent lipid analogs, accumulate predominantly into the liquid disordered phase. For NBD-SM, conflicting data have been published (Ramstedt and Slotte 2006, Sengupta et al. 2008, Sezgin et al. 2012, Wang and Silvius 2000, Wang and Silvius 2003). Therefore, we have characterized the lateral arrangement of NBD-SM in phase-separated GUVs finding that about 75% of this analog are localized in the liquid ordered domain (see **supplementary information**).

Comparing both large sperm head regions, fluorescence lifetimes of NBD-PS and NBD-Ch are higher in the acrosomal than in the postacrosomal part. This means that the probability of molecular interactions of NBD-groups (as possible consequence of their motional freedom in a suggested more fluid or aqueous environment) is higher in the postacrosomal region and concerns particularly analogs with partition into the cytoplasmic leaflet. Whereas close membrane contact as prerequisite for fusion (acrosome reaction) might restrict mobility in the acrosomal part of the head, different conditions in the posterior head region might be required for later reorganization of postacrosomal proteins upon capacitation/acrosome reaction as demonstrated for bovine and human sperm (Luconi et al. 1998, Howes et al. 2001).

3.5.2 Discrepancies between FRAP and FCS measurements

Comparing our data on analog diffusion obtained from FRAP and FCS measurements, the diffusion coefficients as well as the ratio of diffusion coefficients between the two sperm head regions strongly differ in dependence of the detection method used. This indicates that the apparent value of diffusion coefficients (D) depends on the temporal and spatial scale of the measurement.

Similar discrepancies have been described elsewhere recently. Similar to our data on lipids, Adkins et al. (Adkins et al. 2007) detected a 10fold difference in diffusion coefficients calculated from FRAP and FCS measurements for a membrane protein (tagged with yellow fluorescent protein) in HEK293 cells. The authors assumed an overestimation of D values by FCS measurements. Guo et al. (Guo et al. 2008) compared different fluorescence techniques to analyze fluorescent lipid analogs in supported lipid bilayers and GUVs. Again, diffusion coefficients calculated from FRAP were significantly lower than those calculated with FCS. Since their FCS data were in better agreement with diffusion coefficients obtained from single particle tracking (SPT) in supported lipid bilayers where D values are determined from real diffusion pathways of multiple discrete molecules, the authors rather assumed an underestimation of D values by FRAP.

In accordance with the latter authors, we hypothesize that the FRAP measurements in our study also caused a significant underestimation of diffusion velocity compared to FCS derived data. Already in the past, some groups challenged the applicability of conventional FRAP formulas (that were derived for static bleaching lasers) in confocal laser scanning microscopy (CLSM) as presented by Axelrod et al. (Axelrod et al. 1976), and found that the diffusion of molecules between bleach spot and surrounding membrane during the bleaching interval leads to a significant increase in the effective bleach spot size (bleach spot broadening) and cannot be neglected when using CLSM in FRAP experiments (Braga et al. 2004, Kang et al. 2009, Kang et al. 2012). This increase in effective bleach spot size finally causes an underestimation of the diffusion coefficient when conventional data analysis is performed on the recovery data collected. The effect is more pronounced for longer bleaching times, small bleach spots and high diffusion coefficients. Note that due to the scanning nature of the bleaching laser beam in CLSM, an increase in bleach spot size is accompanied by an increase in bleaching time and *vice versa*, which makes it difficult to avoid this aberration. If the labeled marker species consists of subspecies that diffuse with different velocities, these subspecies are differentially influenced by the increase in effective bleach spot size. The kinetics of the recovery curve may then be dominated by slower moving molecules.

Previous FRAP measurements on boar sperm used static lasers with Gaussian profile to create a bleach spot with a diameter of 1.2 or 2.5 µm after 5 ms bleaching time. For the artificial lipid reporter ODAF, D values of about 30 x 10^{-9} cm^2s^{-1} were reported for both boar sperm head regions at 23 or 25°C (Wolfe et al. 1998, James et al. 1999). James et al. found D values of about 70 and 50

x 10^{-9} cm^2s^{-1} for another lipid-like reporter ($DiIC_{12}$) in the acrosomal and postacrosomal region, respectively (James et al. 2004). Note that the mentioned underestimation of D is negligible in these FRAP protocols. Yet the size of these bleach spots seems inadequate to the size and geometry of the sperm head, particularly of the postacrosomal part leading to a point where the FRAP approximation for circular bleach spots in an unbleached region of unlimited size and uniformity in all directions is highly questionable. This is illustrated in **Figure 17**. Therefore we used CLSM to create a smaller bleach spot of 0.686 µm diameter with, due to the scanning nature of the laser beam, a bleaching time of about 300 ms. We detected rather low diffusion coefficients of about 0.5-3 x 10^{-9} cm^2s^{-1} which are in the typical range for membrane proteins being much larger in size and, therefore, diffuse slower. The diffusion coefficients calculated from our study by FCS for NBD-analogs are around 60 x 10^{-9} cm^2s^{-1} and are more consistent with expected motion characteristics of lipid molecules in a membrane (Stöckl et al. 2008). We are aware that due to the described aberrations of D when applying conventional FRAP analysis on confocal FRAP data, the D values revealed by FCS are more representative for the diffusional behavior of the applied lipid analogs.

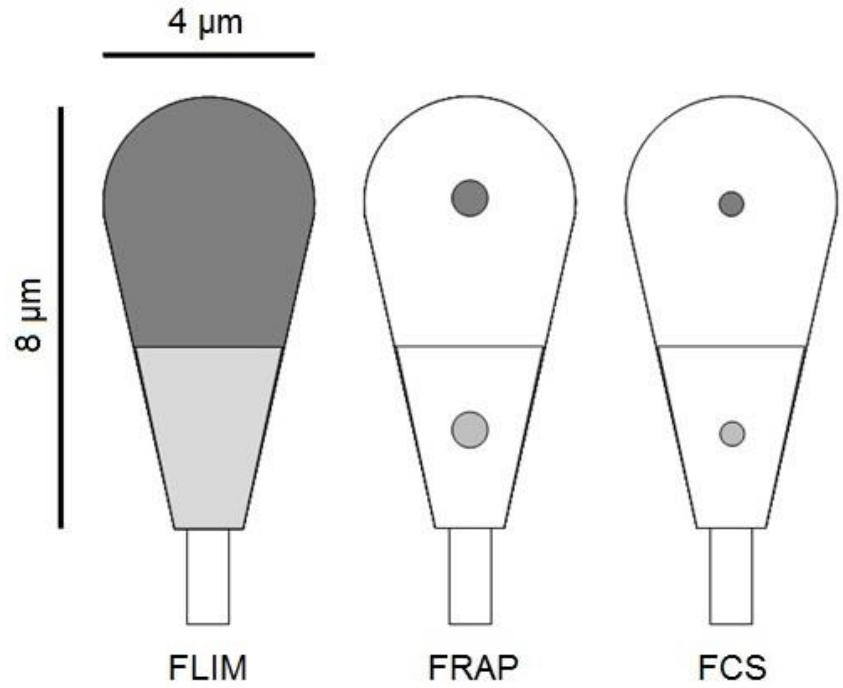

Figure 17: *Visualization of membrane dimensions and measurement parameters of the different methods characterizing the behaviour of fluorescently labeled lipid analogs localized in membrane regions of domestic boar sperm heads. For further explanation on the applied methods (FLIM, FRAP with different bleach spot sizes, FCS) see the introduction. Colors indicate the measured share of the acrosomal (dark grey) and postacrosomal (light grey) region.*

Whereas no difference of NBD-analog diffusion velocity between acrosomal and postacrosomal region was resolved by FCS, FRAP revealed significantly lower D values in the postacrosomal

compared to the acrosomal part of the head for NBD-SM and NBD-PS. Lower D values in the postacrosomal compared to the acrosomal region were also found by FRAP for $DiIC_{12}$ in boar sperm (James et al. 2004) as well as for ODAF in bull, goat, monkey, mouse, and rat but not in boar, dog, and guinea pig sperm (Ladha et al. 1997, Wolfe et al. 1998, Christova et al. 2004). In the case of lower FRAP derived D values in the postacrosome, these were concordantly interpreted by the authors in terms of a less fluid membrane in the posterior head.

Our FCS data matched quite well with the former examinations of ODAF in boar sperm membranes showing relatively homogenous diffusion coefficients over the whole sperm head in the dimension of 10^{-8} cm²/s. While the different dimension of our FRAP derived D values can be explained by the effect of bleach spot broadening as outlined above, this does not explain the inhomogeneity between both sperm head membrane regions seen with this technique. We hypothesize that our lower FRAP derived D values of NBD-PS and NBD-SM in the postacrosome are not necessarily indicative for an overall slower diffusion or membrane fluidity in this part of the head but, on the contrary, for the existence of subpopulations with heterogeneous diffusion coefficients. According to this hypothesis, the lower D values in the posterior region could be caused by a mixture of slowly as well as rapidly diffusing molecules. As a result of the mentioned effect of bleach spot broadening, the latter became unintentionally bleached to a higher extent. When analyzed by FCS, the same average D value as in the acrosomal region was detected without any information about the existence of putative lipid populations with different diffusion velocities. Compared to NBD-SM and NBD-PS, NBD-Ch does obviously not incorporate into different posterior membrane lipid populations with different diffusion behavior or can circumvent limitations in lateral diffusion by flip-flop. Mean D values as calculated from FRAP as well as FCS were similar in the acrosomal and postacrosomal region.

As concluded from comparing FRAP and FCS results (see above), the coexistence of subpopulations with different diffusion velocity is assumed for NBD-SM as well as NBD-PS in the postacrosomal region. The higher fluorescence lifetimes of NBD-PS and NBD-Ch in the acrosomal compared to the postacrosomal part (as possible consequence of decreased motional freedom in a suggested less fluid environment) would throughout be consistent with the assumption that rapidly and slowly diffusing label populations of NBD-SM and NBD-PS co-exist in the postacrosomal region. Fluorescence lifetimes of those differently diffusing analog subpopulations must not necessarily differ since the lifetime of NBD-molecules in the order of several nanoseconds might rather be affected by immediate molecular surroundings. The fluorescence lifetimes can be similar in a continuous lipid phase as well as within molecular platforms/domains which, as a whole, show restricted diffusion in a much larger spatial and temporal scale as detected with FRAP and FCS.

3.6 Conclusions

In conclusion we could show that a combination of different microscopic methods provides a comprehensive picture of lipid dynamics in the cell membrane of vital sperm even if conclusions from each single method are limited and fragmentary in the respective temporal and spatial window. The presented lipid-analog-specific results indicate that the lipid analogs used are suitable to report on the conditions of surrounding membrane domains with different properties. Whereas FLIM analyses did not indicate coexisting distinct liquid ordered and disordered domains in any of the head regions, particularly FRAP in comparison to FCS measurements suggest the incorporation of NBD-SM as well as NBD-PS in postacrosomal subpopulations with different diffusion velocity. FLIM analyses further indicate a more fluid microenvironment of NBD-Ch and NBD-PS in the postacrosomal compared to the acrosomal region indicating a more fluid cytoplasmic leaflet compared to the exoplasmic one. This conclusion is supported by lower fluorescence lifetime and higher D values (FCS) for NBD-PS in both head compartments.

For the first time, fluorescence lifetimes of lipid analogs were determined in the sperm cell membrane and found to be in a range characteristic for the liquid disordered phase in artificial lipid membranes (GUV). Sperm require a fragile membrane with fusion competence for acrosome reaction and fertilization which for instance becomes apparent in the high amount of polyunsaturated fatty acyl residues in sperm lipids. Moreover, boar sperm contain less cholesterol e.g. compared to bull sperm (Parks and Lynch 1992), a lipid which rigidifies membranes. The binding of components, e.g. seminal plasma proteins to sperm could modify their physico-chemical membrane properties. As we have shown recently, bull sperm membranes are stabilized - a requirement for the transit through the female genital tract - by seminal fluid proteins, which directly interact with the lipid phase (Tannert et al. 2007b, Greube et al. 2001). It remains to be investigated whether boar seminal proteins are also able to affect membrane properties e.g. to stabilize the comparatively fluid sperm membrane.

Acknowledgment

This work was supported by the German Research Council (DFG MU1520/2-1) and by the German Ministry of Education and Research (BMBF Number 033 L046).

The authors thank Andreas Herrmann and Thomas Korte (Humboldt-University Berlin) for helpful advice and discussion. The authors also appreciate the excellent technical assistance of Anita Retzlaff (Institute for Reproduction of Farm Animals Schönow e.V.) and Jenny Eichhorst (Leibniz Institute for Molecular Pharmacology).

3.7 Supplementary Material

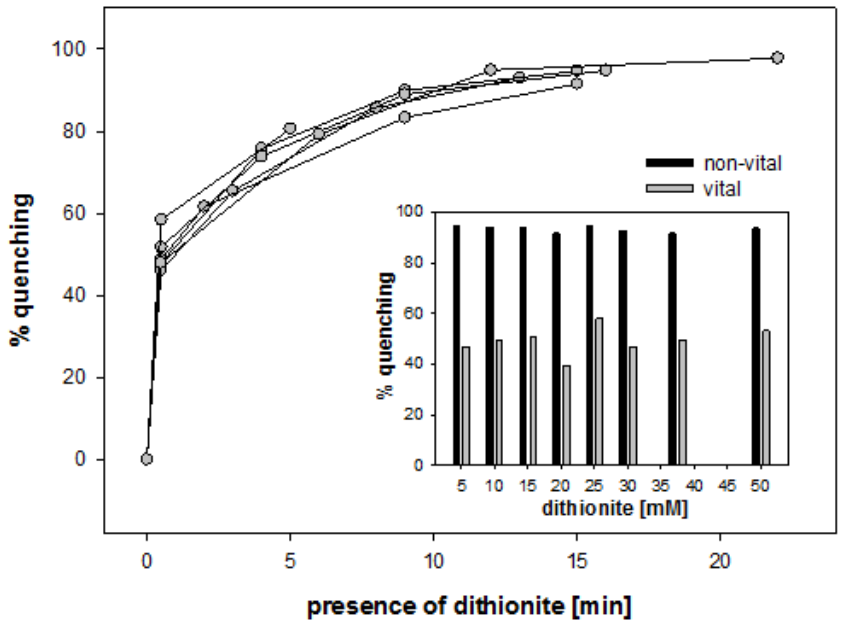

Supplementary Figure 1

Quenching of NBD-cholesterol in the boar sperm membrane by sodium dithionite. NBD-cholesterol labeled sperm cells were incubated with propidium iodide (5 min, 38°C) and analyzed by using flow cytometry to determine the NBD-fluorescence intensity in vital and non-vital cells. Subsequently, cells were treated with dithionite and the fluorescence was measured at different times. The figure shows the increased quenching of NBD-fluorescence, i.e. decrease of fluorescence intensity of vital (i.e. PI-negative) cells in the presence of 25 mM dithionite at room temperature (n=6). The insert shows that the percentage of initially quenched NBD-cholesterol (0.5 min after dithionite addition) is independent of the dithionite concentration in the range from 5 to 50 mM.

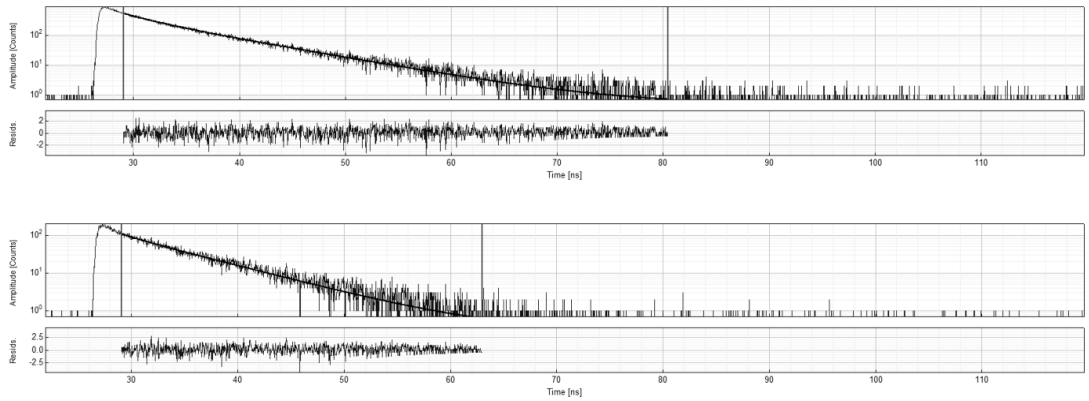

	acrosome	**postacrosome**
τ_1 [ns]	7.064	6
amplitude$_1$ [counts]	341.38	95.26
τ_1 [ns]	2.647	1.563
amplitude$_2$ [counts]	193.78	14.92
τ_1 [ns]	5.46	5.4
X^2	0.797	0.73
background	0.48	0.29
fit range [ns]	29.05-80.5	29.05-63

Supplementary Figure 2: *Typical fluorescence histogram and fit for a FLIM measurement in the acrosomal (top) and postacrosomal (bottom) region of a sperm cell labelled with NBD-SM. Obtained parameters are shown in the table.*

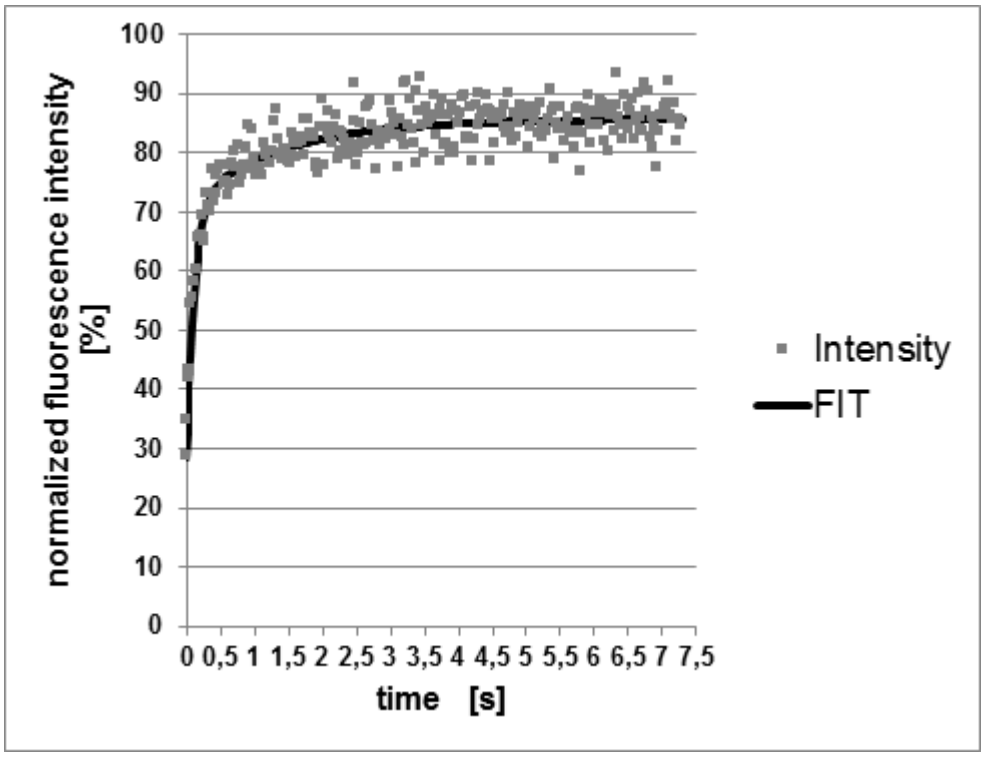
normalized fluorescence intensity [%]
100
90
80
70
60
50
40
30
20
10
0
0 0,5 1 1,5 2 2,5 3 3,5 4 4,5 5 5,5 6 6,5 7 7,5
time [s]
Intensity
FIT

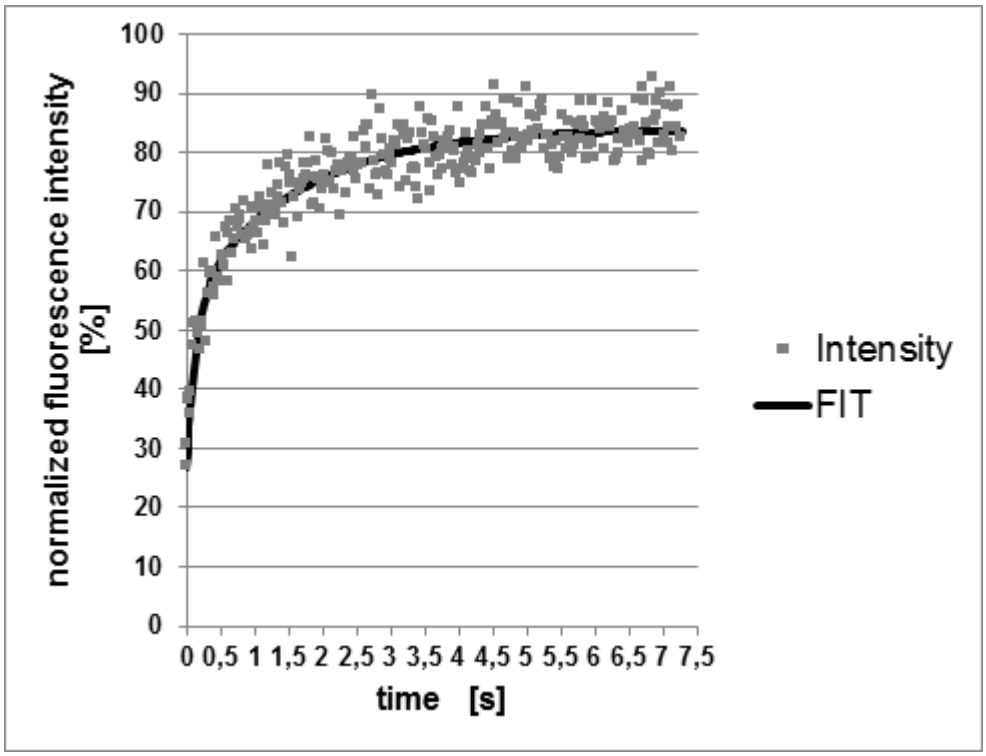
normalized fluorescence intensity [%]
100
90
80
70
60
50
40
30
20
10
0
0 0,5 1 1,5 2 2,5 3 3,5 4 4,5 5 5,5 6 6,5 7 7,5
time [s]
Intensity
FIT

FIT: $$I(t) = A_{\max} + (A_{\min} - A_{\max}) * e^{\frac{-t}{T_1}} + B_{\max} + (B_{\min} - B_{\max}) * e^{\frac{-t}{T_2}}$$

	acrosome	postacrosome
best-fit values		
A_{max}	56.98	41.05
A_{min} (constant)	14.28	13.45
T_1	0.115	0.1399
B_{max}	28.69	43.04
B_{min} (constant)	14.28	13.45
T_2	1.372	1.584
std. error		
A_{max}	1.78E+00	2.17E+00
T_1	1.16E-02	2.50E-02
B_{max}	1.633	1.924
T_2	2.34E-01	1.71E-01
95% confidence intervals		
A_{max}	53.49 to 60.48	36.79 to 45.30
T_1	0.09228 to 0.1378	0.09082 to 0.1889
B_{max}	25.49 to 31.89	39.27 to 46.81
T_2	0.9126 to 1.831	1.250 to 1.918
goodness of fit		
degrees of freedom	286	286
R^2	0.8581	0.8795
absolute sum of squares	2691	3864
Sy.x	3.067	3.676
data		
number of X values	290	290
number of Y replicates	3	3
total number of values	290	290
number of missing values	580	580

Supplementary Figure 3: *Typical recovery curve and fit for a FRAP measurement in the acrosomal (top) and postacrosomal (bottom) region of a sperm cell labelled with NBD-SM. Obtained parameters are shown in the table.*

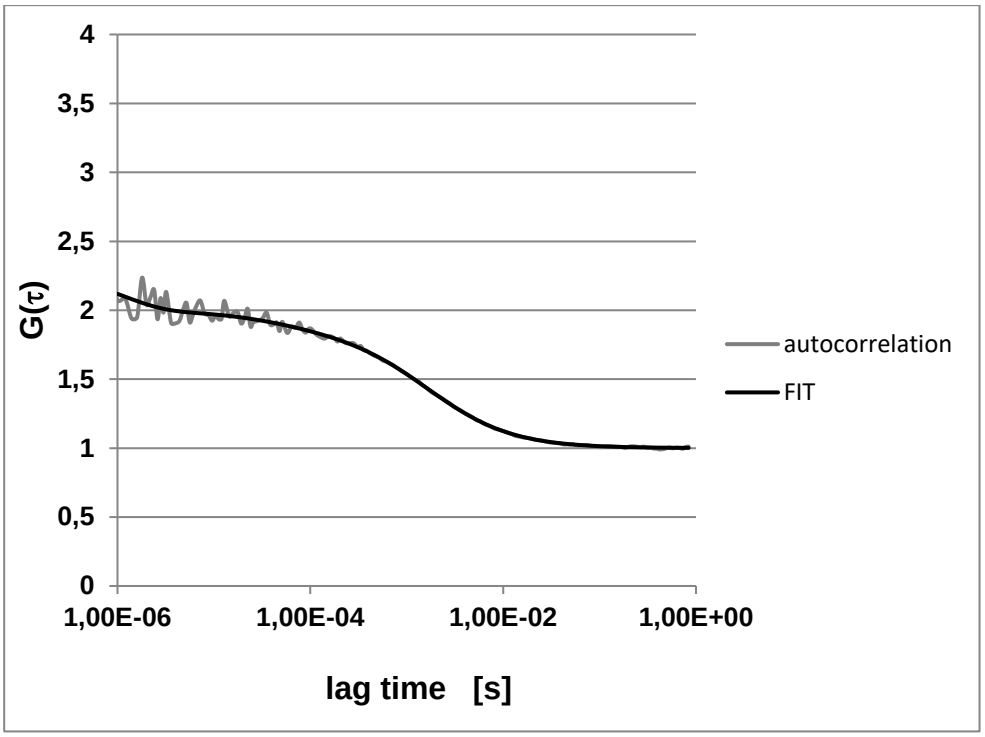
4
3,5
3
2,5
2
1,5
1
0,5
0
G(τ)
1,00E-06
1,00E-04
1,00E-02
1,00E+00
lag time [s]
autocorrelation
FIT

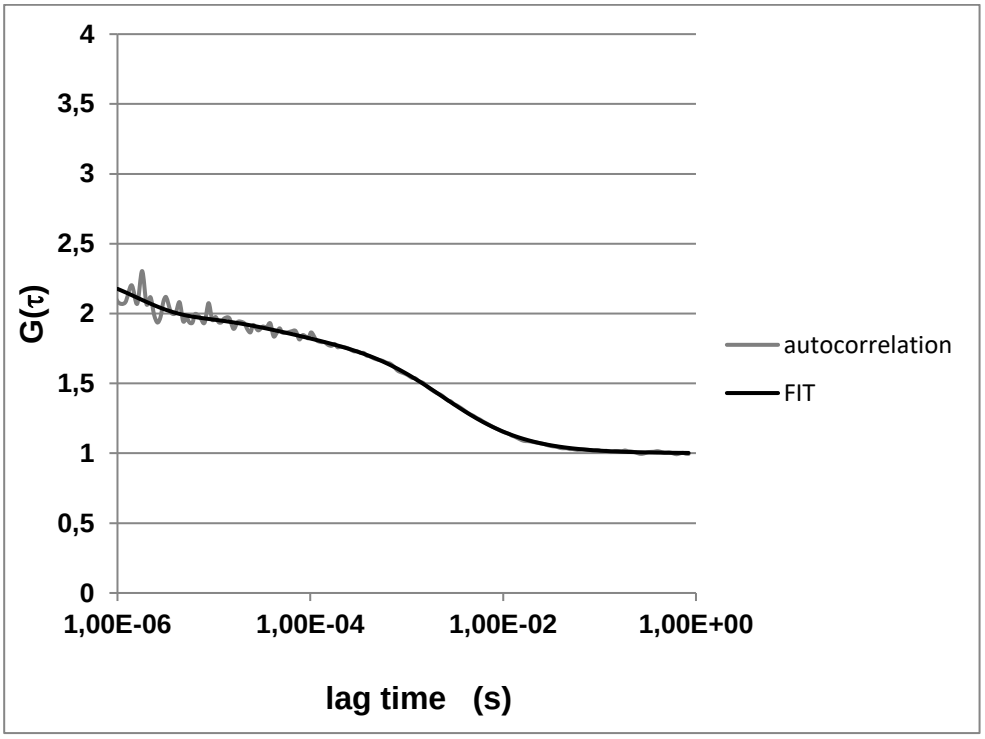
4
3,5
3
2,5
2
1,5
1
0,5
0
G(τ)
1,00E-06
1,00E-04
1,00E-02
1,00E+00
lag time (s)
autocorrelation
FIT

	acrosome	postacrosome
repetition	average	average
count rate [kHz]	23.221	29.953
correlation	1.148	1.106
counts per molecule [kHz]	3.447	3.184
amplitude number particles	6.737	9.406
triplet state fraction [%]	22.906	26.145
triplet state relaxation time [µs]	1.13	1.516
component 1 fraction [%]	16.448	20.668
component 2 fraction [%]	83.552	79.332
component 1 diffusion time [µs]	54.044	40.765
component 2 diffusion time [µs]	1714.579	2409.39
χ^2	1.18E-05	4.19E-06

Supplementary Figure 4: *Normalized autocorrelation and fit of a typical FCS measurement in the acrosomal (top) and postacrosomal (bottom) region of a NBD-SM labelled sperm cell. Obtained parameters are shown in the table.*

Supplementary Information

Preparation of giant unilamellar vesicles (GUVs)

All lipids were purchased from Avanti Polar Lipids (Alabaster, AL) and used without further purification. GUVs were produced by the electroswelling method (Angelova et al. 1992). Lipid mixtures were prepared from stock solutions in chloroform. Finally, 100 nmol of the lateral membrane domain forming lipid mixture DOPC and, either N-stearoyl-D-*erythro*-sphingosylphosphorylcholine (SSM) or porcine brain sphingomyelin (bSM), and cholesterol (in a molar ratio of 1:1:1) including 0.5 mol% of the liquid disordered (*ld*) domain marker 1,2-dioleoyl-*sn*-glycero-3-phosphoethanolamine-N-(lissamine rhodamine B sulfonyl) (N-Rh-DOPE) and 0.5 mol% of N-[6-[(7-nitro-2-1,3-benzoxadiazol-4-yl)amino]hexanoyl]-sphingosine-1-phosphocholine (C6-NBD-SM) were dissolved in 50 µl of chloroform and deposits of 2 µl were spotted onto custom-built titan chambers. The mixture was placed on a heat plate at 50°C to facilitate solvent evaporation, and subsequently given into a high vacuum field for at least 1 h to evaporate remaining traces of solvent. The lipid-coated slides were assembled using Parafilm® (Bemis, Soignies, Belgium) as a spacer for insulation. The electroswelling chamber was filled with 1 ml of sucrose buffer (250 mM sucrose, 15 mM NaN_3, osmolarity of 280 mOsm/kg) and sealed with plasticine. An alternating electrical field of 10 Hz rising from 0.02 V to 1.1 V in the first 56 min was applied for 2.5 h at 55°C, followed by 30 min of 4 Hz and 1.3 V to detach the formed liposomes.

Confocal laser scanning microscopy

For microscopy, GUVs were mixed 1:1 (v/v) with 250 mM glucose buffer (5.8 mM NaH_2PO_4 , 5.8 mM Na_2HPO_4, osmolality of 300 mOsm/kg, pH 7.2) onto a poly-d-lysine coated glass bottom dish (MatTek Coorporation, Ashland, Massachusetts, USA) and were then allowed to settle down for observation. Confocal images of the equatorial plane of the GUVs were taken using an inverted confocal laser scanning microscope (FV1000, Olympus, Hamburg, Germany) using a 60× (N.A. 1.2) water-immersion objective at 25°C. NBD was excited using a 488 nm argon laser (Olympus, Hamburg, Germany) and its fluorescence was detected between 500 and 540 nm. Rhodamine was excited with a 561 nm diode laser (Olympus, Hamburg, Germany) and the emission was recorded between 570 and 670 nm.

Results

The lateral distribution of C6-NBD-SM was investigated in GUVs consisting of DOPC, cholesterol and SSM or bSM. These vesicles are characterized by liquid ordered (*lo*) and disordered (*ld*) domains at room temperature. To identify the *ld* phase, the GUVs additionally contained the fluorescent lipid N-Rh-DOPE which is a well-established marker for this phase. Therefore, this domain shows an intense red fluorescence, while the *lo* phase, which is depleted of N-Rh-DOPE, appears with low fluorescence (Supplementary Figure 5). Notably, the fluorescence of C6-NBD-SM

was larger in the regions of low Rhodamine fluorescence indicating that this analog is concentrated in the liquid ordered domain (Supplementary Figure 5). To quantify the distribution of C6-NBD-SM between the *lo* and the *ld* region, fluorescence intensities in both domains were quantified and the intensity in the *lo* domain was related to the sum of intensities (Johnson et al. 2010). According to that, 74.5 +/- 7.2 % (mean +/- SD, 2 independent preparations, 27 GUVs) of the C6-NBD-SM was localized in the ordered domain of GUVs containing SSM. A similar enrichment of the analog was found in GUVs containing bSM, 78.6 +/- 4.1 % (1 preparation, 7 vesicles). In GUVs consisting solely of DOPC, both fluorescent lipids, N-Rh-DOPE and C6-NBD-SM showed a homogenous fluorescence of the vesicle membrane (not shown).

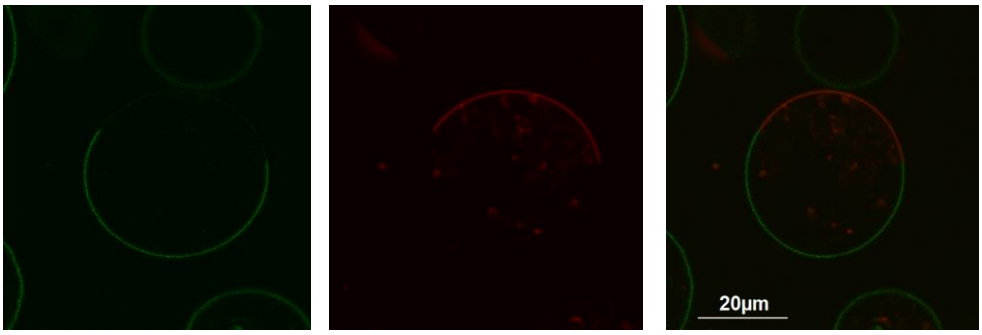

Supplementary Figure 5: *Confocal fluorescence image of GUVs consisting of the canonical raft mixture of DOPC/SSM/cholesterol (1:1:1 molar ratio) and the fluorescent lipids N-Rh-DOPE and C6-NBD-PC (both at 0.5 mol%). The vesicles were observed in the green channel (NBD fluorescence, left image) or in the red channel (Rhodamine fluorescence, mid column) at 25°C. The right image shows the merging of NBD and Rhodamine emission*

References

Angelova MI, Soleau S, Meleard P, Faucon JF, Bothorel P (1992) Preparation of giant vesicles by external AC electric fields. Kinetics and applications. Progress in Colloid and Polymer Science 89:127-131

Johnson SA, Stinson BM, Go MS, Carmona LM, Reminick JI, Fang X, Baumgart T (2010) Temperature-dependent phase behavior and protein partitioning in giant plasma membrane vesicles. Biochim Biophys Acta 1798:1427-1435

Chapter 4: General discussion

The recombinant expression of the porcine spermadhesin AWN and its purification using three chromatography steps was presented in chapter 2. Characterization of the recombinant protein validated the formation of disulphide bridges and a so far unreported affinity for phosphatidic acid (PA) and cardiolipin. Furthermore an interaction between recombinant AWN and male domestic pig sperm cells was observed, showing a distribution over the acrosomal region similar to earlier results with porcine AWN. An arginine-rich stretch near the N-terminus of the recombinant protein was discussed as potential binding site for PA.

In chapter 3, three fluorescence microscopic techniques – FLIM, FRAP and FCS – were applied to examine fluorescence labeled lipid analogs incorporated in domestic pig sperm membranes. While conclusions from each single method are limited and fragmentary in the respective temporal and spatial window, their combination provided a comprehensive picture of lipid dynamics in vital sperm membranes. The presented results were specific for the three different fluorescent phospholipid analogs and indicated that they are suitable to report on the conditions of surrounding membrane domains with different properties.

4.1 AWN

4.1.1 Recombinant expression of AWN (recAWN)

Proteins recombinantly expressed in prokaryotes such as *E.coli* usually lack posttranslational modifications such as glycosylation. Although *E.coli* strains can be created which have the ability to express glycosylated proteins (Wacker et al. 2002), the type of glycosylation might not reflect the situation *in vivo*. Even eukaryotic cell expression systems are not expected to deliver native glycosylation patterns (see Jenkins and Curling 1994 and references therein). Following this reasoning, we expressed unglycosylated AWN in the presented study even though AWN, like other spermadhesins, shows a conserved glycosylation site at N50 with severe impact on its ligand binding potential (Calvete et al. 1993). A further essential argument was the fact that unglycosylated AWN is the isoform that comes into contact with the sperm membrane already in the epididymis (Calvete et al. 1994). Also, this isoform expresses glycoprotein binding behavior which could even be blocked by glycosylation (Calvete et al. 1993). Therefore the unglycosylated isoform of AWN is – in addition to interaction studies with membranes and sperm cells – suitable for future binding studies with zona pellucida and oviductal (epithelia) proteins as well.

A His-tag was chosen to improve the purification potential and detectability of the recombinant protein. This is a small tag at the C-terminus of recAWN that includes 6 successive histidines, additionally a cleavage site for factor Xa was introduced after the AWN sequence and before the His-tag. Therefore it is also possible to remove the tag, if necessary. Since antibodies for poly-His-

tags are commonly in use, this tag opens up several possibilities for immunodetection and antibody based experiments.

As native AWN is a secretory protein which contains two disulphide-bridges, a classical expression in cytoplasma of *E.coli* strains is not possible. Therefore we selected a modified strain that is able to form proteins containing disulfide bonds in the cytoplasm (SHuffle® T7 Express). As an alternative, we also tested the periplasmic expression but this did not yield a higher expression of native soluble protein (not shown). The formation of disulphide bridges was successfully demonstrated by checking the presence of undesired free SH-groups. The molar ratio between the marker for free thiol groups and recAWN was 0.18, implying most of the disulphide bridges to be intact.

Size exclusion chromatography indicated the existence of a multimeric as well as a monomeric form of recAWN with the latter being the dominant form. It was possible to reduce the proportion of the multimeric form after introduction of a prolonged elution gradient in the His-affinity chromatography which also reduced the contamination with proteins originating from the prokaryotic expression organism (unpublished results, Dommaschke 2016).

4.2 Phosphatidic acid

Phosphatidic acid and cardiolipin presented on nitrocellulose-lipid stripes were identified as binding partner for recombinant AWN. Cardiolipin consists of two phosphatidic acids connected by a glycerol backbone and forms a bicyclic structure, presenting the phosphate groups in a way resembling that of PA and explaining the affinity of AWN.

Since cardiolipins are synthesized in mitochondria of mammals (Schlame et al. 2000) and are almost exclusively present in the inner and outer membrane of this organelle in eukaryotic cells (Schlame 2008) , the further discussion focuses on PA as interaction partner for AWN.

4.2.1 Phosphatidic acid – synthesis and distribution in domestic pig sperm membranes

PA can be synthesized by the acetylation of lyso phosphatidic acid (lysoPA), hydrolysis of phosphatidylcholine (PC) or phosphorylation of diacylglycerol (DAG, see **Figure 18**). PA is an important substrate in the phospholipid metabolism of cells where it functions as a precursor for the synthesis of many other lipids. PA's acyl chain saturation can severely differ depending on its origin either from the hydrolysis of PC through phospholipase D or the phosphorylation of phosphatidylinositol-derived DAG through diacylglycerokinase (Hodgkin et al. 1998). PC in domestic pig sperm cells mainly carries one saturated and one polyunsaturated acyl chain (Lessig et al. 2004b) whereas most DAG in domestic pig sperm cells under resting conditions carries two saturated acyl chains (Vazquez and Roldan 1997). PA and cardiolipin with saturated palmitoyl

chains were used on the lipid strips to detect AWN's potential specificity in terms of phospholipid affinity.

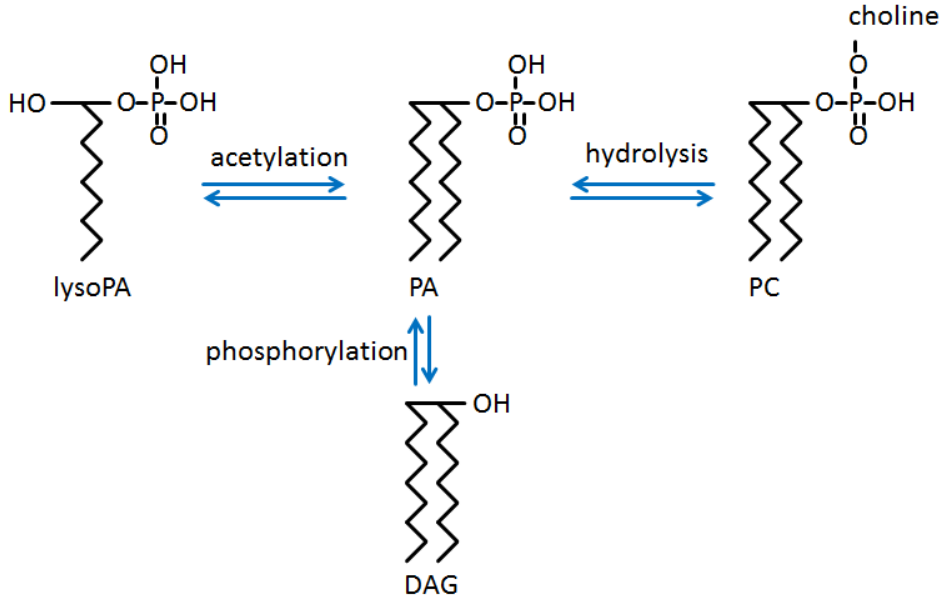

Figure 18: *Schematic view of the different synthesis pathways leading to the synthesis of phosphatidic acid (PA). lysoPA: lyso phosphatidic acid, DAG: diacylglycerol, PC: phosphatidylcholine.*

The PA pool is constantly renewed because of its central position in several synthesis pathways. Even though spermatozoa do not synthesize new proteins (Bedford and Hoskins 1990), they perform *de novo* phospholipid and explicit PA synthesis (Vazquez and Roldan 1997). To elucidate the potential biological function of the detected recAWN interaction with PA, it is important that PA is present in total membrane extracts of ejaculated domestic pig spermatozoa without significantly changing its concentration after capacitation *in vitro* or *in utero* (Evans et al. 1980). It accounts for approximately 1.5 % of the phospholipid content in the membranes of this gamete. In other cells, the PA content can rapidly increase in response to external stimuli (Shukla and Hanahan 1982).

The lateral distribution of PA on domestic pig spermatozoa is unknown. For domestic guinea pig (*Cavia porcellus)* sperm, tests with polymyxin B (PXB) were carried out, showing a distribution of this antibiotic over the fusogenic regions of the acrosomal cap (Bearer and Friend 1980). These authors proposed PA and cardiolipin as anionic binding partners of PXB, suggesting that this was the basis for this localization, and reported an increased binding after proteolysis or capacitation (Bearer and Friend 1982). AWN (Sanz et al. 1992b, Dostalova et al. 1995a) as well as recAWN (see Chapter 2, **Figure 10**) were localized in similar regions on ejaculated domestic pig sperm.

The transversal distribution of PA in sperm membranes is unknown as well. PA seems to lack leaflet preference at physiological pH (Koter et al. 1978). It is possible to induce an asymmetric distribution of PA on either leaflet of large unilamellar vesicles (LUVs) through a pH gradient

(Eastman et al. 1992). Therefore it can be assumed that the transversal distribution of PA maybe controlled by its protonation state *in vivo* (see also **Figure 20**). However, the protonation state of PA is not only influenced by local pH but also by membrane curvature and lipid packing in artificial membrane vesicles (Swairjo et al. 1994).

4.2.2 Functional role of PA

Beside its role as substrate in the phospholipid metabolism of cells, PA can also act as a signaling lipid, for example for the incorporation of cytosolic proteins into the membrane (Delon et al. 2004). An ionophoric function of PA has also been implied (Putney et al. 1980, Cullis et al. 1980). An extensive review on the signaling functions of PA in plants, animals and microorganisms was presented by Wang et al. 2006.

Phospholipids are characterized by so called phase behavior. This term refers to their mode of supramolecular organisation for example in micelles, bilayers or complex structures like the tubular hexagonal or cubic phase (**Figure 19**, see also Frolov et al. 2011, Jouhet 2013 and references therein) and implies transitions between different phases and the formation of phase separations. The characteristics of these phases are determined by the phospholipid structure (fatty acyl chains, e.g. number, length, saturation, and head group structure) and by the environmental conditions (e.g. temperature, pH, ionic strength, presence of divalent cations). The existence of lipid mixtures (e.g. presence of cholesterol) and/or proteins makes the phase behavior of membranes more complex. Therefore, the occurence of phases in biological membranes has been a matter of debate for a long time since these membranes are composed of hundreds of different lipid and protein species. Currently, it is in general accepted that particular lipids can also trigger distinct lipid phases in biological membranes modulating various physiological processes. Some examples are, (i) the formation of lateral domains (so called rafts), and (ii) the segregation of charged phospholipids in the presence of Ca^{2+} ions.

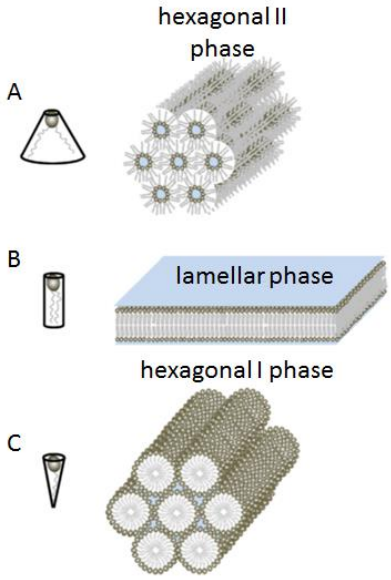

Figure 19: *Influence of phospholipid shape on its spatial organisation. A: Cone shaped lipids with relatively small head groups can organize in hexagonal II and cubic phase (not shown). B: Cylindrical shaped lipids typically organize in lamellar phases like bilayers. C: Inverse cone shaped lipids and lysolipids can form the hexagonal I phase. (Figure adapted from Jouhet 2013)*

PA can have a high impact on membrane curvature and stability (see Kooijman et al. 2003 and references therein) and can therefore play a role in membrane fusion. Its small head group with potentially high charge and hydrogen bonding potential causes a remarkably pH sensitive phase behavior. An extensive overview regarding the physical properties, phase behavior and intermolecular interactions of PA was given by Boggs 1987. Its behavior in membranes may match cone shaped, inverse cone shaped or cylindrical lipids (see **Figure 19**) depending on its protonation which influences the repulsive (charge) and attractive (hydrogen bonding) forces between neighbouring PA molecules (see **Figure 20 B**). The latter seems to be the case at physiological pH (Lu and Benning 2009, Koter et al. 1978, Verkleij et al. 1982, Eibl and Blume 1979).

Figure 20: *Influence of pH on hydrogen bonding potential and occupied membrane area.*

A: Different protonation states of PA depending on pH. Green: hydrogen bonding donor groups, red: hydrogen bonding acceptor groups. Note that PA's charge increases with pH.

B: Lipid shape and repulsive electrostatic forces. Even though the volume of the phosphate head group decreases with deprotonation, the repulsive forces of the negative charges (red) increase the surface area occupied by each phospholipid. Fully protonated PA (left) behaves like a cone shaped lipid inducing negative membrane curvature. At neutral pH, PA forms bilayers like a cylinder shaped lipid, while fully deprotonated PA induces positive membrane curvature through its repulsive head group charges.

C: If PA's head group charges are neutralized, for example by divalent cations, the curvature can be reversed.

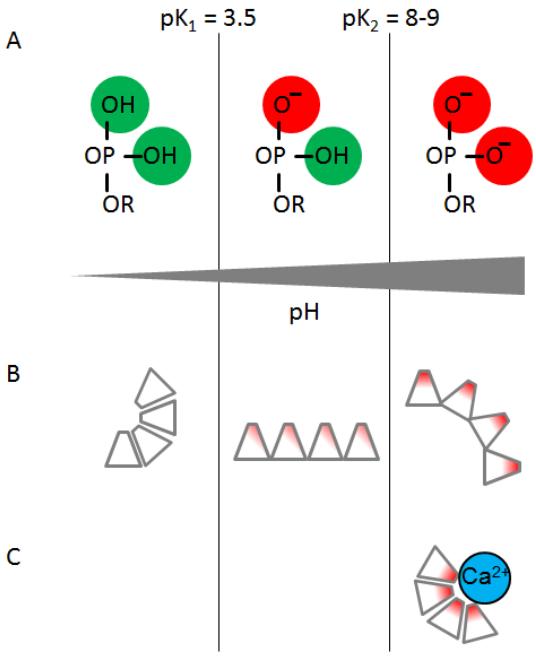

The addition of divalent cations to membrane vesicles containing anionic lipids (Papahadjopoulos et al. 1978) and specifically PA (Simmonds and Halsey 1985, Koter et al. 1978) induced phase transition and fusion of said vesicles, which is detectable by an increase of their size. Depending on pH and presence of divalent cations, PA explicitly expresses phase transitions from a bilayer forming liquid phase to the non-bilayer hexagonal II (H_{II}) phase (**Figure 19 A**, Verkleij 1984). This kind of transition has also been linked to membrane fusion and acrosome reaction of sperm cells (Martinez and Morros 1996). Furthermore, studies with murine and human spermatozoa revealed a PA induced rapid actin polymerisation, leading to hyperactivated movement (Itach et al. 2012). This

movement pattern is also observed without artificial PA addition at the site and time of fertilization and has been linked to functions including, but not limited to, the penetration of the oocyte's zona pellucida and sharp turns during chemotaxis (see Armon and Eisenbach 2011 and references therein).

4.3 AWN-PA binding and its possible functional role

4.3.1 Location and binding mechanism of AWN's PA binding site

The distinctive feature which separates PA from other phospholipids is its exceptionally small head group with one phosphate group at a terminal position, presenting one negative charge at physiological pH. It was stated that the phospholipid is prone to the formation of intermolecular hydrogen bonds while not being able to form intramolecular bonds like other membrane lipids (Boggs 1987).

Several proteins express an affinity to PA without sharing a common sequence but being enriched in basic amino acids, especially lysine and arginine (Kooijman et al. 2007, Wang et al. 2006, Andresen et al. 2002). It was proposed by Kooijman et al. 2007 that these are first attracted by PA's single negative charge at physiological pH prior to hydrogen bonding to the phospholipid. It was further proposed that the positive charge of the amino acid residues then increases the local pH, leading to a second deprotonation of PA and a further rise in binding strength to the protein (Kooijman et al. 2007, visualized in **Figure 22 C**). The effect was stronger with lysine, but also detected for arginine. Contact with poly-lysine peptides also lead to local accumulation of PA and phase separation (Galla and Sackmann 1975a, Galla and Sackmann 1975b), underlining the interactive behavior of this amino acid.

Following this reasoning I propose that the section of amino acids around the three basic arginines ^{3}NRRSRS^{8} (amino acid numbering according to native AWN sequence without signal peptide) within the proposed phospholipid binding site of AWN (Enßlin et al. 1995) is responsible for the interaction of recAWN with PA. It was reported that each arginine has the potential to provide five hydrogen bond donor groups (Shimoni and Glusker 1995). Considering the results about hydrogen bond patterns made by Shimoni and Glusker I propose that each arginine is capable of binding two PA molecules through hydrogen bonds (**Figure 21**, fully deprotonated PA can interact similarly). Since during this process only one positive charge per arginine is brought in the vicinity of the membrane, the repulsive forces between the PAs would be reduced but not eliminated (**Figure 21 C**). Moreover this could lead to the close accumulation of six PAs per AWN molecule bound to the membrane.

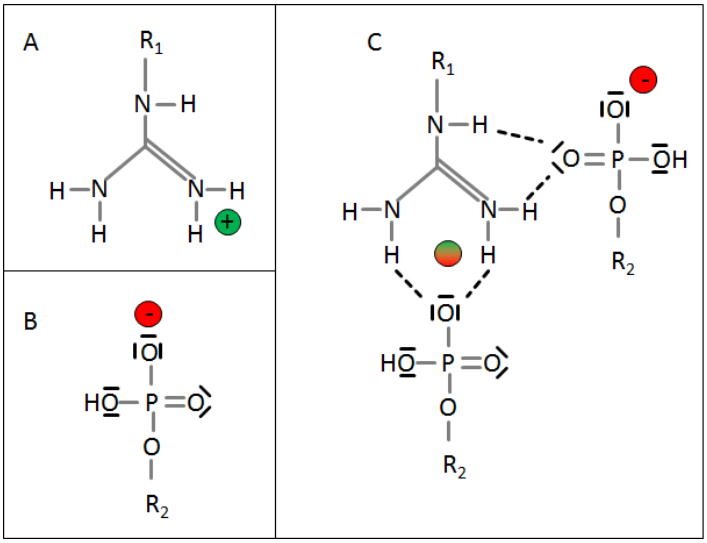

Figure 21: *Vizualisation of hydrogen bonding between arginine and PA. A: schematic view of arginines guanidino group. R_1: amino acid backbone, green circle: positive charge. B: schematic view of PA's negatively charged head group. R_2: Diacylglycerol, red circle: negative charge. C: schematic view of potential hydrogen bonding between arginine and two PAs. The opposing charges are neutralized (bicolored circle) with one negative charge remaining. Dashed lines: potential hydrogen bonds.*

4.3.2 Potential functional role of AWN – PA binding

As AWN has been proposed to form a layer around the acrosomal region of domestic pig sperm cells, it can be assumed that the PA binding will result in its accumulation in this membrane region. By interacting with PA in the membrane, AWN might prevent interactions of this lipid with divalent cations which induce membrane destabilization and fusion in artificial PA containing membrane vesicles (Koter et al. 1978, Simmonds and Halsey 1985). The AWN layer associated with the sperm membrane might therefore serve as a protectant against premature acrosome reaction. In this context it is intriguing that the primal AWN layer originating from the epididymis consists of unglycosylated proteins (Calvete et al. 1994). Unglycosylated AWN expresses binding affinity to carbohydrates of the oocyte's zona pellucida (Dostalova et al. 1995a) through a binding site which does not overlap with the phospholipid binding domain (Calvete et al. 1994, Ekhlasi-Hundrieser et al. 2008a). Interestingly, this primal AWN layer might become exposed at the sperm surface just after the secondary spermadhesin hull is released prior to the contact with the gamete. In turn, the contact with the zona pellucida could trigger the release of any AWN from the sperm to uncover the anionic phospholipids and initiate their phase transition to precede the acrosome reaction.

4.3.3 Similarities in other species

PXB-binding (see 4.2.1) to epididymal domestic guinea pig sperm increased after proteolysis. This might suggest that epididymal proteins similar to AWN are present in this species and mask the charges of PA. Following proteolysis of these proteins, PA is exposed, causing the reported increase in PXB-binding. Recalling that equine HSP-7 differs from AWN in only 3 amino acid substitutions offside the proposed phospholipid binding region, an affinity and function similar to AWN is likely for the equine protein.

4.4 Functional model of AWN's membrane interaction

4.4.1 Potential role of AWN's serine proteinase inhibitor binding potential

A further aspect of the physiological importance of AWN relates to its binding site for serine proteinase inhibitors (SPI), including acrosin inhibitors present in the seminal fluid and even soy bean trypsin inhibitor (Sanz et al. 1992a, Dostalova et al. 1995a). This gives me the opportunity to undertake some hypothetical considerations.

Acrosin is an enzyme whose precursor form is found in the sperm acrosome. It is released during the acrosome reaction and is believed to aid in the binding and penetration of the zona pellucida. The enzyme has an endoproteinase activity, cleaving behind basic amino acids. Its inhibitors can be found in the seminal fluid of pigs and comprise three sperm associated acrosin inhibitor (SAAI) isoforms (Jonakova et al. 1992). These inhibitors have been linked to the protection of the male gametes against enzymes released prematurely from damaged spermatozoa. Studies on domestic cattle (Cesari et al. 2004b), golden hamster (*Mesocricetus auratus,* Cesari et al. 2005), mouse (Honda et al. 2002) rat and human (Cesari et al. 2004a) spermatozoa showed that other serine proteases might also be present on the plasma membrane. In the domestic pig, a membrane bound trypsin like protease was identified in the membrane of porcine cauda epididymal sperm flagella (Okamura et al. 1990). Furthermore acrosin is also present on the plasma membrane of acrosome intact human spermatozoa (Tesarik et al. 1990). Taken together these studies highlight the importance of protease protection even for acrosome intact sperm cells.

The sperm associated acrosin inhibitor form is already present in the domestic pig's epididymis (Jonakova and Cechova 1985, Manaskova-Postlerova et al. 2016, Davidova et al. 2009). Its immunolocalization revealed a distribution over the acrosomal head region similar to AWN (Davidova et al. 2009). Indeed, acrosin inhibitors bind to AWN and this did not hinder AWN to successively contact the zona pellucida which in turn caused the displacement of the inhibitor from the spermadhesin *in vitro* (Sanz et al. 1992a). Therefore it can be argued that the interaction with the zona pellucida glycoproteins releases the SAAI from the membrane *in vivo*, thus enabling acrosin function.

In this context it is interesting to note that Enßlin et al. identified in a zona pellucida binding assay a sperm derived AWN form truncated of the first five amino acids, a stretch which contains a part of the proposed PA binding domain (Enßlin et al. 1995). This was unexpected because several studies were able to collect full length AWN from sperm cells (Sanz et al. 1992d, Sanz et al. 1992b, Sanz et al. 1993, Calvete et al. 1994, Jonakova et al. 1998). These seemingly controversial results might be a consequence of differences in methods, since Enßlin et al. performed a nitrogen cavitation which releases the cell membrane and related proteins from sperm. Since this also damages a part of the acrosome, the serine protease acrosin might become released. When coming into contact with

AWN, the spermadhesin is likely to be enzymatically digested within the sequence ^{1}AWNRRSRS^{8} thereby creating the reported truncated form.

4.4.2 Hypotheses on the functional role of AWN's different binding sites

The variety of binding affinities of AWN, including heparin, zona pelludica glycoproteins, SPI and according to this study PA, lead to the following considerations regarding the functional role of the different ligands. The PA binding most likely mediates the sperm membrane association of the protein, together with some additional effects discussed in **Figure 22** and the corresponding paragraphs. Through competition with PA over the overlapping binding sites, heparin like molecules might be used to regulate AWN's association with sperm and potentially release it from the membrane prior to acrosome reaction. Heparin belongs to the polysaccharide family of glycosaminoglycans (GAGs) which are secreted by the epithelium of the female genital tract, for instance with hyaluronan being localized at the epithelium of the sperm reservoir (Tienthai et al. 2000). Other studies also implied a role for heparin or heparin-like GAGs in sperm-zona pellucida interactions (Coy et al. 2008). GAGs were furthermore linked to the induction of sperm capacitation (Varner et al. 1993) which seems to be mediated by their interaction with heparin binding proteins from the seminal fluid (Miller et al. 1990, Calvete et al. 1996a). Therefore, AWN's heparin binding site might also play a role during the formation of the oviductal sperm reservoir, an idea also proposed by Liberda et al. 2006. This would be consistent with the fact that this interaction is most likely mediated by spermadhesins constituting the multilayer hull around the sperm acrosomal region (Dostalova et al. 1994b) and which therefore lack any immediate membrane contact. Therefore, the overlapping PA/heparin binding site would not be blocked by the phospholipid.

Regarding the other affinity site for SPI and glycoproteins, it seems likely that AWN recruits SPIs during the sperm differentiation in the epididymis (Jonakova and Cechova 1985). It is assumed that the AWN-mediated presence of the inhibitors protects the male gametes from premature degradation through acrosin released from dying spermatozoa as well as from potential plasma membrane associated serine proteases. It is noteworthy that the premier AWN layer around the acrosome is unglycosylated (Calvete et al. 1994), therefore expressing SPI affinity (Calvete et al. 1993) and consequently being successively covered by the protective hull of further spermadhesins during ejaculation. This hull should then protect the SPI carrying binding site from contact to the environment and potential SPI displacement by glycoprotein binding (Sanz et al. 1992a). After capacitation and exit from the oviductal sperm reservoir, the outer spermadhesin layers are released (Töpfer-Petersen et al. 1998). Shortly after that, the spermatozoa reach the oocyte and penetrate the cumulus cells, reaching the zona pellucida. It can be assumed that SPIs bound to the premier AWN layer are then displaced by interaction with zona pellucida glycoproteins competing for the binding site (see **Figure 22 D** and Sanz et al. 1992a). Following this, acrosin activity is enabled at the exact locality needed for successful fertilization.

I furthermore hypothesize that the displacement of SPIs after contact to the zona pellucida leads to the cleavage of AWN by potentially membrane associated serine proteases (**Figure 22 E**). After its subsequent displacement from the sperm membrane, negatively charged PA is presented and can act as a Ca^{2+} ionophore (Cullis et al. 1980, Putney et al. 1980). Ca^{2+} is known to induce the acrosome reaction (Talbot et al. 1976). It was also linked to the attachment of overlaying bilayers by water displacement (Papahadjopoulos et al. 1978). The membrane fusion events during the acrosome reaction will most likely be enhanced through the destabilizing effect on the membrane of deprotonated PA especially if it is locally accumulated.

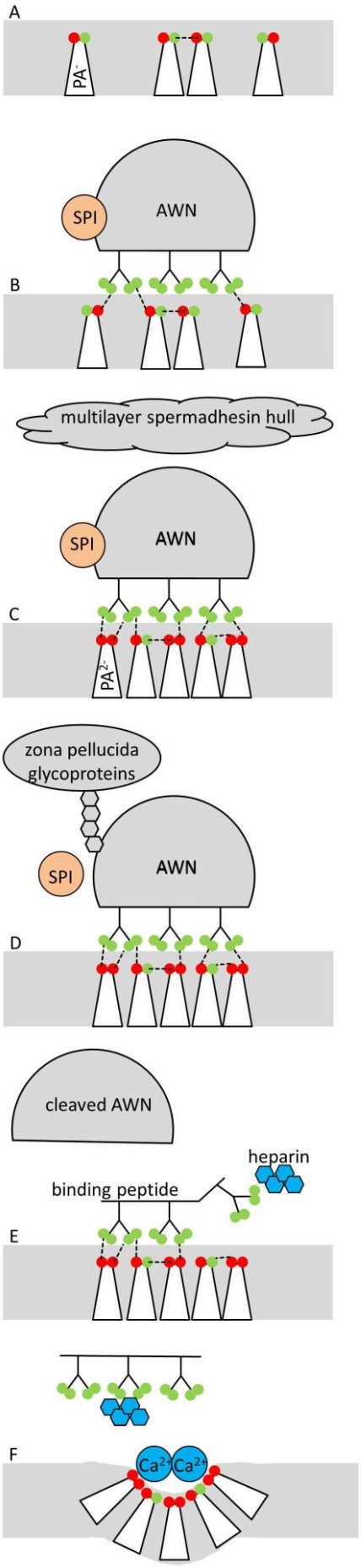

Figure 22: *Graphical presentation of an extended hypothesis on the functional role of AWN and its binding characteristics during fertilization.*

A: PA in the outer leaflet (grey) of the sperm plasma membrane before interaction with AWN is singly charged, presenting a hydrogen bonding donor (green) as well as acceptor group (red). Temporary associations are mediated by hydrogen bonds (dotted line).

B: AWN's arginine rich phospholipid binding domain binds through electrostatic attraction and hydrogen bonding to epididymal spermatozoa. This epididymal AWN fraction is unglycosylated, therefore expressing potential binding affinity to zona pellucida glycoproteins and serine protease inhibitors (SPI). The latter are recruited to the sperm membrane already in the epididymis.

C: The presence of the positively charged arginine residues increases the local pH thereby further deprotonating PA. The repulsive forces of the negative charges are dampened by the attractive hydrogen bonds and AWN's positive charges. A multilayer spermadhesin hull including glycosylated AWN is recruited during ejaculation. The outer layers mediate the binding to the oviductal sperm reservoir and are released after capacitation.

D: Reaching the oocyte, the remaining AWN layer gets into contact with the zona pellucida. Protease inhibitors are released through competitive binding with zona pellucida glycoproteins.

E: Acrosin or plasma membrane localized serine proteases cleave the phospholipid binding domain from AWN. The cleaved short PA-bound peptide is easier accessible to competitive heparin-like ligands and begins to detach.

F: The accumulated, deprotonated and negatively charged PA presents a potent interaction site for Ca^{2+}, which leads to local destabilization/disruption of the membrane. These patches can further function as Ca^{2+} ionophores or take part in membrane fusion events. Ca^{2+} subsequently induces the acrosome reaction.

4.5 Biophysical methods for the experimental validation of AWN's role in fertilization

The ideas and discussions in the previous sections lead to some general hypotheses:

1. AWN originates from the epididymis, directly interacts with the lipid matrix of domestic pig sperm cells and serves as an anchor, attaching further ligands by its variety of binding sites.
2. Physico-chemical sperm membrane properties are influenced by AWN.
3. AWN's binding characteristics themselves are modulated by the interaction with its different ligands.
4. AWN release from the sperm membrane might be triggered by serine protease cleavage. This induces potentially heparin mediated loss of the PA-binding sequence on the sperm membrane followed by membrane destabilization.

Since epididymal AWN and recAWN share a lack of glycosylation, the recombinant protein seems to be suitable to test these hypotheses.

Several biophysical methods are available which provide the means to analyze protein-membrane (lipid) interactions in order to gain further knowledge about this protein and its role in fertilization but come with different advantages and disadvantages each. They mostly require the presence of suitable labels to localize molecules and detect dynamic changes. These labels can be added to recAWN as well as membrane lipids or other binding partners and should ideally not influence the examined processes through their presence. The experiments performed to exclude His-tag induced PA binding of recAWN (see section 2.4 and **Figure 9**) underlined the potential difficulties of labeling a protein with multiple binding sites which might be blocked by the used label. Methods of protein labeling include the expression of fusion proteins with for example GFP (Snapp 2005), usage of antibodies or labeling at primary amines, cysteines or introduced specific tags.

Maekawa and Fairn 2014 provided a general overview on the advantages and disadvantages of different methods for lipid labeling. Acyl chain labeled PA would be a suitable analog for studies on artificial membranes. When applied on cell membranes, a challenge is the fact that PA is a key player in the phospholipid metabolism continuously being processed and synthesized. It therefore has to be checked to what extent the PA analog was processed during such measurements to validate the significance of the results. Labeling the head group of PA would disturb – if not even eliminate – its distinctive ability to form hydrogen bonds and limit AWN's binding affinity to the analog and is therefore not considered any further in the following paragraphs. Another approach would be to use labeled analogs of other membrane lipids to examine the effect of AWN on the physico-chemical properties of sperm membranes.

Other AWN ligands such as heparin are commercially obtainable in fluorophore conjugated versions (amongst other from Thermo Fisher Scientific, Darmstadt, Germany), whereas antibodies

against acrosin inhibitors present in porcine seminal fluid and on domestic pig sperm cells are also in use (Davidova et al. 2009). The arguments about the labeling of recAWN also apply to acrosin inhibitors as well as to zona pellucida proteins (Burkin and Miller 2000).

In the following paragraphs 4.5.1 to 4.5.5 I will discuss several biophysical methods, which were not used in this study, regarding their suitability for studies on interactions between AWN and the sperm membrane.

4.5.1 Electron paramagnetic resonance spectroscopy (EPR)

Electron Paramagnetic Resonance Spectroscopy (EPR) can be used to investigate interactions between proteins and lipids (Marsh 1990). This technique uses the measurement of energy absorption of unpaired electrons in an external magnetic field. These unpaired electrons can be found in transition metals, free radicals and specifically designed spin labels. An advantage of these labels is their relatively small size compared to common fluorescence labels. When the molecular mobility of labels is altered, a change in their EPR spectra is induced and can be detected. This might be caused e.g. when a labeled lipid interacts with a protein when it is immobilized or extracted from the micellar phase (for an example see Müller et al. 1998). Therefore, the interaction between recAWN and artificial membranes containing spin labeled PA could be monitored using EPR as well as its dependence on pH and membrane curvature.

Furthermore, spin labeled lipid analogs can be incorporated in viable spermatozoa similarly to the fluorescent analogs used in Chapter 3 (Müller et al. 1994). The usage of PA analogs would request validation of the amount of PA processing as mentioned before. Analogs of other membrane lipids can be applied to indirectly examine physico-chemical changes in the sperm membrane induced by recAWN-PA interaction.

4.5.2 Nuclear magnetic resonance spectroscopy (NMR)

Quite similar to EPR, nuclear magnetic resonance spectroscopy (NMR) is based on the measurement of energy absorption by atomic nuclei with a spin different from zero as for example the naturally occurring isotopes ^{1}H, ^{13}C or ^{31}P (for an extensive review see Marion 2013). NMR is commonly used to obtain the three-dimensional structure of proteins. The phase of PA can be detected by its distinctive NMR signal even without labeling (Farren et al. 1983), since its spectrum differs significantly from other phospholipids. Similar experiments can be performed to evaluate lateral membrane compression (Traikia et al. 2002). This might be used to detect possible changes in the phase behavior of PA and phospholipid packing in the membrane in response to the interaction with or loss of contact to AWN (see **Figure 22**).

4.5.3 Surface plasmon resonance (SPR)

Surface plasmon resonance monitors changes in the refraction index of a material, e. g. a membrane, which influences the reflection behavior of a laser beam (for a review see Homola 2008). With such a refraction-based approach, there is no need for probe labeling, but the studied molecules have to be located in a thin layer. The method can be used for interaction studies between molecules and ligands and to determine the binding kinetics of this interaction. Therefore, experiments similar to previous studies on the interaction of the bovine seminal plasma protein PDC-109 with artificial membranes (Thomas et al. 2003) would be suitable to gain further knowledge on the interplay between AWN and PA and the role of phospholipid composition of the membrane. Another approach could include the immobilization of recAWN on a sensor chip and successive binding studies of sperm cells (see Quinn et al. 1997 for a similar application on red blood cells). This could be used to validate the presence and accessibility of PA on the membrane of sperm cells from different stages of the fertilization process. A further application might arise from the presented lack of recAWN binding to spermatozoa with lost acrosome (see Chapter 2, **Figure 10**) which could be used for sperm sorting prior to artificial insemination.

4.5.4 Circular dichroism (CD) spectroscopy

Circular dichroism (CD) spectroscopy is a technique based on the absorption of polarized light by biological molecules (Woody 1995). Amongst other applications it can be used to investigate the secondary structure of proteins, conformational changes and binding of ligands. This could be used to study conformational changes of AWN induced by interaction with sperm or artificial membranes.

4.5.5 Fluorescence spectroscopy

Fluorescence spectroscopy is another technique suitable to examine interactions of proteins with membranes (see Greube et al. 2004). Besides the measurement of fluorescence labeled molecules, the autofluorescence spectrum of an unlabeled protein caused by its tryptophan, tyrosine and phenylalanine residues can also be recorded to examine interactions of proteins with artificial membrane vesicles. If the protein gets into close contact or even integrates into the vesicle, the immediate environment of the fluorescent amino acids can change which leads to a shift in the fluorescence spectrum or quantum yield. Similar effects can be caused by conformational changes induced by interactions between molecules. Yet autofluorescence measurements in whole cells with their broad variety of proteins are not reasonable. In these cases like in most fluorescence based approaches the molecule in question – either AWN or its potential interaction partner – has to be labeled with a fluorophore. Another approach used for protein-lipid-interaction studies is Förster Resonance Transfer (FRET, Loura et al. 2010). Here the potential interaction partners are labeled with different fluorophores with overlapping excitation and emission spectra. If both molecules are

in close proximity, excitation of the fluorophore with the lower excitation wavelength leads to energy transfer and fluorescence emission from the other fluorescence label which can be detected by fluorescence spectroscopy. As mentioned before it has to be considered that these dyes might influence the *in vivo* behavior of the studied molecules by their size, mass or polarity.

Summing up, EPR and NMR are more suitable for studies on membranes and their lipids, SPR for examination of interaction kinetics, CD spectroscopy for the evaluation of protein structure and its changes and fluorescence spectroscopy for the validation of interactions between labeled molecules and potential interaction partners.

4.5.6 Applicability and advantages of FLIM, FRAP and FCS for AWN studies

All the methods discussed in paragraph 4.5.1 to 4.5.5 are used to study the cells, membranes or molecules of interest and their interactions in solutions without the possibility to discriminate individual cells and their properties. In contrast, the methods presented in Chapter 3 (FLIM, FRAP, FCS, Schröter et al. 2016) are all based on the use of a confocal laser scanning microscope (CLSM) which permits the examination of single cells and their subdomains. This is of special importance in highly structured cells such as spermatozoa, where functionally important differences between the tail, midpiece as well as the acrosomal and postacrosomal head region are expected. Furthermore, the high resolution of the CLSM and the option of applying dyes for viability control permit the discrimination of damaged, malformed and dead spermatozoa, thereby substantially improving the value of the data gained. Last but not least the measurements can be performed under conditions mimicking the *in vivo* situation regarding temperature and buffer presence.

Fluorescence labeled PA can be incorporated in artificial membranes and vesicles. If several fluorescence labeled PA molecules interact with recAWN as proposed in **Figure 22 B**, their close proximity would lead to an increase of non-emitting energy transfer between the fluorophores, a process called self-quenching. Since these energy transfer processes compete with fluorescent energy loss in a time dependent manner, they lead to a detectable decrease of fluorescence lifetimes. If a similar experiment is performed in sperm cells, it has to be checked whether the metabolization of the PA analog is low enough to gain significant results as mentioned above.

Fluorescence labeled analogs of other membrane lipids can be used to indirectly study PA's interaction with AWN and its local accumulation also in sperm cells. PA is assumed to interact tightly with other potentially labeled phospholipids in membranes via its pronounced intermolecular hydrogen bonding potential (Boggs 1987). If this bonding potential is instead involved in the interaction with AWN this might lead to a separation of PA from other membrane incorporated lipid analogs. This might result in an increased mobility and accessibility of these analogs to external quenchers, decreasing their fluorescence lifetime. Furthermore, an interaction between PA and AWN will likely induce changes in lipid packing, membrane thickness and accessibility of

phospholipid head groups to surrounding water molecules. All three effects might effectively influence the fluorescence lifetime of other labeled lipid analogs which can be monitored in all areas of the cell by FLIM.

Regarding the hypotheses presented in **Figure 22** and the corresponding paragraphs above it would be of special interest to perform further studies including fluorescence labeled acrosin inhibitors, which are commercially available from Thermo Fisher Scientific (Darmstadt, Germany), amongst others. Fluorescence techniques as well as classical fluorescence microscopy could be used to determine the presence of the inhibitors on the spermatozoa and their interaction with AWN. The use of epididymal sperm would be of great value, since the unglycosylated recAWN is likely to mimic the first AWN fraction which comes into contact with the spermatozoa in the epididymis.

As elaborated before, FRAP is commonly used to study molecular movements and calculate diffusion coefficients. Unfortunately, the evidence in this work demonstrates that this technique is not ideally suited for studies of lipid analogs in the membrane of sperm. One reason is the very small size of the area of the sperm membrane and its subdomains in particular. This is inconsistent with one of FRAP's basic assumptions, an approximately infinite size of the unbleached region compared to the size of the bleach spot. Another problem arises from the usage of a laser scanning mode to achieve sufficiently small bleaching spots. This led to a relatively long bleaching time, inconsistent with the FRAP assumption that this event is fast enough to neglect diffusion during bleaching. However, FRAP allows for other interesting studies regarding the interaction between AWN and sperm membranes. The possibility to create bleaching areas with variable size and form permits the examination of diffusion barriers as source for the possible accumulation of PA in the acrosomal head region. This might be tested by incorporating a fluorescent PA analog in sperm cells and eliminating fluorescence in the postacrosomal region to monitor the ability of the label to cross the equatorial segment.

Since FCS provides more trustworthy results for diffusion coefficients in sperm membranes and therefore membrane fluidity, this technique might be suitable to examine multiple effects on phase behavior implied for PA. The formation of a hydrogen bonding system of PA, either homogenous or under the participation of other phospholipids, will greatly influence its diffusive behavior. This might also be examined indirectly using NBD-SM, -PS or -Ch, to avoid the aforementioned problems regarding labeled PA analogs. Furthermore, the interaction with Ca^{2+} or AWN leading to local accumulation of several PA molecules, phase separation or even transition to a non-bilayer phase could be examined with FCS. For example, the association of AWN to PA proposed in **Figure 22 B** could be detected since fluorescence caused by the transit of these interacting molecules through the confocal volume would differ significantly from freely diffusing molecules. Self-quenching of AWN-bound fluorescence labeled PA-analogs in close proximity could be avoided either by careful adjusting its concentration in the examined membrane or by fluorescence

labeling of AWN. This local accumulation of PA molecules and interaction with AWN might also influence the membrane fluidity and therefore might be examined indirectly using NBD-SM, -PS or -Ch.

4.6 Advantages of recombinant expression of AWN for interaction studies

Recombinant expression provides several advantages and possibilities for further studies including the creation of fluorescent fusion proteins (Snapp 2005). Yet this option is not suitable for our recAWN due to its small size compared to fluorescent groups like GFP (26.9 kDa) which might therefore have a severe influence on the proteins function.

As mentioned before, our recAWN is likely to mimic the properties of AWN of epididymal origin because of its lack of glycosylation. The phospholipid ligand identified here could be used to separate glycosylated AWN from seminal plasma by using a PA-based affinity chromatography. This would encourage comparative studies on AWN which originates from different source tissues, thereby providing a way to shed some light into the mechanism of spermadhesin multi-layer formation around domestic pig sperm cells. Both protein variants (native and recombinant) can be fluorescence labeled through the linkage of fluorophores to primary amines, for example by NHS esters, as used in Chapter 2 (Schröter et al. 2016). Such a reaction might block functional sites and motives of the studied protein, as seems to be the case in recAWN, where PA affinity was abolished after labeling. A shift of the pH of the reaction buffer to lower values can be used to preferentially label the N-terminal amines instead of other groups (Selo et al. 1996), even though this seems to depend on protein properties (Modesti 2011). It remains to be tested whether this would preserve AWN function in the labeled protein. Another common approach is the labeling of thiol groups. Even though AWN possesses 4 cysteines, all of them are involved in structural disulfide bridges, therefore discouraging this approach.

Besides its role in protein purification and as target for antibodies, the His-tag of recAWN can also be used for reversible labeling of the protein using the tag affinity to nickel ions (Krishnan et al. 2007). This approach has the advantage that the fluorophore would be added offside the amino acids corresponding to the natural occurring AWN sequence at the artificial C-terminal His-tag of recAWN. The label would also be positioned far distant from the proposed phospholipid binding site.

Labeling the C-terminal His-tag and the N-terminus of the protein would provide the opportunity to validate a potential serine protease cleavage site at the N-terminus of AWN since both cleavage products would be fluorescent. If the protein is cleaved to induce its release from the sperm membrane (see **Figure 22 E**) the loss of the C-terminal fluorescence signal could be monitored while still retaining the N-terminal fluorescence of the binding peptide (**Figure 22 E**) on the membrane.

Other possibilities arising from the recombinant expression of proteins are distinct site directed mutations which can be especially valuable to determine the importance of amino acids for binding characteristics (for an example see Ekhlasi-Hundrieser et al. 2008a). Given the importance of the PA binding domain as revealed by my work, it would be of high interest to perform mutagenesis studies where arginine residues in the proposed binding domain ^{3}NRRSRS^{8} are replaced by other amino acids, or where this sequence is even excluded in order to confirm its role for heparin and PA specific binding.

Zusammenfassung

Spermadhesine sind Seminalplasmaproteine von Huftieren mit vielfältigen Funktionen während der Fortpflanzung. Von besonderem Interesse ist dabei das porcine (*Sus scrofa domestica*) Spermadhesin AWN, welches bereits in der Epididymis direkt mit der Spermienmembran interagiert. Im Zuge dieser Arbeit wurde es daher, versehen mit einem C-terminalen His-tag, rekombinant in *E.coli* exprimiert. Die Aufreinigung aus dem Zelllysat erfolgte durch Affinitätschromatographien, welche den His-tag sowie eine bereits postulierte Heparin-Affinität nutzten, sowie durch eine anschließende Größenausschlusschromatographie. Die Ausbildung der für natives AWN postulierten Disulfidbrücken konnte durch einen Fluorescein-Maleimid-Assay nachgewiesen werden.

Mittels Immuncytochemie konnte nachgewiesen werden, dass das rekombinante AWN an Eberspermien bindet. Um künftig die Interaktion des AWN sowie weiterer Spermadhesine mit Eberspermien genauer untersuchen zu können, wurden fluoreszenzmikroskopische Methoden – Fluorescence Lifetime Imaging Microscopy (FLIM), Fluorescence Recovery after Photobleaching (FRAP) und Fluorescence Correlation Spectroscopy (FCS) – für die Messung an porcinen Spermien etabliert und zur Membrancharakterisierung genutzt. Alle drei Methoden erlauben selektive Messungen an einzelnen Zellen und Regionen der Spermienmembran bei gleichzeitiger Unterscheidung der Zellen bezüglich Vitalität und Entwicklungszustand. Sie unterscheiden sich dabei in ihrer zeitlichen und räumlichen Auflösung und damit in ihrer Eignung für verschiedene biologische Fragestellungen.

Das Screening der Bindung von rekombinantem AWN an Lipidstreifen ergab eine bisher nicht beschriebene selektive Affinität zu Phosphatidsäure (PA). Dies eröffnet unter Anderem neue Perspektiven für die Nutzung von PA-Matrizen zur Aufreinigung von AWN auch in seiner glykosylierten Isoform aus dem Seminalplasma.

Die Ergebnisse der Lipidstreifenassays legen nahe, dass die Interaktion des AWN mit der Spermienmembran auf seiner Affinität zu PA basieren könnte und führten zu einer umfassenden Hypothese bezüglich seiner Rolle während der Spermienpassage durch den Genitaltrakt. Die Bindung von AWN würde zunächst einen potenziellen Schutz bzw. die Stabilisierung von Ansammlungen geladener PA Moleküle in der Spermienmembran bewirken. Erst bei Erreichen der Zona Pellucida der Eizelle könnte die Ablösung von AWN induziert und die ionophore und membrandestabilisierende Eigenschaft der PA genau dann aktiviert werden, wenn diese Reaktivität für die Akrosomreaktion nötig ist.

Die vorliegende Arbeit bereitet die Grundlage für ein Verständnis der funktionellen Rolle der Spermadhesine im Befruchtungsprozess. Die postulierte duale Funktion von AWN sowohl bei der Stabilisierung der Spermienmembran als auch ihrer Vorbereitung auf Fusionsereignisse kann

perspektivisch auch artübergreifend zur Optimierung der assistierten Reproduktion genutzt werden, insbesondere wenn zur Arterhaltung nur epididymale Spermien zur Verfügung stehen.

Summary

Spermadhesins are seminal plasma proteins of ungulates with multiple functions during reproduction. The porcine (*Sus scrofa domestica*) spermadhesin AWN is of special interest as it begins to interact with the sperm membrane already in the epididymis. Therefore, AWN together with an additional C-terminal His-tag was recombinantly expressed in *E.coli*. The purification of recombinant protein from the cell lysate was performed by affinity chromatographies exploiting the His-tag as well as an already postulated heparin affinity followed by size exclusion chromatography. The formation of disulfide bridges postulated for native AWN could be verified by a fluorescein-maleimide-assay.

Next, using immunocytochemistry, the binding of recombinant AWN to domestic pig sperm cells was demonstrated. Several methods were then established to facilitate the examination of the interaction of AWN and other spermadhesins with domestic pig sperm in future. Three types of fluorescence microscopic measurements, fluorescence lifetime imaging microscopy (FLIM), fluorescence recovery after photobleaching (FRAP) and fluorescence correlation spectroscopy (FCS), were successfully established to investigate porcine sperm cells and characterise its membrane. All three methods allowed selective measurements of single cells and sperm membrane subregions after discrimination of individual cells by their viability and functional stages. The three methods differ in their temporal and spatial resolution and therefore their suitability to address diverse biological questions.

The screening for the binding of recombinant AWN to lipid stripes revealed a so far unreported selective binding to phosphatidic acid (PA). This opens up new perspectives for the usage of PA-matrices for the purification of AWN also in its glycosylated isoform from the seminal plasma. It resolves also some longstanding methodological controversies in the literature.

The results of the lipid-stripe-assays imply that the interaction of AWN with the sperm membrane could be mediated by the proteins affinity to PA. This led to an integrated hypothesis regarding its role during the sperm passage through the genital tract. Initially, the binding of AWN might potentially protect or respectively stabilize accumulations of several charged PA molecules in the sperm membrane. Later, only after the arrival at the oocyte's zona pellucida, AWN's displacement would be induced and the ionophoric and membrane destabilizing properties of the PA would be activated exactly when their reactivity is needed for the acrosome reaction.

This work sets the stage for understanding the functional role of spermadhesins during the fertilization process. Especially the proposed dual function of AWN in the stabilization of the membrane as well as in its preparation for fusion processes might be used to optimize assisted reproduction in endangered wildlife porcine species, particularly if only epididymal sperm cells are available for species conservation.

References

Adkins E. M.; Samuvel D. J.; Fog J. U.; Eriksen J.; Jayanthi L. D.; Vaegter C. B.; Ramamoorthy S.; Gether U., 2007: Membrane mobility and microdomain association of the dopamine transporter studied with fluorescence correlation spectroscopy and fluorescence recovery after photobleaching. Biochemistry, *46* 10484-10497.

Almeida P. F.; Pokorny A.; Hinderliter A., 2005: Thermodynamics of membrane domains. Biochim Biophys Acta, *1720* 1-13.

Amaro M.; Sachl R.; Jurkiewicz P.; Coutinho A.; Prieto M.; Hof M., 2014: Time-resolved fluorescence in lipid bilayers: selected applications and advantages over steady state. Biophys J, *107* 2751-2760.

Andresen B. T.; Rizzo M. A.; Shome K.; Romero G., 2002: The role of phosphatidic acid in the regulation of the Ras/MEK/Erk signaling cascade. Febs Letters, *531* 65-68.

Angelova M. I.; Soleau S.; Meleard P.; Faucon J. F.; Bothorel P., 1992: Preparation of giant vesicles by external AC electric fields. Kinetics and applications. Progress in Colloid and Polymer Science, *89* 127-131.

Armon L.; Eisenbach M., 2011: Behavioral mechanism during human sperm chemotaxis: involvement of hyperactivation. PLoS One, *6* e28359.

Assreuy A. M. S.; Calvete J. J.; Alencar N. M. N.; Cavada B. S.; Rocha-Filho D. R.; Melo S. C.; Cunha F. Q.; Ribeiro R. A., 2002: Spermadhesin PSP-I/PSP-II heterodimer and its isolated subunits induced neutrophil migration into the peritoneal cavity of rats. Biology of Reproduction, *67* 1796-1803.

Axelrod D.; Koppel D. E.; Schlessinger J.; Elson E.; Webb W. W., 1976: Mobility measurement by analysis of fluorescence photobleaching recovery kinetics. Biophys J, *16* 1055-1069.

Bearer E. L.; Friend D. S., 1980: Anionic lipid domains: correlation with functional topography in a mammalian cell membrane. Proc Natl Acad Sci U S A, *77* 6601-6605.

Bearer E. L.; Friend D. S., 1982: Modifications of anionic-lipid domains preceding membrane fusion in guinea pig sperm. J Cell Biol, *92* 604-615.

Bedford J. M.; Hoskins D. D., 1990: The mammalian spermatoozoon: Morphology, biochemistry and physiology. In: G. E. Lamming, (ed), Marshall's Physiology of Reproduction, Vol. 2. Churchill Livingstone, Edinburgh, pp. 379–568.

Bergeron A.; Villemure M.; Lazure C.; Manjunath P., 2005: Isolation and characterization of the major proteins of ram seminal plasma. Mol Reprod Dev, *71* 461-470.

Boerke A.; Tsai P. S.; Garcia-Gil N.; Brewis I. A.; Gadella B. M., 2008: Capacitation-dependent reorganization of microdomains in the apical sperm head plasma membrane: functional relationship with zona binding and the zona-induced acrosome reaction. Theriogenology, *70* 1188-1196.

Boggs J. M., 1987: Lipid intermolecular hydrogen bonding: influence on structural organization and membrane function. Biochim Biophys Acta, *906* 353-404.

Bolanos-Garcia V. M.; Davies O. R., 2006: Structural analysis and classification of native proteins from E. coli commonly co-purified by immobilised metal affinity chromatography. Biochim Biophys Acta, *1760* 1304-1313.

Bork P.; Beckmann G., 1993: The CUB domain. A widespread module in developmentally regulated proteins. J Mol Biol, *231* 539-545.

Bou Khalil M.; Chakrabandhu K.; Xu H.; Weerachatyanukul W.; Buhr M.; Berger T.; Carmona E.; Vuong N.; Kumarathasan P.; Wong P. T.; Carrier D.; Tanphaichitr N., 2006: Sperm capacitation induces an increase in lipid rafts having zona pellucida binding ability and containing sulfogalactosylglycerolipid. Dev Biol, *290* 220-235.

Braga J.; Desterro J. M.; Carmo-Fonseca M., 2004: Intracellular macromolecular mobility measured by fluorescence recovery after photobleaching with confocal laser scanning microscopes. Mol Biol Cell, *15* 4749-4760.

Braun B. C.; Vargas A.; Jewgenow K., 2012: The molecular detection of relaxin and its receptor RXFP1 in reproductive tissue of Felis catus and Lynx pardinus during pregnancy. Reproduction, *143* 399-410.

Bromfield J. J.; Schjenken J. E.; Chin P. Y.; Care A. S.; Jasper M. J.; Robertson S. A., 2014: Maternal tract factors contribute to paternal seminal fluid impact on metabolic phenotype in offspring. Proc Natl Acad Sci U S A, *111* 2200-2205.

Burkin H. R.; Miller D. J., 2000: Zona pellucida protein binding ability of porcine sperm during epididymal maturation and the acrosome reaction. Dev Biol, *222* 99-109.

Cajazeiras J. B.; Melo L. M.; Albuquerque E. S.; Radis-Baptista G.; Cavada B. S.; Freitas V. J., 2009: Analysis of protein expression and a new prokaryotic expression system for goat

(Capra hircus) spermadhesin Bdh-2 cDNA. Genetics and molecular research : GMR, *8* 1147-1157.

Calvete J. J.; Dostalova Z.; Sanz L.; Adermann K.; Thole H. H.; Töpfer-Petersen E., 1996a: Mapping the heparin-binding domain of boar spermadhesins. FEBS Lett, *379* 207-211.

Calvete J. J.; Enßlin M.; Mburu J.; Iborra A.; Martinez P.; Adermann K.; Waberski D.; Sanz L.; Töpfer-Petersen E.; Weitze K. F.; Einarsson S.; Rodriguez-Martinez H., 1997: Monoclonal antibodies against boar sperm zona pellucida-binding protein AWN-1. Characterization of a continuous antigenic determinant and immunolocalization of AWN epitopes in inseminated sows. Biol Reprod, *57* 735-742.

Calvete J. J.; Mann K.; Schäfer W.; Raida M.; Sanz L.; Töpfer-Petersen E., 1995: Boar spermadhesin PSP-II: location of posttranslational modifications, heterodimer formation with PSP-I glycoforms and effect of dimerization on the ligand-binding capabilities of the subunits. FEBS Lett, *365* 179-182.

Calvete J. J.; Sanz L.; Dostalova Z.; Töpfer-Petersen E., 1993: Characterization of AWN-1 glycosylated isoforms helps define the zona pellucida and serine proteinase inhibitor-binding region on boar spermadhesins. FEBS Lett, *334* 37-40.

Calvete J. J.; Sanz L.; Enßlin M.; Töpfer-Petersen E., 1996b: Sperm surface proteins. Reproduction in domestic animals = Zuchthygiene, *31* 101-105.

Calvete J. J.; Solis D.; Sanz L.; Diaz-Maurino T.; Töpfer-Petersen E., 1994: Glycosylated boar spermadhesin AWN-1 isoforms. Biological origin, structural characterization by lectin mapping, localization of O-glycosylation sites, and effect of glycosylation on ligand binding. Biological chemistry Hoppe-Seyler, *375* 667-673.

Cardin A. D.; Weintraub H. J., 1989: Molecular modeling of protein-glycosaminoglycan interactions. Arteriosclerosis, *9* 21-32.

Carroll R. L., 1988: Vertebrate paleontology and evolution. Freeman, New York.

Cesari A.; Katunar M. R.; Monclus M. A.; Vincenti A.; de Rosas J. C.; Fornes M. W., 2005: Serine protease activity, bovine sperm protease, 66 kDa (BSp66), is present in hamster sperm and is involved in sperm-zona interaction. Reproduction, *129* 291-298.

Cesari A.; Katunar M. R.; Monclus M. A.; Vincenti A.; Fornes M. W., 2004a: BSp66 protease is widespread in the acrosomal region of sperm from several mammalian species. Biochem Bioph Res Co, *324* 874-877.

Cesari A.; Sanchez J. J.; Biancotti J. C.; Vazquez-Levin M. H.; Kaiser G.; Palma G. A.; Alberio R.; Vincenti A. E.; Fornes M. W., 2004b: Immunolocalization of bovine sperm protease BSp120 by light and electron microscopy during capacitation and the acrosome reaction: Its role in in vitro fertilization. Molecular Reproduction and Development, *69* 411-418.

Chattopadhyay A., 1990: Chemistry and biology of N-(7-nitrobenz-2-oxa-1,3-diazol-4-yl)-labeled lipids: fluorescent probes of biological and model membranes. Chemistry and physics of lipids, *53* 1-15.

Chattopadhyay A.; London E., 1987: Parallax method for direct measurement of membrane penetration depth utilizing fluorescence quenching by spin-labeled phospholipids. Biochemistry, *26* 39-45.

Christova Y.; James P.; Mackie A.; Cooper T. G.; Jones R., 2004: Molecular diffusion in sperm plasma membranes during epididymal maturation. Mol Cell Endocrinol, *216* 41-46.

Coy P.; Canovas S.; Mondejar I.; Saavedra M. D.; Romar R.; Grullon L.; Matas C.; Aviles M., 2008: Oviduct-specific glycoprotein and heparin modulate sperm-zona pellucida interaction during fertilization and contribute to the control of polyspermy. Proc Natl Acad Sci U S A, *105* 15809-15814.

Cullis P. R.; Dekruijff B.; Hope M. J.; Nayar R.; Schmid S. L., 1980: Phospholipids and Membrane-Transport. Can J Biochem Cell B, *58* 1091-1100.

Daleke D. L., 2003: Regulation of transbilayer plasma membrane phospholipid asymmetry. Journal of lipid research, *44* 233-242.

Davidova N.; Jonakova V.; Manaskova-Postlerova P., 2009: Expression and localization of acrosin inhibitor in boar reproductive tract. Cell Tissue Res, *338* 303-311.

de Almeida R. F.; Loura L. M.; Prieto M., 2009: Membrane lipid domains and rafts: current applications of fluorescence lifetime spectroscopy and imaging. Chemistry and physics of lipids, *157* 61-77.

Delon C.; Manifava M.; Wood E.; Thompson D.; Krugmann S.; Pyne S.; Ktistakis N. T., 2004: Sphingosine kinase 1 is an intracellular effector of phosphatidic acid. J Biol Chem, *279* 44763-44774.

Dommaschke N., 2016: Biochemische und biophysikalische Analysen zur Interaktion von Spermadhäsinen mit Membranen. Bachelor of Science Bachelor Thesis, Humboldt-Universität zu Berlin.

Dostalova Z.; Calvete J. J.; Sanz L.; Hettel C.; Riedel D.; Schoneck C.; Einspanier R.; Töpfer-Petersen E., 1994a: Immunolocalization and quantitation of acidic seminal fluid protein (aSFP) in ejaculated, swim-up, and capacitated bull spermatozoa. Biological chemistry Hoppe-Seyler, *375* 457-461.

Dostalova Z.; Calvete J. J.; Sanz L.; Töpfer-Petersen E., 1994b: Quantitation of boar spermadhesins in accessory sex gland fluids and on the surface of epididymal, ejaculated and capacitated spermatozoa. Biochim Biophys Acta, *1200* 48-54.

Dostalova Z.; Calvete J. J.; Sanz L.; Töpfer-Petersen E., 1995a: Boar spermadhesin AWN-1. Oligosaccharide and zona pellucida binding characteristics. European journal of biochemistry / FEBS, *230* 329-336.

Dostalova Z.; Calvete J. J.; Töpfer-Petersen E., 1995b: Interaction of non-aggregated boar AWN-1 and AQN-3 with phospholipid matrices. A model for coating of spermadhesins to the sperm surface. Biological chemistry Hoppe-Seyler, *376* 237-242.

Dyballa N.; Metzger S., 2009: Fast and sensitive colloidal coomassie G-250 staining for proteins in polyacrylamide gels. Journal of visualized experiments : JoVE.

Eastman S. J.; Hope M. J.; Wong K. F.; Cullis P. R., 1992: Influence of phospholipid asymmetry on fusion between large unilamellar vesicles. Biochemistry, *31* 4262-4268.

Eckford P. D.; Sharom F. J., 2005: The reconstituted P-glycoprotein multidrug transporter is a flippase for glucosylceramide and other simple glycosphingolipids. Biochem J, *389* 517-526.

Eibl H.; Blume A., 1979: The influence of charge on phosphatidic acid bilayer membranes. Biochim Biophys Acta, *553* 476-488.

Einspanier R.; Amselgruber W.; Sinowatz F.; Henle T.; Ropke R.; Schams D., 1993: Localization and concentration of a new bioactive acetic seminal fluid protein (aSFP) in bulls (Bos taurus). Journal of reproduction and fertility, *98* 241-244.

Einspanier R.; Krause I.; Calvete J. J.; Töpfer-Petersen E.; Klostermeyer H.; Karg H., 1994: Bovine seminal plasma aSFP: localization of disulfide bridges and detection of three different isoelectric forms. FEBS Lett, *344* 61-64.

Ekhlasi-Hundrieser M.; Calvete J. J.; Von Rad B.; Hettel C.; Nimtz M.; Töpfer-Petersen E., 2008a: Point mutations abolishing the mannose-binding capability of boar spermadhesin AQN-1. Biochim Biophys Acta, *1784* 856-862.

Ekhlasi-Hundrieser M.; Gohr K.; Wagner A.; Tsolova M.; Petrunkina A.; Töpfer-Petersen E., 2005: Spermadhesin AQN1 is a candidate receptor molecule involved in the formation of the oviductal sperm reservoir in the pig. Biol Reprod, *73* 536-545.

Ekhlasi-Hundrieser M.; Müller P.; Töpfer-Petersen E., 2008b: Male secretory proteins - sperm tools for fertilisation. In: H. J. Glander; S. Grundewald; U. Paasch, (eds), Biology of male germ cells. Shaker Publisher GmbH, Aachen, Germany, pp. 173-210.

Ekhlasi-Hundrieser M.; Sinowatz F.; Greiser De Wilke I.; Waberski D.; Töpfer-Petersen E., 2002: Expression of spermadhesin genes in porcine male and female reproductive tracts. Mol Reprod Dev, *61* 32-41.

Elson E. L., 2001: Fluorescence correlation spectroscopy measures molecular transport in cells. Traffic, *2* 789-796.

Elson E. L., 2011: Fluorescence correlation spectroscopy: past, present, future. Biophys J, *101* 2855-2870.

Elson E. L.; Magde D., 1974: Fluorescence correlation spectroscopy. I. Conseptual basis and theory. Biopolymers, *13* 1-27.

Enßlin M.; Calvete J. J.; Thole H. H.; Sierralta W. D.; Adermann K.; Sanz L.; Töpfer-Petersen E., 1995: Identification by affinity chromatography of boar sperm membrane-associated proteins bound to immobilized porcine zona pellucida. Mapping of the phosphorylethanolamine-binding region of spermadhesin AWN. Biological chemistry Hoppe-Seyler, *376* 733-738.

Evans R. W.; Weaver D. E.; Clegg E. D., 1980: Diacyl, alkenyl, and alkyl ether phospholipids in ejaculated, in utero-, and in vitro-incubated porcine spermatozoa. Journal of lipid research, *21* 223-228.

Farren S. B.; Hope M. J.; Cullis P. R., 1983: Polymorphic phase preferences of phosphatidic acid: A 31P and 2H NMR study. Biochem Biophys Res Commun, *111* 675-682.

Fery-Forgues S.; Fayet J. P.; Lopez A., 2003: Drastic changes in the fluorescence properties of NBD probes with the polarity of the medium: involvement of a TICT state? . J Photochem Photobiol A:Chem, *70* 229-243.

Flesch F. M.; Gadella B. M., 2000: Dynamics of the mammalian sperm plasma membrane in the process of fertilization. Biochim Biophys Acta, *1469* 197-235.

Frolov V. A.; Shnyrova A. V.; Zimmerberg J., 2011: Lipid polymorphisms and membrane shape. Cold Spring Harbor perspectives in biology, *3* a004747.

Fromm J. R.; Hileman R. E.; Caldwell E. E.; Weiler J. M.; Linhardt R. J., 1997: Pattern and spacing of basic amino acids in heparin binding sites. Archives of biochemistry and biophysics, *343* 92-100.

Fuchs B.; Jakop U.; Goritz F.; Hermes R.; Hildebrandt T.; Schiller J.; Müller K., 2009: MALDI-TOF "fingerprint" phospholipid mass spectra allow the differentiation between ruminantia and feloideae spermatozoa. Theriogenology, *71* 568-575.

Gadella B. M.; Miller N. G.; Colenbrander B.; van Golde L. M.; Harrison R. A., 1999: Flow cytometric detection of transbilayer movement of fluorescent phospholipid analogues across the boar sperm plasma membrane: elimination of labeling artifacts. Mol Reprod Dev, *53* 108-125.

Galla H. J.; Sackmann E., 1975a: Chemically induced lipid phase separation in model membranes containing charged lipids: a spin label study. Biochim Biophys Acta, *401* 509-529.

Galla H. J.; Sackmann E., 1975b: Chemically induced phase separation in mixed vesicles containing phosphatidic acid. An optical study. J Am Chem Soc, *97* 4114-4120.

Greube A.; Müller K.; Töpfer-Petersen E.; Herrmann A.; Müller P., 2001: Influence of the bovine seminal plasma protein PDC-109 on the physical state of membranes. Biochemistry, *40* 8326-8334.

Greube A.; Müller K.; Töpfer-Petersen E.; Herrmann A.; Müller P., 2004: Interaction of fibronectin type II proteins with membranes: The stallion seminal plasma protein SP-1/2. Biochemistry, *43* 464-472.

Guo L.; Har J. Y.; Sankaran J.; Hong Y.; Kannan B.; Wohland T., 2008: Molecular diffusion measurement in lipid bilayers over wide concentration ranges: a comparative study. Chemphyschem, *9* 721-728.

Gur Y.; Breitbart H., 2006: Mammalian sperm translate nuclear-encoded proteins by mitochondrial-type ribosomes. Genes & development, *20* 411-416.

Gur Y.; Breitbart H., 2008: Protein synthesis in sperm: dialog between mitochondria and cytoplasm. Mol Cell Endocrinol, *282* 45-55.

Haase B.; Schlotterer C.; Hundrieser M. E.; Kuiper H.; Distl O.; Töpfer-Petersen E.; Leeb T., 2005: Evolution of the spermadhesin gene family. Gene, *352* 20-29.

Hachen A.; Jewgenow K.; Krause E.; Braun B. C., 2012: Recombinant feline oviductin--a powerful tool for functional IVF studies in the domestic cat. Reproduction in domestic animals = Zuchthygiene, *47 Suppl 6* 88-92.

Haldar S.; Chattopadhyay A., 2013: Application of NBD-Labeled Lipids in Membrane and Cell Biology. In: Y. Mely; G. Duportail, (eds), Fluorescent Methods to Study Biological Membranes Springer, pp. 37–50.

Haupts U.; Maiti S.; Schwille P.; Webb W. W., 1998: Dynamics of fluorescence fluctuations in green fluorescent protein observed by fluorescence correlation spectroscopy. Proc Natl Acad Sci U S A, *95* 13573-13578.

Hodgkin M. N.; Pettitt T. R.; Martin A.; Michell R. H.; Pemberton A. J.; Wakelam M. J., 1998: Diacylglycerols and phosphatidates: which molecular species are intracellular messengers? Trends in biochemical sciences, *23* 200-204.

Homola J., 2008: Surface plasmon resonance sensors for detection of chemical and biological species. Chemical reviews, *108* 462-493.

Honda A.; Yamagata K.; Sugiura S.; Watanabe K.; Baba T., 2002: A mouse serine protease TESP5 is selectively included into lipid rafts of sperm membrane presumably as a glycosylphosphatidylinositol-anchored protein. Journal of Biological Chemistry, *277* 16976-16984.

Howes E. A.; Hurst S. M.; Jones R., 2001: Actin and actin-binding proteins in bovine spermatozoa: potential role in membrane remodeling and intracellular signaling during epididymal maturation and the acrosome reaction. Journal of andrology, *22* 62-72.

Ikawa M.; Inoue N.; Benham A. M.; Okabe M., 2010: Fertilization: a sperm's journey to and interaction with the oocyte. J Clin Invest, *120* 984-994.

Im J. S.; Yu K. O.; Illarionov P. A.; LeClair K. P.; Storey J. R.; Kennedy M. W.; Besra G. S.; Porcelli S. A., 2004: Direct measurement of antigen binding properties of CD1 proteins using fluorescent lipid probes. J Biol Chem, *279* 299-310.

International Sheep Genomics C.; Archibald A. L.; Cockett N. E.; Dalrymple B. P.; Faraut T.; Kijas J. W.; Maddox J. F.; McEwan J. C.; Hutton Oddy V.; Raadsma H. W.; Wade C.; Wang J.; Wang W.; Xun X., 2010: The sheep genome reference sequence: a work in progress. Animal genetics, *41* 449-453.

Itach S. B.; Finklestein M.; Etkovitz N.; Breitbart H., 2012: Hyper-activated motility in sperm capacitation is mediated by phospholipase D-dependent actin polymerization. Dev Biol, *362* 154-161.

James P. S.; Hennessy C.; Berge T.; Jones R., 2004: Compartmentalisation of the sperm plasma membrane: a FRAP, FLIP and SPFI analysis of putative diffusion barriers on the sperm head. J Cell Sci, *117* 6485-6495.

James P. S.; Wolfe C. A.; Ladha S.; Jones R., 1999: Lipid diffusion in the plasma membrane of ram and boar spermatozoa during maturation in the epididymis measured by fluorescence recovery after photobleaching. Mol Reprod Dev, *52* 207-215.

Jamil K., 1984: Plasma membrane cytoskeletal complex of the mammalian spermatozoa. Arch Androl, *13* 177-193.

Jenkins N.; Curling E. M. A., 1994: Glycosylation of Recombinant Proteins - Problems and Prospects. Enzyme Microb Tech, *16* 354-364.

Johnson S. A.; Stinson B. M.; Go M. S.; Carmona L. M.; Reminick J. I.; Fang X.; Baumgart T., 2010: Temperature-dependent phase behavior and protein partitioning in giant plasma membrane vesicles. Biochim Biophys Acta, *1798* 1427-1435.

Jonakova V.; Calvete J. J.; Mann K.; Schäfer W.; Schmid E. R.; Töpfer-Petersen E., 1992: The complete primary structure of three isoforms of a boar sperm-associated acrosin inhibitor. FEBS Lett, *297* 147-150.

Jonakova V.; Cechova D., 1985: Demonstration of an anionic acrosin inhibitor in spermatozoa epididymal fluid and seminal plasma of the boar. Andrologia, *17* 466-471.

Jonakova V.; Kraus M.; Veselsky L.; Cechova D.; Bezouska K.; Ticha M., 1998: Spermadhesins of the AQN and AWN families, DQH sperm surface protein and HNK protein in the heparin-binding fraction of boar seminal plasma. Journal of reproduction and fertility, *114* 25-34.

Jonakova V.; Manaskova P.; Kraus M.; Liberda J.; Ticha M., 2000: Sperm surface proteins in mammalian fertilization. Mol Reprod Dev, *56* 275-277.

Jones R.; Howes E.; Dunne P. D.; James P.; Bruckbauer A.; Klenerman D., 2010: Tracking diffusion of GM1 gangliosides and zona pellucida binding molecules in sperm plasma membranes following cholesterol efflux. Dev Biol, *339* 398-406.

Jones R.; James P. S.; Howes L.; Bruckbauer A.; Klenerman D., 2007: Supramolecular organization of the sperm plasma membrane during maturation and capacitation. Asian J Androl, *9* 438-444.

Jouhet J., 2013: Importance of the hexagonal lipid phase in biological membrane organization. Frontiers in plant science, *4* 494.

Julien M.; Tournier J. F.; Tocanne J. F., 1993: Differences in the transbilayer and lateral motions of fluorescent analogs of phosphatidylcholine and phosphatidylethanolamine in the apical plasma membrane of bovine aortic endothelial cells. Exp Cell Res, *208* 387-397.

Kaiser R. D.; London E., 1998: Determination of the depth of BODIPY probes in model membranes by parallax analysis of fluorescence quenching. Biochim Biophys Acta, *1375* 13-22.

Kang M.; Day C. A.; Drake K.; Kenworthy A. K.; DiBenedetto E., 2009: A generalization of theory for two-dimensional fluorescence recovery after photobleaching applicable to confocal laser scanning microscopes. Biophys J, *97* 1501-1511.

Kang M.; Day C. A.; Kenworthy A. K.; DiBenedetto E., 2012: Simplified equation to extract diffusion coefficients from confocal FRAP data. Traffic, *13* 1589-1600.

Kawano N.; Yoshida K.; Miyado K.; Yoshida M., 2011: Lipid rafts: keys to sperm maturation, fertilization, and early embryogenesis. J Lipids, *2011* 264706.

Klein A. S.; Schaefer M.; Korte T.; Herrmann A.; Tannert A., 2012: HaCaT keratinocytes exhibit a cholesterol and plasma membrane viscosity gradient during directed migration. Exp Cell Res, *318* 809-818.

Kol M. A.; van Dalen A.; de Kroon A. I.; de Kruijff B., 2003: Translocation of phospholipids is facilitated by a subset of membrane-spanning proteins of the bacterial cytoplasmic membrane. J Biol Chem, *278* 24586-24593.

Kooijman E. E.; Chupin V.; de Kruijff B.; Burger K. N., 2003: Modulation of membrane curvature by phosphatidic acid and lysophosphatidic acid. Traffic, *4* 162-174.

Kooijman E. E.; Tieleman D. P.; Testerink C.; Munnik T.; Rijkers D. T.; Burger K. N.; de Kruijff B., 2007: An electrostatic/hydrogen bond switch as the basis for the specific interaction of phosphatidic acid with proteins. J Biol Chem, *282* 11356-11364.

Koter M.; de Kruijff B.; van Deenen L. L., 1978: Calcium-induced aggregation and fusion of mixed phosphatidylcholine-phosphatidic acid vesicles as studied by 31P NMR. Biochim Biophys Acta, *514* 255-263.

Krishnan B.; Szymanska A.; Gierasch L. M., 2007: Site-specific fluorescent labeling of poly-histidine sequences using a metal-chelating cysteine. Chem Biol Drug Des, *69* 31-40.

Kurz A.; Viertel D.; Herrmann A.; Müller K., 2005: Localization of phosphatidylserine in boar sperm cell membranes during capacitation and acrosome reaction. Reproduction, *130* 615-626.

Kwon W. S.; Rahman M. S.; Lee J. S.; Kim J.; Yoon S. J.; Park Y. J.; You Y. A.; Hwang S.; Pang M. G., 2014: A comprehensive proteomic approach to identifying capacitation related proteins in boar spermatozoa. BMC genomics, *15* 897.

Ladha S.; James P. S.; Clark D. C.; Howes E. A.; Jones R., 1997: Lateral mobility of plasma membrane lipids in bull spermatozoa: heterogeneity between surface domains and rigidification following cell death. J Cell Sci, *110 (Pt 9)* 1041-1050.

Laemmli U. K., 1970: Cleavage of structural proteins during the assembly of the head of bacteriophage T4. Nature, *227* 680-685.

Lange S.; Sylvester M.; Schumann M.; Freund C.; Krause E., 2010: Identification of phosphorylation-dependent interaction partners of the adapter protein ADAP using

quantitative mass spectrometry: SILAC vs (18)O-labeling. Journal of proteome research, *9* 4113-4122.

Leeb T., 2007: The horse genome project--sequence based insights into male reproductive mechanisms. Reproduction in domestic animals = Zuchthygiene, *42 Suppl 2* 45-50.

Lessig J.; Gey C.; Suss R.; Schiller J.; Glander H. J.; Arnhold J., 2004a: Analysis of the lipid composition of human and boar spermatozoa by MALDI-TOF mass spectrometry, thin layer chromatography and 31P NMR spectroscopy. Comp Biochem Physiol B Biochem Mol Biol, *137* 265-277.

Lessig J.; Gey C.; Suss R.; Schiller J.; Glander H. J.; Arnhold J., 2004b: Analysis of the lipid composition of human and boar spermatozoa by MALDI-TOF mass spectrometry, thin layer chromatography and P-31 NMR spectroscopy. Comp Biochem Phys B, *137* 265-277.

Liberda J.; Manaskova P.; Prelovska L.; Ticha M.; Jonakova V., 2006: Saccharide-mediated interactions of boar sperm surface proteins with components of the porcine oviduct. Journal of reproductive immunology, *71* 112-125.

Lin S.; Struve W. S., 1991: Time-resolved fluorescence of nitrobenzoxadiazole-aminohexanoic acid: effect of intermolecular hydrogen-bonding on non-radiative decay. Photochemistry and photobiology, *54* 361-365.

Loura L. M. S.; Prieto M.; Fernandes F., 2010: Quantification of protein-lipid selectivity using FRET. Eur Biophys J Biophy, *39* 565-578.

Lu B.; Benning C., 2009: A 25-amino acid sequence of the Arabidopsis TGD2 protein is sufficient for specific binding of phosphatidic acid. J Biol Chem, *284* 17420-17427.

Luconi M.; Barni T.; Vannelli G. B.; Krausz C.; Marra F.; Benedetti P. A.; Evangelista V.; Francavilla S.; Properzi G.; Forti G.; Baldi E., 1998: Extracellular signal-regulated kinases modulate capacitation of human spermatozoa. Biol Reprod, *58* 1476-1489.

Mackie A. R.; James P. S.; Ladha S.; Jones R., 2001: Diffusion barriers in ram and boar sperm plasma membranes: directionality of lipid diffusion across the posterior ring. Biol Reprod, *64* 113-119.

Mädler S.; Bich C.; Touboul D.; Zenobi R., 2009: Chemical cross-linking with NHS esters: a systematic study on amino acid reactivities. J Mass Spectrom, *44* 694-706.

Maekawa M.; Fairn G. D., 2014: Molecular probes to visualize the location, organization and dynamics of lipids. Journal of Cell Science, *127* 4801-4812.

Magde D.; Elson E. L.; Webb W. W., 1974: Fluorescence correlation spectroscopy. II. An experimental realization. Biopolymers, *13* 29-61.

Manaskova-Postlerova P.; Cozlova N.; Dorosh A.; Sulc M.; Guyonnet B.; Jonakova V., 2016: Acrosin inhibitor detection along the boar epididymis. International journal of biological macromolecules, *82* 733-739.

Marion D., 2013: An introduction to biological NMR spectroscopy. Molecular & cellular proteomics : MCP, *12* 3006-3025.

Marriott G.; Clegg R. M.; Arndt-Jovin D. J.; Jovin T. M., 1991: Time resolved imaging microscopy. Phosphorescence and delayed fluorescence imaging. Biophys J, *60* 1374-1387.

Marsh D., 1990: Lipid-protein interactions in membranes. FEBS Lett, *268* 371-375.

Martinez P.; Morros A., 1996: Membrane lipid dynamics during human sperm capacitation. Front Biosci, *1* d103-117.

McGee W. M.; Mentinova M.; McLuckey S. A., 2012: Gas-Phase Conjugation to Arginine Residues in Polypeptide Ions via N-Hydroxysuccinimide Ester-Based Reagent Ions. Journal of the American Chemical Society, *134* 11412-11414.

Melo L. M.; Teixeira D. I.; Havt A.; da Cunha R. M.; Martins D. B.; Castelletti C. H.; de Souza P. R.; Filho J. L.; Freitas V. J.; Cavada B. S.; Radis-Baptista G., 2008: Buck (Capra hircus) genes encode new members of the spermadhesin family. Mol Reprod Dev, *75* 8-16.

Meyvis T. K.; De Smedt S. C.; Van Oostveldt P.; Demeester J., 1999: Fluorescence recovery after photobleaching: a versatile tool for mobility and interaction measurements in pharmaceutical research. Pharmaceutical research, *16* 1153-1162.

Miller B. T.; Collins T. J.; Rogers M. E.; Kurosky A., 1997: Peptide biotinylation with amine-reactive esters: differential side chain reactivity. Peptides, *18* 1585-1595.

Miller D.; Ostermeier G. C., 2006: Towards a better understanding of RNA carriage by ejaculate spermatozoa. Human reproduction update, *12* 757-767.

Miller D. J.; Winer M. A.; Ax R. L., 1990: Heparin-binding proteins from seminal plasma bind to bovine spermatozoa and modulate capacitation by heparin. Biol Reprod, *42* 899-915.

Modesti M., 2011: Fluorescent labeling of proteins. Methods Mol Biol, *783* 101-120.

Moura A. A.; Koc H.; Chapman D. A.; Killian G. J., 2006: Identification of proteins in the accessory sex gland fluid associated with fertility indexes of dairy bulls: a proteomic approach. Journal of andrology, *27* 201-211.

Mukherjee S.; Kalipatnapu S.; Pucadyil T. J.; Chattopadhyay A., 2006: Monitoring the organization and dynamics of bovine hippocampal membranes utilizing differentially localized fluorescent membrane probes. Mol Membr Biol, *23* 430-441.

Mukherjee S.; Maxfield F. R., 2004: Membrane domains. Annu Rev Cell Dev Biol, *20* 839-866.

Müller K.; Pomorski T.; Müller P.; Zachowski A.; Herrmann A., 1994: Protein-dependent translocation of aminophospholipids and asymmetric transbilayer distribution of phospholipids in the plasma membrane of ram sperm cells. Biochemistry, *33* 9968-9974.

Müller P.; Erlemann K. R.; Müller K.; Calvete J. J.; Töpfer-Petersen E.; Marienfeld K.; Herrmann A., 1998: Biophysical characterization of the interaction of bovine seminal plasma protein PDC-109 with phospholipid vesicles. Eur Biophys J Biophy, *27* 33-41.

Müller P.; Plazzo A. P.; Herrmann A., 2011: Transbilayer movement and distribution of cholesterol. In: P. F. Devaux, (ed), Membrane asymmetry and transmembrane motion of lipids. Wiley, pp. 75-96.

Nascimento A. S.; Cajazeiras J. B.; Nascimento K. S.; Nogueira S. M.; Sousa B. L.; Teixeira E. H.; Melo L. M.; da Cunha R. M.; Silva A. L.; Cavada B. S., 2012: Expression, purification and structural analysis of recombinant rBdh-2His(6), a spermadhesin from buck (Capra hircus) seminal plasma. Reproduction, fertility, and development, *24* 580-587.

Nolan J. P.; Magargee S. F.; Posner R. G.; Hammerstedt R. H., 1995: Flow cytometric analysis of transmembrane phospholipid movement in bull sperm. Biochemistry, *34* 3907-3915.

Okamura N.; Onoe S.; Kawakura K.; Tajima Y.; Sugita Y., 1990: Effects of a Membrane-Bound Trypsin-Like Proteinase and Seminal Proteinase-Inhibitors on the Bicarbonate-Sensitive Adenylate-Cyclase in Porcine Sperm Plasma-Membranes. Biochimica Et Biophysica Acta, *1035* 83-89.

Ostasov P.; Sykora J.; Brejchova J.; Olzynska A.; Hof M.; Svoboda P., 2013: FLIM studies of 22- and 25-NBD-cholesterol in living HEK293 cells: plasma membrane change induced by cholesterol depletion. Chemistry and physics of lipids, *167-168* 62-69.

Papahadjopoulos D.; Portis A.; Pangborn W., 1978: Calcium-induced lipid phase transitions and membrane fusion. Annals of the New York Academy of Sciences, *308* 50-66.

Parker G. A., 1982: Why Are There So Many Tiny Sperm - Sperm Competition and the Maintenance of 2 Sexes. Journal of theoretical biology, *96* 281-294.

Parker G. A.; Pizzari T., 2010: Sperm competition and ejaculate economics. Biological reviews of the Cambridge Philosophical Society, *85* 897-934.

Parks J. E.; Lynch D. V., 1992: Lipid composition and thermotropic phase behavior of boar, bull, stallion, and rooster sperm membranes. Cryobiology, *29* 255-266.

Peterson R. N.; Gillott M.; Hunt W.; Russell L. D., 1987: Organization of the boar spermatozoan plasma membrane: evidence for separate domains (subdomains) of integral membrane proteins in the plasma membrane overlying the principal segment of the acrosome. J Cell Sci, *88 (Pt 3)* 343-349.

Pomorski T.; Herrmann A.; Zachowski A.; Devaux P. F.; Müller P., 1994: Rapid determination of the transbilayer distribution of NBD-phospholipids in erythrocyte membranes with dithionite. Mol Membr Biol, *11* 39-44.

Pomorski T.; Hrafnsdottir S.; Devaux P. F.; van Meer G., 2001: Lipid distribution and transport across cellular membranes. Seminars in cell & developmental biology, *12* 139-148.

Pucadyil T. J.; Mukherjee S.; Chattopadhyay A., 2007: Organization and dynamics of NBD-labeled lipids in membranes analyzed by fluorescence recovery after photobleaching. The journal of physical chemistry. B, *111* 1975-1983.

Putney J. W.; Weiss S. J.; Vandewalle C. M.; Haddas R. A., 1980: Is Phosphatidic-Acid a Calcium Ionophore under Neurohumoral Control. Nature, *284* 345-347.

Quinn J. G.; O'Kennedy R.; Smyth M.; Moulds J.; Frame T., 1997: Detection of blood group antigens utilising immobilised antibodies and surface plasmon resonance. Journal of immunological methods, *206* 87-96.

Ramm S. A.; Edward D. A.; Claydon A. J.; Hammond D. E.; Brownridge P.; Hurst J. L.; Beynon R. J.; Stockley P., 2015: Sperm competition risk drives plasticity in seminal fluid composition. Bmc Biol, *13*.

Ramstedt B.; Slotte J. P., 2006: Sphingolipids and the formation of sterol-enriched ordered membrane domains. Biochim Biophys Acta, *1758* 1945-1956.

Reinert M.; Calvete J. J.; Sanz L.; Mann K.; Töpfer-Petersen E., 1996: Primary structure of stallion seminal plasma protein HSP-7, a zona-pellucida-binding protein of the spermadhesin family. European journal of biochemistry / FEBS, *242* 636-640.

Rodriguez-Martinez H.; Iborra A.; Martinez P.; Calvete J. J., 1998: Immunoelectronmicroscopic imaging of spermadhesin AWN epitopes on boar spermatozoa bound in vivo to the zona pellucida. Reproduction, fertility, and development, *10* 491-497.

Rodriguez-Martinez H.; Kvist U.; Ernerudh J.; Sanz L.; Calvete J. J., 2011: Seminal plasma proteins: what role do they play? American journal of reproductive immunology, *66 Suppl 1* 11-22.

Rutherfurd K. J.; Swiderek K. M.; Green C. B.; Chen S.; Shively J. E.; Kwok S. C., 1992: Purification and characterization of PSP-I and PSP-II, two major proteins from porcine seminal plasma. Archives of biochemistry and biophysics, *295* 352-359.

Sanz L.; Calvete J. J.; Jonakova V.; Töpfer-Petersen E., 1992a: Boar spermadhesins AQN-1 and AWN are sperm-associated acrosin inhibitor acceptor proteins. FEBS Lett, *300* 63-66.

Sanz L.; Calvete J. J.; Mann K.; Gabius H. J.; Töpfer-Petersen E., 1993: Isolation and biochemical characterization of heparin-binding proteins from boar seminal plasma: a dual role for spermadhesins in fertilization. Mol Reprod Dev, *35* 37-43.

Sanz L.; Calvete J. J.; Mann K.; Schäfer W.; Schmid E. R.; Amselgruber W.; Sinowatz F.; Ehrhard M.; Töpfer-Petersen E., 1992b: The complete primary structure of the spermadhesin AWN, a zona pellucida-binding protein isolated from boar spermatozoa. FEBS Lett, *300* 213-218.

Sanz L.; Calvete J. J.; Mann K.; Schäfer W.; Schmid E. R.; Töpfer-Petersen E., 1991: The amino acid sequence of AQN-3, a carbohydrate-binding protein isolated from boar sperm. Location of disulphide bridges. FEBS Lett, *291* 33-36.

Sanz L.; Calvete J. J.; Mann K.; Schäfer W.; Schmid E. R.; Töpfer-Petersen E., 1992c: The complete primary structure of the boar spermadhesin AQN-1, a carbohydrate-binding protein involved in fertilization. European journal of biochemistry / FEBS, *205* 645-652.

Sanz L.; Calvete J. J.; Schäfer W.; Mann K.; Töpfer-Petersen E., 1992d: Isolation and biochemical characterization of two isoforms of a boar sperm zona pellucida-binding protein. Biochim Biophys Acta, *1119* 127-132.

Schlame M., 2008: Cardiolipin synthesis for the assembly of bacterial and mitochondrial membranes. Journal of lipid research, *49* 1607-1620.

Schlame M.; Rua D.; Greenberg M. L., 2000: The biosynthesis and functional role of cardiolipin. Prog Lipid Res, *39* 257-288.

Schröter F.; Jakop U.; Teichmann A.; Haralampiev I.; Tannert A.; Wiesner B.; Müller P.; Müller K., 2016: Lipid dynamics in boar sperm studied by advanced fluorescence imaging techniques. European biophysics journal : EBJ, *45* 149-163.

Seigneuret M.; Zachowski A.; Hermann A.; Devaux P. F., 1984: Asymmetric lipid fluidity in human erythrocyte membrane: new spin-label evidence. Biochemistry, *23* 4271-4275.

Selo I.; Negroni L.; Creminon C.; Grassi J.; Wal J. M., 1996: Preferential labeling of alpha-amino N-terminal groups in peptides by biotin: application to the detection of specific anti-peptide antibodies by enzyme immunoassays. Journal of immunological methods, *199* 127-138.

Sengupta P.; Hammond A.; Holowka D.; Baird B., 2008: Structural determinants for partitioning of lipids and proteins between coexisting fluid phases in giant plasma membrane vesicles. Biochim Biophys Acta, *1778* 20-32.

Sezgin E.; Levental I.; Grzybek M.; Schwarzmann G.; Mueller V.; Honigmann A.; Belov V. N.; Eggeling C.; Coskun U.; Simons K.; Schwille P., 2012: Partitioning, diffusion, and ligand binding of raft lipid analogs in model and cellular plasma membranes. Biochim Biophys Acta, *1818* 1777-1784.

Shimoni L.; Glusker J. P., 1995: Hydrogen bonding motifs of protein side chains: descriptions of binding of arginine and amide groups. Protein science : a publication of the Protein Society, *4* 65-74.

Shukla S. D.; Hanahan D. J., 1982: Agepc (Platelet Activating Factor) Induced Stimulation of Rabbit Platelets - Effects on Phosphatidylinositol, Di-Phosphoinositides and Tri-Phosphoinositides and Phosphatidic-Acid Metabolism. Biochem Bioph Res Co, *106* 697-703.

Simmonds A. C.; Halsey M. J., 1985: General and local anaesthetics perturb the fusion of phospholipid vesicles. Biochim Biophys Acta, *813* 331-337.

Simons K.; Gerl M. J., 2010: Revitalizing membrane rafts: new tools and insights. Nature reviews. Molecular cell biology, *11* 688-699.

Snapp E., 2005: Design and use of fluorescent fusion proteins in cell biology. Current protocols in cell biology / editorial board, Juan S. Bonifacino ... [et al.], *Chapter 21* Unit 21 24.

Soleilhavoup C.; Riou C.; Tsikis G.; Labas V.; Harichaux G.; Kohnke P.; Reynaud K.; de Graaf S. P.; Gerard N.; Druart X., 2016: Proteomes of the Female Genital Tract During the Oestrous Cycle. Molecular & cellular proteomics : MCP, *15* 93-108.

Soleilhavoup C.; Tsikis G.; Labas V.; Harichaux G.; Kohnke P. L.; Dacheux J. L.; Guerin Y.; Gatti J. L.; de Graaf S. P.; Druart X., 2014:seminal plasma proteome and its impact on liquid preservation of spermatozoa. Journal of proteomics, *109* 245-260.

Souza C. E.; Rego J. P.; Lobo C. H.; Oliveira J. T.; Nogueira F. C.; Domont G. B.; Fioramonte M.; Gozzo F. C.; Moreno F. B.; Monteiro-Moreira A. C.; Figueiredo J. R.; Moura A. A., 2012: Proteomic analysis of the reproductive tract fluids from tropically-adapted Santa Ines rams. Journal of proteomics, *75* 4436-4456.

Stöckl M.; Plazzo A. P.; Korte T.; Herrmann A., 2008: Detection of lipid domains in model and cell membranes by fluorescence lifetime imaging microscopy of fluorescent lipid analogues. J Biol Chem, *283* 30828-30837.

Swairjo M. A.; Seaton B. A.; Roberts M. F., 1994: Effect of vesicle composition and curvature on the dissociation of phosphatidic acid in small unilamellar vesicles--a 31P-NMR study. Biochim Biophys Acta, *1191* 354-361.

Talbot P.; Summers R. G.; Hylander B. L.; Keough E. M.; Franklin L. E., 1976: The role of calcium in the acrosome reaction: an analysis using ionophore A23187. The Journal of experimental zoology, *198* 383-392.

Tannert A.; Kurz A.; Erlemann K. R.; Müller K.; Herrmann A.; Schiller J.; Töpfer-Petersen E.; Manjunath P.; Müller P., 2007a: The bovine seminal plasma protein PDC-109 extracts phosphorylcholine-containing lipids from the outer membrane leaflet. European biophysics journal : EBJ, *36* 461-475.

Tannert A.; Töpfer-Petersen E.; Herrmann A.; Müller K.; Müller P., 2007b: The lipid composition modulates the influence of the bovine seminal plasma protein PDC-109 on membrane stability. Biochemistry, *46* 11621-11629.

Tanphaichitr N.; Carmona E.; Bou Khalil M.; Xu H.; Berger T.; Gerton G. L., 2007: New insights into sperm-zona pellucida interaction: involvement of sperm lipid rafts. Front Biosci, *12* 1748-1766.

Tedeschi G.; Oungre E.; Mortarino M.; Negri A.; Maffeo G.; Ronchi S., 2000: Purification and primary structure of a new bovine spermadhesin. European journal of biochemistry / FEBS, *267* 6175-6179.

Teichmann A.; Gibert A.; Lampe A.; Grzesik P.; Rutz C.; Furkert J.; Schmoranzer J.; Krause G.; Wiesner B.; Schulein R., 2014: The specific monomer/dimer equilibrium of the corticotropin-releasing factor receptor type 1 is established in the endoplasmic reticulum. J Biol Chem, *289* 24250-24262.

Teixeira D. I.; Cavada B. S.; Sampaio A. H.; Havt A.; Bloch C., Jr.; Prates M. V.; Moreno F. B.; Santos E. A.; Gadelha C. A.; Gadelha T. S.; Crisostomo F. S.; Freitas V. J., 2002: Isolation and partial characterisation of a protein from buck seminal plasma (Capra hircus), homologous to spermadhesins. Protein and peptide letters, *9* 331-335.

Tesarik J.; Drahorad J.; Testart J.; Mendoza C., 1990: Acrosin Activation Follows Its Surface Exposure and Precedes Membrane-Fusion in Human Sperm Acrosome Reaction. Development, *110* 391-&.

Thomas C. J.; Anbazhagan V.; Ramakrishnan M.; Sultan N.; Surolia I.; Swamy M. J., 2003: Mechanism of membrane binding by the bovine seminal plasma protein, PDC-109: a surface plasmon resonance study. Biophys J, *84* 3037-3044.

Tienthai P.; Kjellen L.; Pertoft H.; Suzuki K.; Rodriguez-Martinez H., 2000: Localization and quantitation of hyaluronan and sulfated glycosaminoglycans in the tissues and intraluminal fluid of the pig oviduct. Reproduction, fertility, and development, *12* 173-182.

Töpfer-Petersen E., 1999a: Carbohydrate-based interactions on the route of a spermatozoon to fertilization. Human reproduction update, *5* 314-329.

Töpfer-Petersen E., 1999b: Molecules on the sperm's route to fertilization. The Journal of experimental zoology, *285* 259-266.

Töpfer-Petersen E.; Calvete J. J.; Sanz L.; Sinowatz F., 1995: Carbohydrate-and heparin-binding proteins in mammalian fertilization. Andrologia, *27* 303-324.

Töpfer-Petersen E.; Ekhlasi-Hundrieser M.; Tsolova M., 2008: Glycobiology of fertilization in the pig. Int J Dev Biol, *52* 717-736.

Töpfer-Petersen E.; Romero A.; Varela P. F.; Ekhlasi-Hundrieser M.; Dostalova Z.; Sanz L.; Calvete J. J., 1998: Spermadhesins: a new protein family. Facts, hypotheses and perspectives. Andrologia, *30* 217-224.

Traikia M.; Warschawski D. E.; Lambert O.; Rigaud J. L.; Devaux P. F., 2002: Asymmetrical membranes and surface tension. Biophys J, *83* 1443-1454.

van Gestel R. A.; Brewis I. A.; Ashton P. R.; Helms J. B.; Brouwers J. F.; Gadella B. M., 2005: Capacitation-dependent concentration of lipid rafts in the apical ridge head area of porcine sperm cells. Mol Hum Reprod, *11* 583-590.

Varner D. D.; Bowen J. A.; Johnson L., 1993: Effect of heparin on capacitation/acrosome reaction of equine sperm. Arch Androl, *31* 199-207.

Vazquez J. M.; Roldan E. R. S., 1997: Phospholipid metabolism in boar spermatozoa and role of diacylglycerol species in the de novo formation of phosphatidylcholine. Molecular Reproduction and Development, *47* 105-112.

Verkleij A. J., 1984: Lipidic intramembranous particles. Biochim Biophys Acta, *779* 43-63.

Verkleij A. J.; De Maagd R.; Leunissen-Bijvelt J.; De Kruijff B., 1982: Divalent cations and chlorpromazine can induce non-bilayer structures in phosphatidic acid-containing model membranes. Biochim Biophys Acta, *684* 255-262.

Wacker M.; Linton D.; Hitchen P. G.; Nita-Lazar M.; Haslam S. M.; North S. J.; Panico M.; Morris H. R.; Dell A.; Wren B. W.; Aebi M., 2002: N-linked glycosylation in Campylobacter jejuni and its functional transfer into E-coli. Science, *298* 1790-1793.

Wagner A.; Ekhlasi-Hundrieser M.; Hettel C.; Petrunkina A.; Waberski D.; Nimtz M.; Töpfer-Petersen E., 2002: Carbohydrate-based interactions of oviductal sperm reservoir formation-studies in the pig. Mol Reprod Dev, *61* 249-257.

Wang T. Y.; Silvius J. R., 2000: Different sphingolipids show differential partitioning into sphingolipid/cholesterol-rich domains in lipid bilayers. Biophys J, *79* 1478-1489.

Wang T. Y.; Silvius J. R., 2003: Sphingolipid partitioning into ordered domains in cholesterol-free and cholesterol-containing lipid bilayers. Biophys J, *84* 367-378.

Wang X.; Devaiah S. P.; Zhang W.; Welti R., 2006: Signaling functions of phosphatidic acid. Prog Lipid Res, *45* 250-278.

Wolfe C. A.; James P. S.; Mackie A. R.; Ladha S.; Jones R., 1998: Regionalized lipid diffusion in the plasma membrane of mammalian spermatozoa. Biol Reprod, *59* 1506-1514.

Woody R. W., 1995: Circular dichroism. Methods in enzymology, *246* 34-71.

Wüstner D., 2007: Fluorescent sterols as tools in membrane biophysics and cell biology. Chemistry and physics of lipids, *146* 1-25.

Wüstner D.; Mukherjee S.; Maxfield F. R.; Müller P.; Herrmann A., 2001: Vesicular and nonvesicular transport of phosphatidylcholine in polarized HepG2 cells. Traffic, *2* 277-296.

Wüstner D.; Pomorski T.; Herrmann A.; Müller P., 1998: Release of phospholipids from erythrocyte membranes by taurocholate is determined by their transbilayer orientation and hydrophobic backbone. Biochemistry, *37* 17093-17103.

Xiao Q.; Zhang F.; Nacev B. A.; Liu J. O.; Pei D., 2010: Protein N-terminal processing: substrate specificity of Escherichia coli and human methionine aminopeptidases. Biochemistry, *49* 5588-5599.

Zachowski A., 1993: Phospholipids in animal eukaryotic membranes: transverse asymmetry and movement. Biochem J, *294 (Pt 1)* 1-14.